INVESTIGATING IN VIVO UTILIZATION OF VLP VACCINES ADJUVANTED WITH SINGLE, DUAL, OR TRIPLE PATHOGEN-ASSOCIATED MOLECULAR PATTERNS

A THESIS SUBMITTED TO

THE GRADUATE SCHOOL OF ENGINEERING AND SCIENCE

OF BILKENT UNIVERSITY

IN PARTIAL FULFILLMENT OF THE REQUIREMENTS FOR

THE DEGREE OF

MASTER OF SCIENCE

IN

MOLECULAR BIOLOGY AND GENETICS

By

Yasemin Ceylan

August 2023

INVESTIGATING IN VIVO UTILIZATION OF VLP VACCINES ADJUVANTED WITH SINGLE, DUAL, OR TRIPLE PATHOGEN-ASSOCIATED MOLECULAR PATTERNS

By Yasemin Ceylan

August 2023

We certify that we have read this thesis and that in our opinion it is fully adequate, in scope and in quality, as a thesis for the degree of Master of Science.

İhsan Gürsel (Advisor)

Serkan İsmail Göktuna

Haluk Barbaros Oral

Approved for the Graduate School of Engineering and Science

Orhan Arıkan

Director of the School of Engineering and Science

ABSTRACT

INVESTIGATING IN VIVO UTILIZATION OF VLP VACCINES ADJUVANTED WITH SINGLE, DUAL, OR TRIPLE PATHOGEN-ASSOCIATED MOLECULAR PATTERNS

Yasemin Ceylan

M.Sc. in Molecular Biology and Genetics

Advisor: Ihsan Gursel

August 2023

COVID-19 was first identified in Wuhan, a Chinese city, and it has been a part of our lives since late December 2019. The WHO declared this disease, caused by SARS-CoV-2, a pandemic due to its high transmission rate, a status that remained in effect until May 2023. The escalating death toll and virus spread expedited vaccine development efforts. Various platforms for vaccine development have been utilized, including inactivated virus, mRNA, and subunit vaccines. Given the virus's propensity for mutations due to its high transmission rate, the chosen platform must be easy to produce, effective, and safe for immunocompromised individuals. One such platform is virus-like particles (VLPs). VLP vaccines consist of viral proteins without genetic material and are known for their ease of production. A VLP vaccine, adjuvanted with Alum and K-type CpG ODN against SARS-CoV-2, is tested in Phase II clinical trials. In addition to CpG ODN, this study aimed to evaluate the efficacy of other adjuvants and their combinations to explore potential clinical advantages. The additional adjuvants included poly(I:C) and a member of cyclic dinucleotides, 2,3-cGAMP, which are Toll-like receptor 3 (TLR3) and STING agonists, respectively. Nine groups of male mice (C57BL/6, 6–8 weeks old) received intraperitoneal injections three times with a mixture of VLP vaccine using different combinations of adjuvants, including CpG ODN, CDN, and poly(I:C). Blood samples were collected from the tail vein two weeks after each injection. Antibody ELISA was employed to assess humoral immunity against each combination of vaccines, with plates coated using in-house recombinant 6P-Spike and commercial recombinant RBD. ELISA results indicated that VLPs combined with CpG plus poly(I:C) and VLPs combined with all three adjuvants induced high levels of total IgG against RecS. Two weeks after the third injection, the animals' spleens were isolated, and cytokine profiles were assessed through an antigen recall assay. As a result, only one group exhibited the expected cytokine profile: VLPs combined with the triple adjuvant combination. This profile demonstrated the requisite Th1-biased cytokine response necessary for vaccine development. This study suggests that the triple adjuvant combination holds promise as a vaccine adjuvant for addressing future pandemics.

Key Words: COVID-19, SARS-CoV-2, Virus-like Particle Vaccine, K3 CpG ODN, poly(I:C), 2,3-cGAMP, CDN, Humoral immune response, Cellular immune response

ÖZET

SARS-CoV-2 VLP AŞISININ TEKLİ, İKİLİ VEYA ÜÇLÜ PATOJENLERE ÖZGÜ MOLEKÜLER ÖRÜNTÜLERDEN OLUŞAN DESTEKLEYİCİ MADDELERLE KARIŞTIRILARAK ELDE EDİLMİŞ FORMÜLLERİN HAYVANLARDA KULLANIMININ İNCELENMESİ

Yasemin Ceylan

Moleküler Biyoloji ve Genetik, Yüksek Lisans

Danışman: İhsan Gürsel

Ağustos 2023

COVID-19 hastalığı ilk olarak Çin'in Wuhan şehrinde görüldü ve Aralık 2019'dan beri hayatımızın bir parçası. İlerleyen zamanlarda Dünya Sağlık Örgütü SARS-CoV-2 enfeksiyonundan oluşan bu hastalığı virüsün bulaş hızı sebebiyle pandemi olarak ilan etti. Artan ölümler ve bulaş hızı aşı geliştirme çabalarını hızlandırdı. İnaktif virüs, mRNA ve altbirim aşı platformları dahil birçok aşı platformu kullanıldı. Bunlardan biri de virüs benzeri parçacık aşıları. Bu aşı platformu virüsün sahip olduğu proteinleri içerirken, genetik materyalini içermemektedir ve üretmesi kolaydır. SARS-CoV-2'ye karşı VLP aşısı üretildi ve Alum ve CpG ODN ile formüle edilen aşı Faz-II aşamasında test edilerek etkinlik düzeyi belirlendi. CpG ODN'e ek olarak, bu çalışmada TLR3 agonisti olan poly(I:C) ve STING agonisti olan 2,3-cGAMP kullanılmıştır. Bu yardımcı maddelerin etkinlikleri ve ilerideki pandemilerde kullanılmak üzere klinik çalışmalar için potansiyellerini test etmek istedik. 6 ila 8 haftalık C57BL/6 hayvanlarından dokuz adet enjeksiyon grubu oluşturuldu ve VLP aşısının CpG, poly(I:C) ve 2,3-cGAMP ile tekli, ikili ya da üçlü olacak şekilde karışımları karın içine enjekte edildi. Her enjeksiyondan iki hafta sonra hayvanların kuyruklarından kanlar toplandı. Her bir grubun hümoral bağışıklık yanıtı antikor ELISAsı ile ölçüldü ve deneydeki plakalar rekombinant 6p-Spike ve Delta+ RBD ile kaplanmıştır. ELISA sonuçları CpG ve poly(I:C)

formüle edilmiş ve üçlü ajanlarla birleştirilmiş VLP aşısının RecS'e karşı güçlü antikor cevapları oluşturduğunu göstermiştir. Son enjeksiyondan iki hafta sonra hayvanların dalakları izole edilip hücrelerin sitokin profilleri belirlenmeye çalışılmıştır. Antikor hatırlatma deneyi sonucunda üç ajanla formüle edilmiş VLP aşısı enjekte edilen grup beklenen sitokin profilini oluştrurmuştur. Bu çalışma gösteriyor ki bu üçlü ajan kombinasyonu ileride klinik çalışmalar için umut vericidir.

Anahtar Kelimeler: COVID-19, SARS-CoV-2, Virüs Benzeri Parçacık aşısı, K3 CpG ODN, poly(I:C), 2,3-cGAMP, CDN, hümoral bağışıklık yanıtı, hücresel bağışıklık yanıtı.

ACKNOWLEDGEMENTS

First, I want to thank Prof. Dr. Ihsan Gursel for allowing me to work with a mind like his. He gave me a chance to work with many valuable people and gain much experience in this academic environment. His support, encouragement, and point of view during my Master's studies helped me to obtain priceless experience.

I want to thank my thesis jury members, Prof. Dr. Haluk Barbaros Oral and Assist. Prof. Dr. Serkan Ismail Göktuna for their valuable time and opinions.

I would also thank all IG lab members, but especially Muzaffer Yıldırım and Tolunay Ataç for their friendship and support. I am also thankful for İrem Fatma Abraş, Pınar Gür Çetinkaya, and Tuğçe Canavar Yıldırım, who stand near me through though times and improve my motivation all the time with their cheerful and supportive attitude. They were my luck during my master's. I will always appreciate their warm heart and wisdom. I am thrilled that our paths crossed. They taught many priceless lessons inside and outside of the lab.

I have special thanks to members of other labs in Bilkent: İlke Sarı, Nurmuhammet Satlykov, Beliz Uzun, Dilan Akdoğan, Yücehan Yazıcı, Umut Tank, Ladin Işık Köse, Ümran Borucu, Pelin Gülizar Ersan, Ünal Metin Tokat, and Oğuzhan Tarman. Without them, my master's would not be this fun and fulfilling. I am incredibly thankful for İlke and Dilan's friendship and valuable insights. I will always be grateful for the time we spent together!

I am grateful to have my best friends, Hüseyin Karabürk and Ezgi June Olgaç. We met with Hüso by our mutual friends, and he became my lifeline. Although we are on different continents and timelines, he was and is there for me at any time. We made and will make fun of everything and laugh til we cry. He is one of a kind, and I am so lucky that he is forever in my life. Regarding Ezgi, we became close in our senior year at METU, and since then, she has opened up her warm heart and became my support system. I love her, her heart, and everything about her. We made many mistakes together, and many more to come!

I want to express my deepest gratitude to my lovely family, mother, Atiye, father, Bedii, and my dearest siblings Yusuf, Mahmut, and our 'kazandibi' Nisa. Their unconditional love and support made me come this far in my life. I am and always will be grateful for having such a great family.

TABLE OF CONTENTS

LIST OF TABLES

LIST OF FIGURES

ABBREVIATIONS

2′3′-cyclic GMP–AMP	2,3-cGAMP
2019-novel coronavirus	2019-nCoV
Acute respiratory distress syndrome	ARDS
A Disintegrin and metalloproteinase domain-containing protein	ADAM
Angiotensin-Converting Enzyme 2	ACE2
Absent in Melanoma 2	AIM2
AIM2-like receptor	ALR
Alkaline phosphatase	ALP
Aluminum hydroxide	Alum
Antigen-presenting cell	APC
Betacoronavirus	β−CoV
B cell receptors	BCR
Bovine serum albumin	BSA
Cathepsin L	CTSL
Cluster of Differentiation	CD
Coronavirus disease 2019	COVID-19
Coronavirus Study Group	CSG
Cytosine poly guanine	CpG
CpG oligodeoxynucleotide	CpG ODN
Cytotoxic T lymphocyte	CTL
Cyclic GMP-AMP synthase	cGAS
C-type lectin receptors	CLR
C terminal Domain	CTD
Cyclic dinucleotide	CDN
Dendritic cell	DC
Dimethyl sulfoxide	DMSO
Deoxyribonucleic acid	DNA
Dulbecco’s Phosphate Saline Buffer	DPBS
Envelope protein	E

Enzyme-Linked Immunosorbent Assay	ELISA
Endoplasmic reticulum	ER
ER-Golgi intermediate compartment	ERGIC
European Centre for Disease and Prevention and Control	ECDC
Fetal bovine serum	FBS
Follicular T cells	Tfh
Fusion peptide	FP
Heptapeptide repeat sequence	HR
Human embryonic kidney-293 fast-transfection	HEK293-FT
Human papilloma virus	HPV
Interferon	IFN
Immunoglobulin	Ig
Interleukin	IL
Interferon-gamma inducible protein	IP
Interleukin-1 receptor-activated kinase	IRAK
Interferon regulatory factor	IRF
Lipid nanoparticle	NLP
Membrane protein	M
Melanoma differentiation-associated protein	MDA
Middle East respiratory syndrome	MERS
Major histocompatibility complex	MHC
Messenger ribonucleic acid	mRNA
Myeloid differentiation primary response gene 88	MyD88
Natural killer	NK
Natural killer cells	NKC
Non-structural proteins	nsp1
Nucleocapsid protein	N
Nuclear factor-κB	NF-κB
N terminal domain	NTD
Neuropilin-1	NRP-1
Nucleotide-binding oligomerization domain	NOD

NOD-like Receptors	NLR
Open reading frame	ORF
Optical density	OD
Phylogenetic Assignment of Named Global Outbreak Lineages	PANGO
Pathogen-associated molecular patterns	PAMP
Peripheral blood mononuclear cell	PBMC
Pattern recognition receptors	PRR
PE-conjugated streptavidin	SA-PE
Polymerase chain reaction	PCR
Plasmacytoid dendritic cells	pDC
Phosphatidylinositol 3-kinases	PI3K
p-Nitrophenyl Phosphate	PNPP
Polyinosinic:polycytidylic acid	poly(I:C)
Red blood cells	RBC
Retinoic acid-inducible gene	RIG
RIG- I-like receptors	RLR
Receptor-binding domain	RBD
Ribonucleic acid	RNA
Double stranded RNA	ds-RNA
Reactive oxygen species	ROS
Room temperature	RT
Replication/transcription complex	RTC
R-phycoerythrin	PE
Spike protein	S
Streptavidin	SA
Severe acute respiratory syndrome coronavirus	SARS-CoV
Severe Acute Respiratory Syndrome Coronavirus-2	SARS-CoV-2
Sodium Dodecyl Sulfate Polyacrylamide Gel Electrophoresis	SDS-PAGE
Stimulator of interferon gene	STING
T cell receptors	TCR
T helper cells	Th

T helper cells class 1	Th1
T helper cells class 2	Th2
T helper cells class 9	Th9
T helper cells class 17	Th17
T helper cells class 22	Th22
Toll-like receptors	TLR
Transmembrane	TM
Transmembrane serine protease 2	TMPRSS2
Tumour Necrosis Factor	TNF
Tumor necrosis factor receptor-associated factor 6	TRAF6
TIR domain-containing adaptor inducing interferon-β	TRIF
Regulatory T cells	Treg
A variant of interest	VOI
A variant of concern	VOC
A variant under monitoring	VUM
Virus-like-particle	VLP
Wild-type	WT
World Health Organization	WHO

CHAPTER 1

INTRODUCTION

1.1. SARS-CoV-2 and COVID-19 Pandemic

In December 2019, a newly recognized ß-coronavirus caused pneumonia cases in the Chinese city of Wuhan. World Health Organization defined it as 2019-novel coronavirus (2019-nCoV) on 12 January 2020. Nearly a month, on 11 February 2020, the WHO named this pneumonia coronavirus disease 2019 (COVID-19), the Coronavirus Study Group (CSG) of the International Committee suggested a name for the new coronavirus; that is, SARS-CoV-2.[1] It showed high transmissibility and caused the deaths of many people. As of April 12, 2023, 762.791.152 people got infected with the virus, while 6.897.025 of those died because of the virus, according to the WHO.[2]

1.1.1. Origin of Severe Acute Respiratory Syndrome Coronavirus 2 (SARS-CoV-2)

As the number of inpatients increased due to COVID-19, the genome of the virus was sequenced immediately and has been shown to have a 96% sequence homology to bat coronavirus[4] that belongs to the betacoronavirus family.[3] Two well-known examples of human-infecting β−CoV are the severe acute respiratory syndrome coronavirus (SARS-CoV) and Middle East respiratory syndrome coronavirus (MERS-CoV). Features of this group of viruses include having an enveloped single-stranded RNA as genetic material[5], which is known to be a causative agent of respiratory tract infections. [6]

1.1.2. Structure of SARS-CoV-2

SARS-CoV-2 consists of a positive sense RNA as the genetic material, about 29.9 kb.[93] It encodes for four main structural proteins, which are spike protein (S), membrane protein (M), nucleocapsid protein (N), and envelope protein (E), and sixteen non-structural proteins (nsp1-16)[7]. Figure 1.1 summarizes the SARS-CoV-2 genome and its structure.[8]

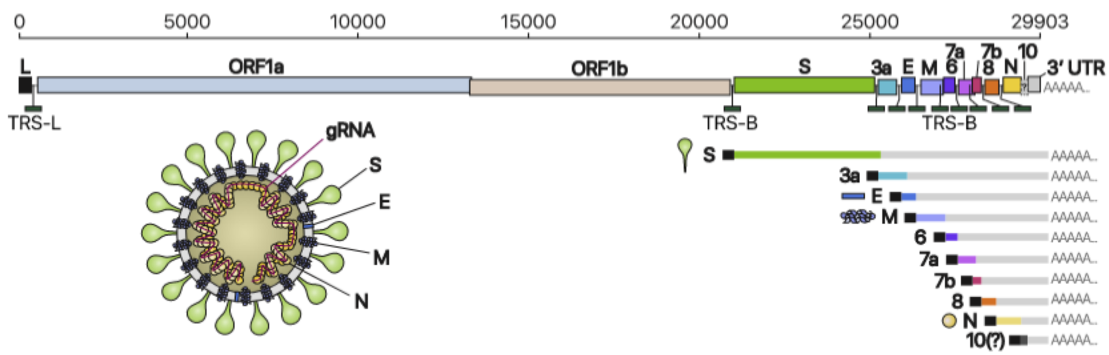

Figure 1.1. Representation of SARS-CoV-2 virion and its genomic architecture.[8]

Gene name	Region (nucleotide positions)	Encoded proteins
ORF1ab	266 – 21555	Polyproteins pp1a and pp1ab that produce the non-structural proteins: leader protein (nsp1), nsp2, nsp3, nsp4, 3C-like proteinase (nsp5A), nsp6, nsp7, nsp8, nsp9, nsp10, RNA-dependent RNA polymerase (RdRP; nsp12), helicase (nsp13), 3′–to–5′ exonuclease (nsp14), endoRNAse (nsp15) and 2′–O–ribose methyltransferase (nsp16)
S	21563 – 25384	Spike glycoprotein (structural protein)
ORF3a	25393 – 26220	ORF3a protein (accessory protein)
E	26245 – 26472	Envelope protein (structural protein)
M	26523 – 27191	Membrane glycoprotein (structural protein)
ORF6	27202 – 27387	ORF6 protein (accessory protein)
ORF7a	27394 – 27759	ORF7a protein (accessory protein)
ORF7b	27756 – 27887	ORF7b protein (accessory protein)
ORF8	27894 – 28259	ORF8 protein (accessory protein)
N	28274 – 29533	Nucleocapsid phosphoprotein (structural protein)
ORF10	29558 – 29674	ORF10 protein (accessory protein)

Figure 1.2. Summary of SARS-CoV-2 genes and respective encoded proteins.[20]

Glycosylated spikes are found on the surface of the virus to bind the angiotensin-converting enzyme 2 (ACE2) receptor on the host cell to facilitate entry into the cell. S protein consists of 1273 aminoacids in which, about 700 of which form the N-terminal S1 subunit, and the remaining amino acids shape the S2 subunit [5] and the roles of these subunits are receptor binding and membrane fusion, respectively. While S2 consists of five primary structures: heptapeptide repeat sequence 1 (HR1), HR2, TM domain, cytoplasm domain, and the fusion peptide (FP), N terminal domain (NTD), and receptor binding domain (RBD) comprise the S1. The trimeric structure of the virus-encoded S protein is uncovered with cryo-electron microscopy and X-ray crystallography.[9] Although homotrimers of the spike are found in an inactive state, upon binding to ACE2 in the host cell, it is cleaved by the host's proteases, such as transmembrane protease serine 2 (TMPRSS2) into S1 and S2 subunits. This first cleavage is a necessary process called priming that enhances the viral entry into the cell and starts the replication process.[35]

The membrane protein is the most abundant viral structural glycoprotein.[10] It is one of the crucial functional components that becomes a platform for the new viral components to be produced by bringing host factors and viral components. Studies have shown that the interactions between membrane protein and other structural components are essential for full viral assembly and efficient viral RNA packaging; the crown-like structure of S.[12,13,14] Envelope protein is a small transmembrane protein like M protein. Although it is produced at high concentrations in the host cell, the amount in the virion envelope is small. This is because it is used in virion assembly and budding in the endoplasmic reticulum (ER), Golgi, and the ER-Golgi intermediate compartment (ERGIC), where intracellular trafficking occurs. Together with membrane protein, they ensure the correct positioning of Spike trimers.[14,15] N protein has separate domains: NTD and CTD. The major role of nucleocapsid protein is to pack viral RNA into ribonucleocapsid particles by recognizing and binding to the genome. Although the exact mechanism is not clear yet, it is known that two domains of the protein use different mechanisms to bind RNA.[16,17,18] Despite their separate roles, studies have shown that the interaction of these structural proteins is critical for efficient virion assembly, trafficking, and virus-like particle formation.[12,14,18]

1.1.3 Mechanisms of SARS-CoV-2 entry into cells

As mentioned earlier, binding of the spike protein on the envelope of the virus to its cognate receptor, ACE2, on the host cell membrane commences the entry. Although it is widely known that RBD is the part binding to ACE2 to facilitate the entry, some studies suggest that NTD also takes part in it, but this needs further studies.[28,29] Two cleavages happen on the S protein. One is at the S1/S2 site involving proproteins convertase furin to separate fusion domains and RBD, while the other is on the S2' site following the ACE2 binding, which is associated with the activity of two major cellular proteases: transmembrane serine protease-2 TMPRSS2 or cathepsin L (CTSL). The latter eases the fusion of the target cell membrane and virus by making the fusion peptides more accessible. In recent studies, additional proteases, such as ADAM10 and ADAM17, are taking part in the cleavage of the spike protein.[94] Neuropilin-1 (NRP-1) has been shown to bind the furin-cleaved S1, thereby enhancing the viral entry via endocytosis.[30] CD147, AXL, KREMEN1, ASGR1, CD209 (CLEC4M), CLEC4G, transferrin receptor, or TIM1 may serve as an alternative to ACE2 receptor for the SARS-CoV-2 viral entry in the cells or tissues where it is not expressed.[6] Although this is not known to be biologically relevant yet, they may have a critical role in the viral entry, as shown in Figure 1.3.

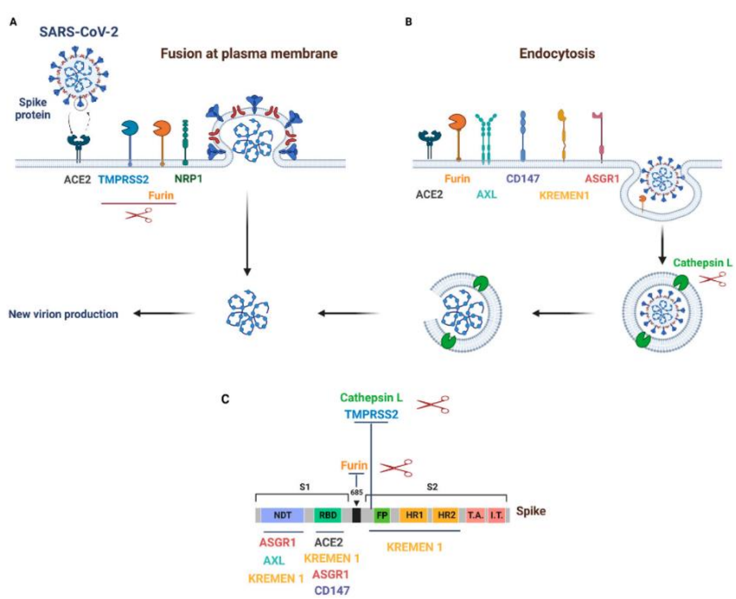

Figure 1.3. Receptors and cofactors that ease the fusion of SARS-CoV-2. Two main mechanisms of entry (**A**) ACE2 and TMPRSS2-dependent fusion of the SARS-CoV-2 with the

host membrane, (**B**) endocytosis of the virus which involves cathepsin L. (**C**) location of the SARS-CoV-2 binding sites of the receptors on Spike protein.[19]

The cleavage between S1 and S2 interface happens at the producer cell during maturation. Upon binding to the host receptor, S1 undergoes a conformational change, exposing the S2' site. Then, the route of entry decides which protease would be responsible for the cleavage of S2'. Two main routes exist to follow for the viral entry: either cell surface or endosomal. When the former happens, TMPRSS2 cleaves the S2' site, whereas it is cathepsin L (CTSL) for the latter case. After the entry, the viral genome is released into the cytosol, followed by transcription and translation of the structural and accessory proteins.[19] Figure 1.4 summarizes the lifecycle of the virus and drugs that may interfere with the cell cycle of the virus at different stages.

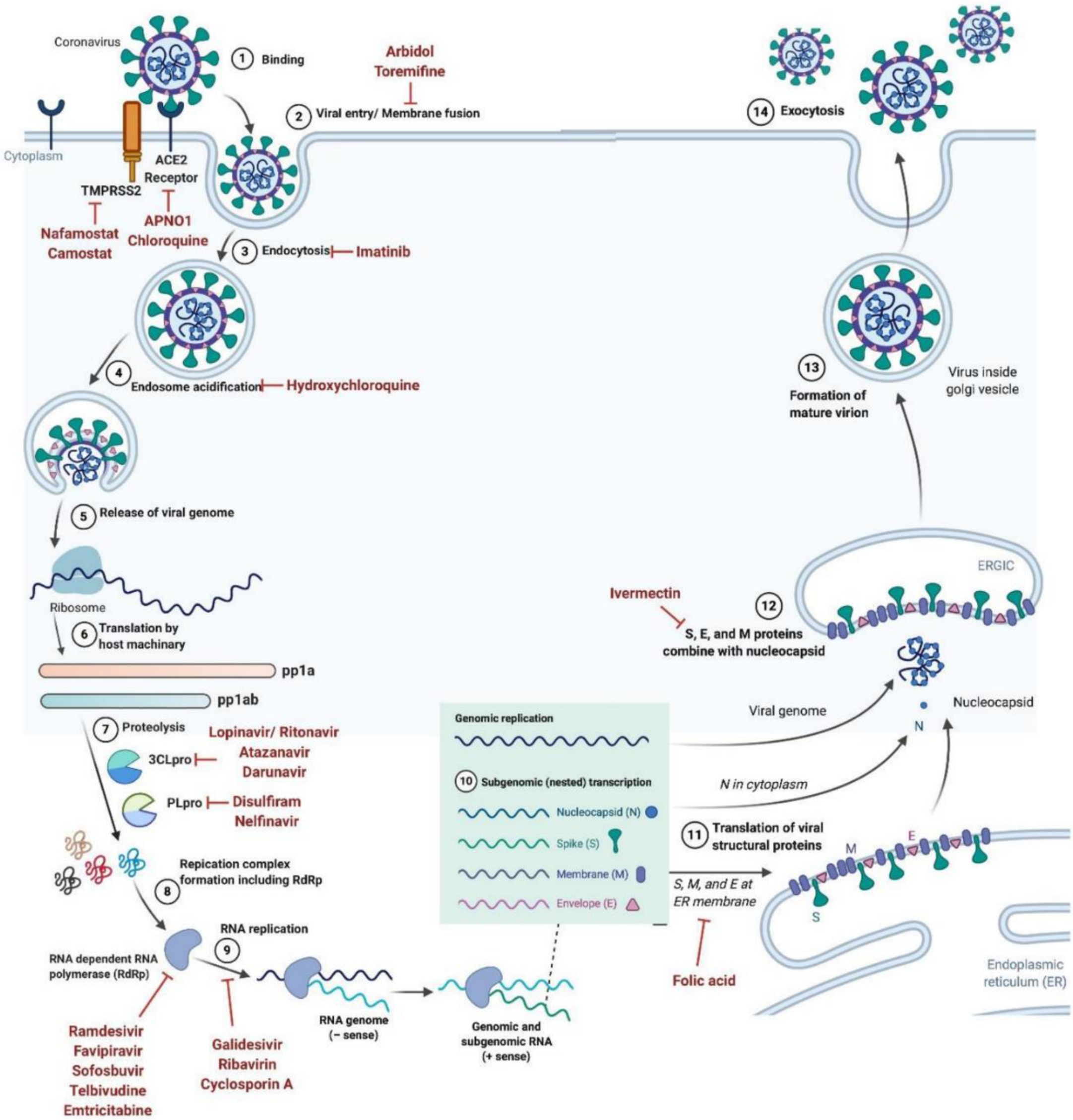

Figure 1.4. **The life cycle of SARS-CoV-2 and drugs interfere with the cycle**.[10]

1.1.4 Transmission and Pathogenesis of SARS-CoV-2

It is determined that the source of COVID-19 is bats from the seafood market in Wuhan, China. However, a study shows there must be an intermediate host before the virus can be transmitted to human since bat-derived CoV hardly infect human.[1] For SARS-CoV-2 to transmit from one person to another, they must be exposed to respiratory droplets bearing the virus. Three ways exist for the exposure to the droplets: (1) breathing in air droplets, (2) contacting mucous membranes containing the virus, (3) transfer of respiratory particles with exposed mucosal areas in the mouth, nose or eye by splashing or spraying.[31]

Clinical features of SARS-CoV-2 vary from one to another ranging from asymptomatic to severe illness that leads to death. Common symptoms of COVID-19 are fever, fatigue, dry cough, muscle and joint pain, and brain fog. In addition to these flu-like symptoms, some may show respiratory failure, diarrhea, and olfactory and gustatory dysfunctions.[32] Since ACE2 is expressed in various cells, those initial flu-like symptoms can develop acute respiratory distress syndrome (ARDS) that might lead to death. In this case, an increase in the viral number would induce hypoxia, and the products are released into the bloodstream, hyperactivating macrophages, T cells, and the complement system. This systemic inflammation can give rise to multiorgan dysfunction resulting in death. Thus, the range in the symptoms indicates the role of the immune system for each individual.[33,34]

1.1.5 Variants of SARS-CoV-2

The expansion of SARS-CoV-2 in humans led to the emergence of various lineages of the virus, thus, making the naming complicated. Although the nomenclature of the virus depends on the source, the two most employed ones are PANGO and WHO nomenclature. The former one makes use of two letters (i.e., A and B), referring to two initial lineages, and numbers are used for the sub lineages that emerged from these initial ones, such as B.1. Numbers are added to the end for each newly produced sublevels, i.e., B.1.1.7. The latter classifies the sublevels and clades based on their relevance to the pandemic. Subsequently, WHO used three main terms to categorize these sublevels: VUM (variant under monitoring), VOI (a variant of interest), and VOC (variant of concern). Greek letters, such as Beta and Delta variants, are used for the nomenclature. [20]

VUM refers to a SARS-CoV-2 variant that might have a potential risk of becoming a VOI or VOC but needs time to assess its potential risks. VOI is a variant with changes in the genome influencing transmissibility, immune escape, therapeutics escape, or disease severity, as well as spreading among significant populations in many countries to represent a possible danger to global public health. In contrast, VOC is a variant that shows association with one or more following points: lessening the effects of current protection methods, therapeutics, vaccines, or diagnostics, destructive changes in the epidemiology of the virus, increased transmissibility, and/ or change in the disease profile in the clinic in addition to meeting the criteria for VOI.[22] Figure 1.5 illustrates the evolutionary history of SARS-CoV-2 variant of concerns.[21]

Currently, there are no VOCs for SARS-CoV-2 meeting the criteria. However, many sub lineages of Omicron are classified as VOI, and their lineages and additional mutations are annotated as BA.2.75 (x), BA.2.75 (x), XBB (z), XBB.1.5-like (a). According to ECDC, three other omicron variants are under monitoring, labeled CH.1.1, XBB.1.16, and XBB.1.5-like + F456L as of 27 July 2023. Since the pandemic has declared over, a new class of variants has emerged, de-escalated variants. The following variants fell into this category based on at least one of the points: (a) the variant has no impact epidemiologically while circulating, (b) the variant does not circulate anymore, or (c) it has been shown scientifically that the variant has no concerning property. These variants include but are not limited to Alpha (B.1.1.7), Delta (B.1.617.2), Epsilon (B.1.427/B.1.429), Beta (B.1.351) variants.[36]

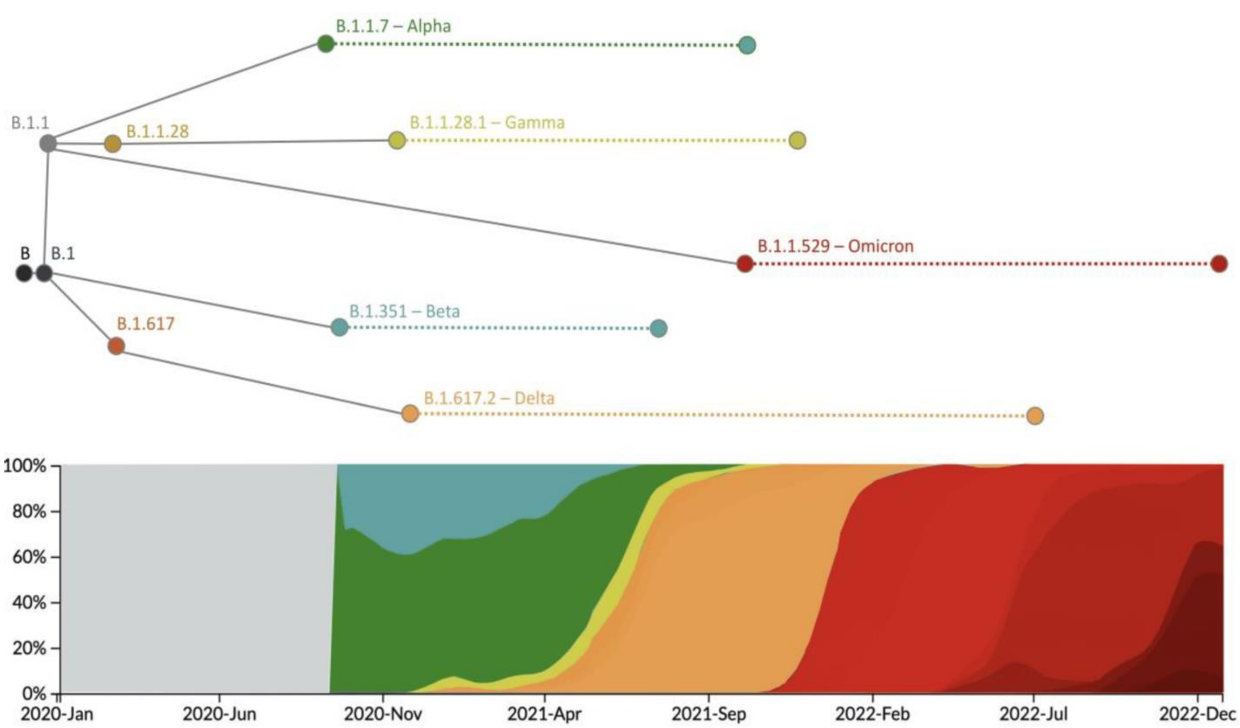

Figure 1.5. Evolutionary history of some SARS-CoV-2 variants.[21]

1.2 Immune System

The human immune system gets invaded continuously by various things that are not recognized as self. The Immune system comprises the molecules, cells, and lymphoid organs protecting the body from these invasions. The immune system is classified into two categories mainly: innate and adaptive immunity, although these interact with each other to fight effectively against invaders (pathogens). Those pathogens are first recognized by innate immune cells, and if not cleared from the system, they are presented to players of adaptive immunity to augment antigen-specific response.

1.2.1 Innate Immunity

Innate immunity serves as the first line of defense against pathogens or pathogen-associated molecular patterns (PAMPs). It includes innate cells as well as epithelial surfaces. Pathogen first encounters epithelial barriers such as skin, gut, lungs, eye/nose/oral cavity, separating the internal milieu from the external world. These barriers not only present mechanical barriers through tight junctions between cells to prevent easy entry of pathogens but also employ chemical and microbiological barriers. Most epithelial barriers are associated with commensal bacteria, nonpathogenic bacteria, which compete with the invading pathogens for the nutrients and sites on the epithelial surfaces. These microorganisms can secrete antimicrobial peptides and antimicrobial enzymes to kill pathogens or weaken their effects. Antimicrobial peptides and enzymes function by digesting bacterial cell walls and lysing the bacterial cell membranes, respectively. This immediate response does not depend on the specific antigen and only protects the body from infection. [23,26]

When the epithelial barriers are breached, innate immunity comes into play. Then, the second part of the response begins, which is to distinguish self from non-self and activate effector cells and inflammation.[37] To recognize pathogen-associated molecular patterns (PAMPs), evolutionarily conserved germline-encoded pathogen recognition receptors (PRRs) are employed. While some PRRs are facing towards extracellular milieu some are located in endosomal compartments. They are classified into two groups: transmembrane receptors and those that reside in intracellular compartments. The former encompasses C-type lectin receptors

(CLRs) and Toll-like receptors (TLRs), while the latter includes retinoic acid-inducible gene- (RIG-) I-like receptors (RLRs), the nucleotide-binding oligomerization domain- (NOD-) like receptors (NLRs), and AIM2-like receptor (ALR).[24,25] Phagocytes located near the breach, unless pathogens are cleared, are activated upon recognizing these PRRs. Then, these cells secrete pro-inflammatory cytokine and chemokine to attract more phagocytic cells to the infection site. After the release of these pro-inflammatory molecules, neutrophils, monocytes, and dendritic cells start to become a bridge between innate and adaptive immune systems as well as phagocyting pathogens.[37,38]

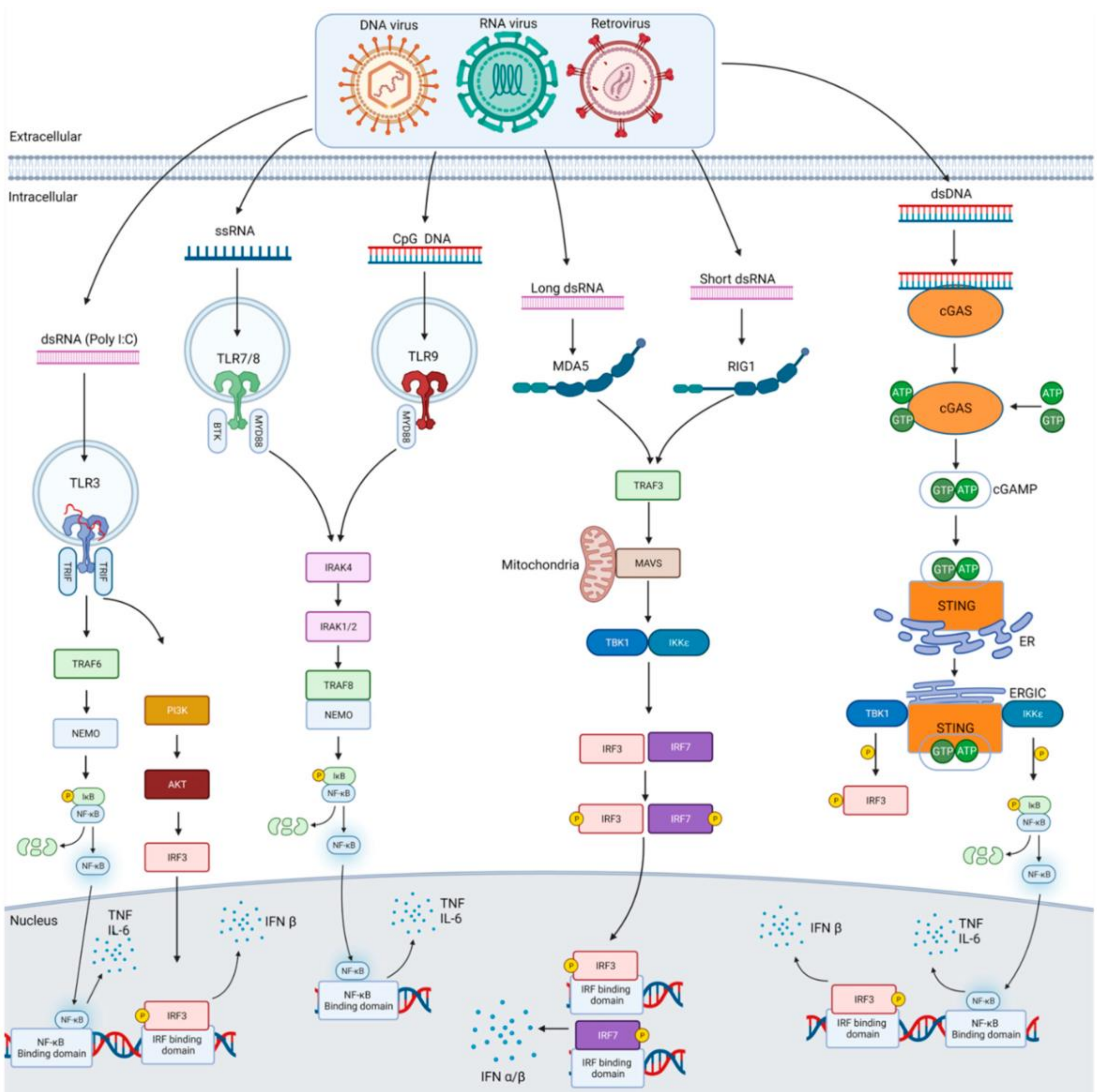

Figure 1.6. Summary of PRRs and their response after recognition of virus.[91]

1.2.1.1 SARS-CoV-2 and its Relationship with Innate Immunity

Innate immunity senses danger signals through PRRs. Recognition of SARS-CoV-2 upon entry is performed by two main classes of cytosolic and endosomal RNA sensors: RLRs and TLRs. The single-stranded viral genome can activate at least six TLRs: TLR2, TLR3, TLR4, TLR7, TLR8 and TLR9. It has been shown that viral structural and nonstructural proteins can be recognized by TLR2 and TLR4 outside the cell.[39] TLR4s in macrophages can identify S1 subunit, while TLR2 can recognize the envelope protein of the virus and initiate the downstream signaling pathways.[39,40,41] TLR3 can recognize double-stranded RNA of SARS-CoV-2 during replication. TLR7/TLR8 can identify genomic DNA released from the virions and signal for the production of proinflammatory cytokines.[42] Although research on TLR9 is still limited, it is known that it is activated when SARS-CoV-2 infects endothelial cells. TLRs signal through two main adaptor molecules, MyD88 and TRIF. Most TLRs employ MyD88 to initiate the downstream signaling to produce proinflammatory cytokines. On the contrary, TLR3, as an exception, signals only through TRIF. As a result of downstream signaling of both adaptor molecules, Type-I interferon and pro-inflammatory cytokines are released, which delays the pathogenesis. RIG-I and MDA-5 recognize viral genomes and signals to produce Type III IFN. Some structural and nonstructural proteins can activate NLRP3 inflammasome and lead to the production of IL1ß and IL18. These cytokines trigger pyroptosis as well as inflammatory cytokine production. In addition to the receptors, as mentioned earlier, cGAS can be activated upon the release of mitochondrial DNA because of SARS-CoV-2 infection damaging mitochondria. Upon cGAS activation, the STING signaling pathway can be employed to produce proinflammatory cytokines. Nonetheless, some accessory proteins can suppress antiviral immunity by inhibiting cGAS-STING signaling. Figure 1.7 summarizes how the TLR, RLR and NLR mechanisms act upon SARS-CoV-2 infection. Even though PAMP recognition is invaluable to fighting SARS-CoV-2 infection, excessive response causes cytokine storms resulting in increased severity of COVID-19. Thus, controlled release of cytokine is important for clearance of the virus and severity of COVID-19.[43-46]

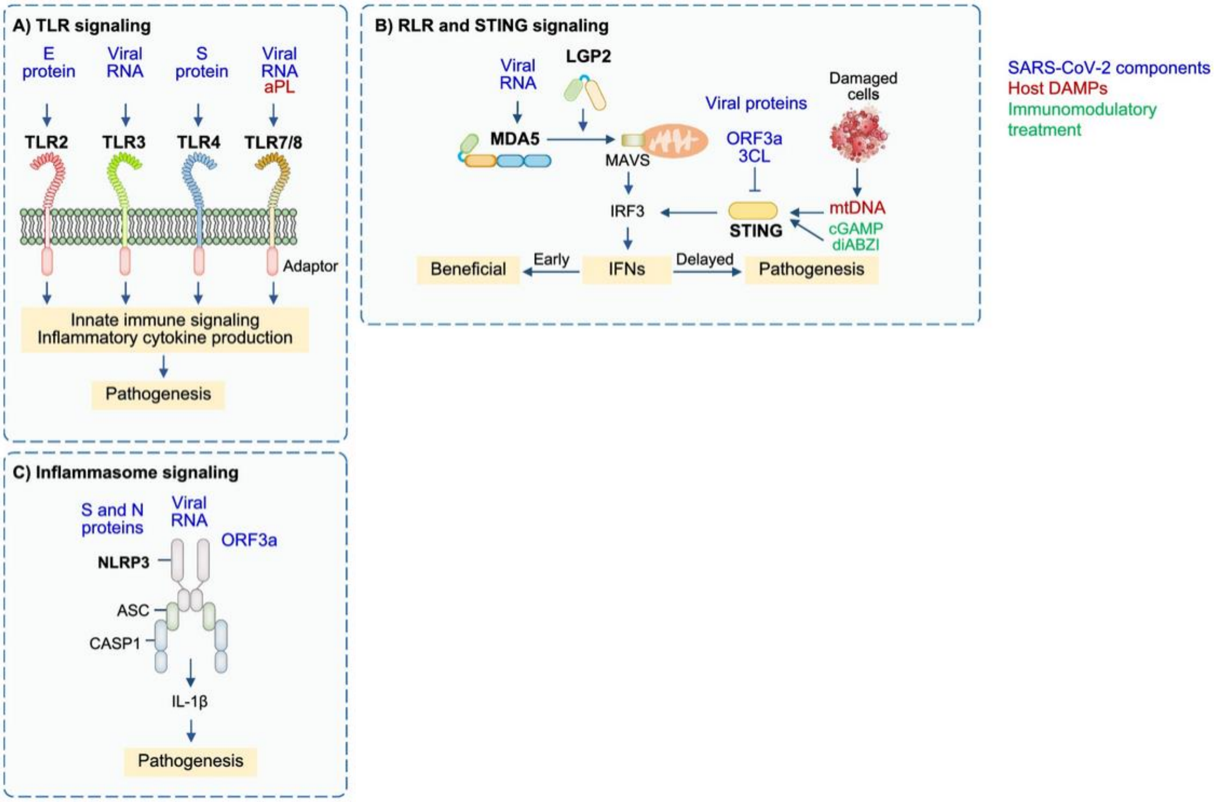

Figure 1.7. Illustration of which part of the virus activates specific PRRs. (**A**) TLR activation, (**B**) RLR and STING activation, (**C**) Inflammasome activation upon infection with SARS-CoV-2.[46]

1.2.2 Adaptive Immunity

Adaptive immunity, unlike innate one, is antigen-specific and produces memory cells to kill the pathogen more quickly when reinfected. It encompasses cellular (T cells) and humoral immune response (B cells). They are employed when all the elements of innate immunity fail to eradicate the pathogen from the body. The bridge between them is antigen-presenting cells (APCs).[27, 28] APCs take up the antigens of a pathogen at the infection site and are drained to secondary lymphoid organs. In addition to antigen, these cells have costimulatory molecules on their cell surface, which act together with the antigen to stimulate naïve T cells to become effectors. On the other hand, B cells require effector T helper cells to produce a proper antibody response.[47]

Two types of major histocompatibility complexes, MHC I and MHC II, are responsible for antigen representation. In comparison, all nucleated cells express MHC I; only macrophages and dendritic cells possess MHC II. An antigen as itself or loaded onto MHC molecules on APC arrives in secondary lymphoid tissues, where naïve T cells reside. The MHC type decides which of two effector classes of T cells will differentiate into either helper T cells or cytotoxic T cells. Peptide complexed MHC I binds to T cells bearing CD4 cell-surface protein and those with MHC II to CD8+ cytotoxic T lymphocytes. The latter is responsible for the most direct action of the T cell; that is, it recognizes cells infected with the virus by binding the antigens displayed on the host's cell surface and kills the cell before the viral replication ends and new viruses are produced. CD4+ helper T cells, in contrast, can function in several ways after they differentiate into effector cells.[48,49]

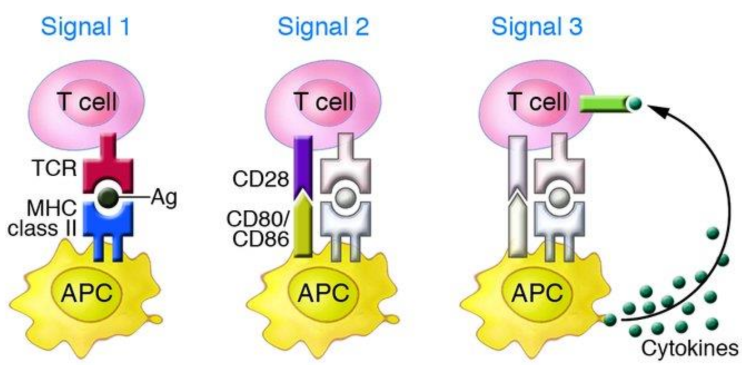

Figure 1.8. Three signals for T cell activation.[49]

Three signals are required for fully differentiated functional T cells. The first signal is the binding of antigen peptide-loaded MHC I/II to T cell receptor (TCR), followed by the existence of a costimulatory molecule on the same APC. The last signal is the appropriate cytokine milieu to induce the differentiation of naïve T cells. Depending on the MHC type and appropriate signals, the effector function of the T cell is decided. CD4+ helper T cells play a crucial role in the activation of macrophages, CD8+ cytotoxic T cells, and stimulation of antibody production by B cells. Figure 1.8 illustrates the three signals required for functional T-cell production.[49,50]

CD4+ helper T cells are classified based on their immunological functions. Th1 cells mainly secrete IFN-γ, a proinflammatory cytokine inducing TLR expression by innate immune cell.

Th1 milieu provides an environment for the B cell class switching to IgG2c in mice C57BL/6. The secretion of IL4, IL5, and IL13 characterizes Th2 cells. These cytokines are mostly known for protection against multicellular parasites and their involvement in allergies and atopic illnesses. IL4 is mainly crucial for B cell plasma differentiation and class switching to IgG1 and IgE, as well as promoting dendritic cell differentiation and maturation. IL5 stimulates antibody production and induces eosinophil differentiation and maturation, whereas IL13 acts as a B cell co-stimulator and inhibits the production of proinflammatory cytokines in monocytes. The other subsets are Th17, Th22, Th9, Tfh and Treg, producing IL17, IL22, IL9, IL21 and IL10, respectively. Their roles vary from immune homeostasis to tissue inflammation. Figure 1.9 summarizes the lineages of Th cells and their roles. In a healthy individual Th1/Th2 ratio should be around one, meaning the homeostasis of the immune system. When the response is th1-skewed, excessive production of proinflammatory cytokine causes tissue damage. On the other hand, a Th2-skewed response may lead to hypersensitivity or atopy. Thus, desired response in vaccines is a Th1-skewed one since it increases the proinflammatory responses of the immune system.[49,51-54]

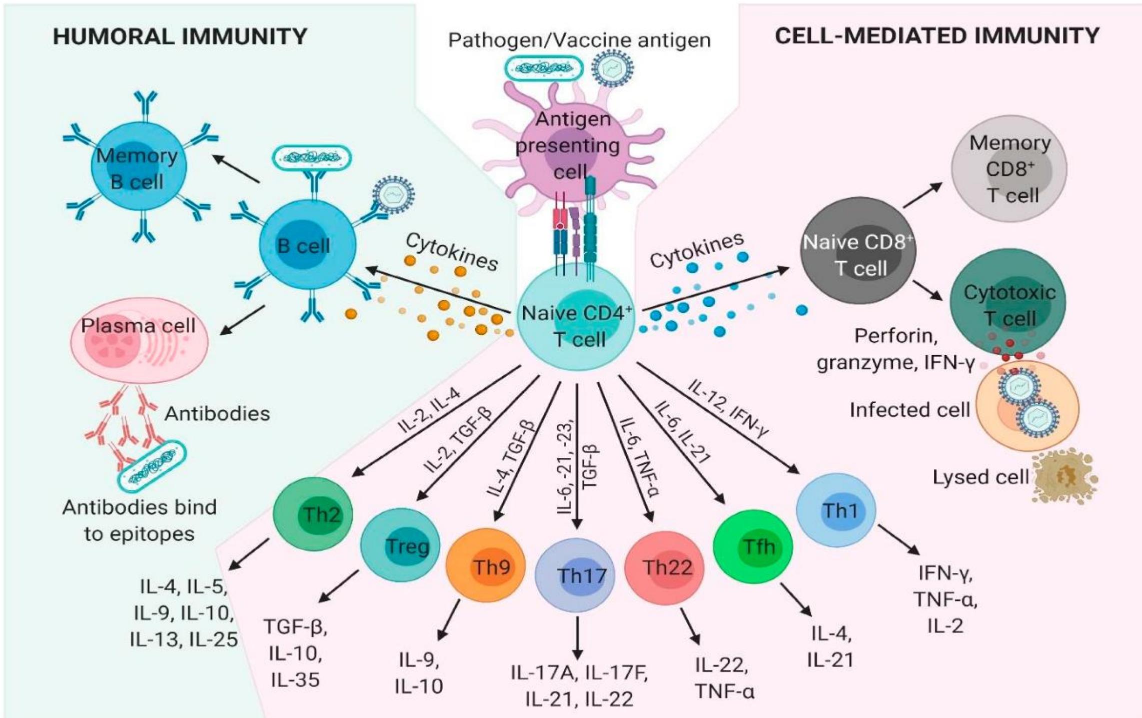

Figure 1.9. Possible humoral and cell-mediated adaptive immune responses upon infection or vaccination.[56]

B cells are responsible for the humoral immune response of the adaptive arm. Naïve B cells are activated by binding an antigen to the B cell receptor (BCR) and then become either plasma cells or memory cells, depending on the cytokine milieu. Primarily IgM, immunoglobulin bearing low affinity, is secreted upon the first encounter with the antigen since production of antigen-specific antibodies takes at least two weeks. After complete differentiation, IgG and IgA are produced because of class-switching, and they have a higher affinity against the antigen. The first encounter with the pathogen leads to memory B and T cell formation and innate immune cells. Thus, the response will be quicker when infected for the second time.[55,56]

1.2.2.1 SARS-CoV-2 and its Relationship with Adaptive Immunity

Many studies revealed the inevitable role of adaptive immunity in the control of SARS-CoV-2. The virus has ways of evading the immune system, but it is handled by the immune system like other RNA viruses. CD4+ T and CD8+ T cells are recruited upon SARS-CoV-2 infection to eliminate virions and control the intracellular pathogen. Studies have shown that S, N, M, nonstructural proteins, and ORF3a proteins are the main targets of T cells. Timing of the T cell response is vital in the determination of the severity of the disease. Impaired Tfh function and germinal center are two factors found in deceased patients showing their importance. In some studies, scientists observed more impaired CD4+ T cells and overexpression of CD8+ T cells in severe COVID-19 patients than in mild patients though the total number of T cells is reduced during infection. These studies show the value of proper immune response. Immediate humoral responses are IgM and IgA, followed by specific IgGs within 7-10 days post-infection. IgG antibodies against RBD are associated with the neutralizing antibody levels of S protein. It has been shown that IgG levels are robust for 20 weeks, which reduces the probability of reinfection with the same pathogen. However, some individuals showed an early decline in the IgG levels in weeks 5-7, while some lasted up to 34-42 weeks. More studies need to be conducted to comprehend how long antibody responses last in symptomatic and asymptomatic patients.[43,45,57,58]

1.3 Vaccines

Vaccines have become one of the most essential tools to prevent infections and their transmission. Since the introduction of the vaccine in the 18th century, development in science has accelerated the number of vaccine availability to humans against many diseases, including cancer. The rapid spread of SARS-CoV-2 increment in deaths revealed the urgent need for vaccines to control the pandemic. Creating protective artificial adaptive immunity is accomplished by a well-formulated vaccine with antigens and proper choice of adjuvant for immune stimulation.[55]

1.3.1 Vaccines against SARS-CoV-2

Many vaccine platforms have been tested since the beginning of the pandemic, including whole pathogen vaccines, protein subunit vaccines, viral and nonviral vector vaccines, virus-like particle (VLP), and nucleic acid vaccines, as depicted in Figure 1.10. Whole pathogen vaccines are either inactivated or attenuated. Inactivated vaccines contain the whole virus killed by heat, chemicals, or radiation.

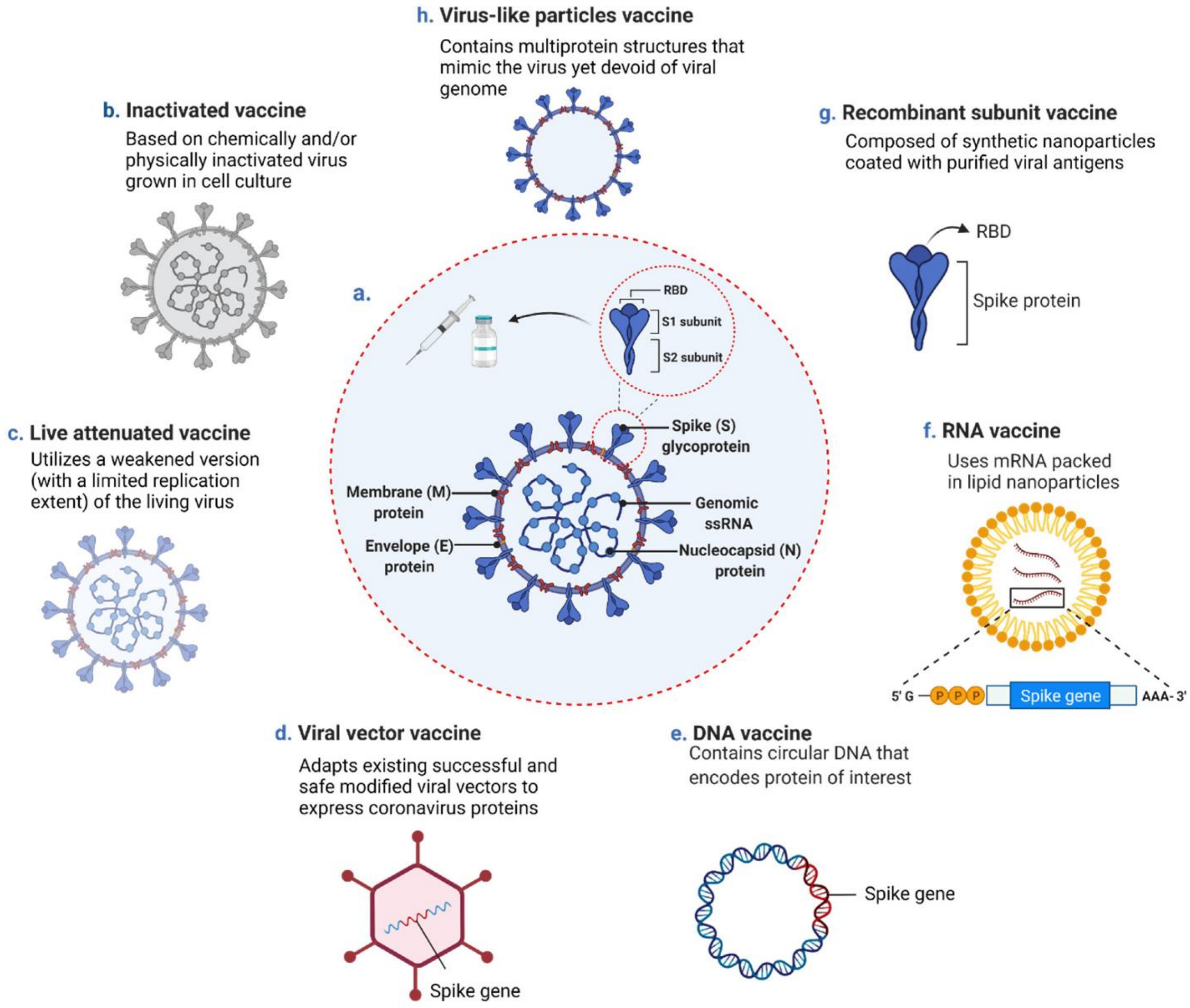

Figure 1.10. Vaccine platforms against SARS-CoV-2[90]

They usually induce less strong and lasting immunity when compared with live-attenuated vaccines. To improve immunogenicity, booster injections, and immunostimulatory adjuvants are employed. 22 inactivated vaccine candidates are in clinical trials for COVID-19. Inactivated COVID-19 Vaccine by SinoPharm BIBP, CoronaVac, and Covaxin are three inactivated virus used vaccines listed for emergency use for COVID-19 by WHO. Live attenuated vaccines contain a weakened form of the pathogen that induces a robust and adequate immune response but does not cause disease. Although they closely mimic natural immunity and do not require immunostimulatory adjuvants, they are unsuitable for immunocompromised people because of the potential reversion to virulence. Two vaccines are under clinical trials for covid19, and none is approved for the market yet.[59,65,67]

Virus' ability to inject their RNA or DNA into host cells and to activate intra- and extra-cellular TLR makes them great candidates for vaccine. The logic is that a non-replicating virus carries the target gene and infects the host cell to augment the immune response. This platform allows proper folding and modification of proteins when introduced into the target cell. Vaxzeria (AstraZeneca) and COVISHIELD (Serum Institute of India Pvt. Ltd) are vaccines using replication-deficient chimpanzee adenovirus vector; JCOVDEN (Ad26.COV2-S) use replication-deficient Adenovirus type 26 to encode SARS-CoV-2 S gene in the host cell, and Convidecia is a single dose Ad5 viral vector-based vaccine produced by CanSino Biologics Inc. 25 non-replicating viral vector vaccines, and 4 replicating viral vector vaccines are in the clinical phase. [60,63,67]

Nucleic acid, DNA, and mRNA vaccines are safer, cheaper, and quicker alternatives to the traditional vaccine. The former is based on inserting the target gene encoding for the target antigen into a plasmid. There is no approved DNA vaccine for human use. The latter vaccine platform delivers messenger RNA encoding for Spike protein in lipid nanoparticles (NLP) for the antigen production in the host resulting in endocytosis of this particle and inducing an anti-viral immune response. COMIRNATY (BioNTech Manufacturing GmbH) original and mixed with Omicron BA.1 nd B.4-5 and SPIKEVAX (Moderna Biotech) are based on this technology and approved by WHO for emergency use in COVID-19. They are all encoded for prefusion stabilized Spike protein to enhance neutralizing antibody response. Due to its high efficacy, 43 out of 183 vaccines in the clinical phase are based on the mRNA platform.[62,64,65,67]

Subunit vaccines are composed of part/s of a pathogen. It can contain one or more antigens to trigger protective immunity. Not including the whole pathogen makes these vaccines suitable for immunocompromised individuals, young children, and the elderly. However, this platform elicits an immune response when introduced with an adjuvant. Two approved vaccines: COVOVAX™ by Serum Institute of India Pvt. Ltd and NUVAXOVID™ by Novavax get the advantage of this technology. They both contain recombinant SARS-CoV-2 Spike protein, but the former is adjuvanted with Matrix-M1 while the latter is with saponin-based Matrix-M. [59,63,67,71]

The high transmissibility of SARS-CoV-2 led to many variants. The mutations mainly occur receptor binding domain (RBD) of Spike protein or on other parts of the Spike; this decreases the efficacy of the approved vaccines since they only contain Spike protein. Virus-like particle vaccines provide a comprehensive antigen presentation and immunogenicity due to their structural similarity to native viruses. One prominent advantage of this platform is lacking virulent components, which makes it safer than whole-pathogen vaccines. Its safety and efficacy can be comprehended by checking already approved Hepatitis B and HPV vaccines. Many virus-like particle vaccines are in clinical phases, but one stands out. It has four structural proteins of SARS-CoV-2, namely S, M, N, and E, and it is adjuvanted with CpG oligonucleotide (CpG ODN) and Alum to skew the response towards Th1. The super-stable hexaproline spike protein with three other structural proteins can provide advantageous humoral immunity and extend the T cell response.[68-70]

1.3.2 Adjuvants

Most immune-evoking vaccines are whole-pathogen since they mimic natural immunity and induce memory B and T cell production. However, those vaccines can induce undesired side effects such as allergic, reactogenic, and autoimmune reactions. In addition, the pathogen gaining its pathogenic features back is another drawback in these whole pathogen vaccines for immunocompromised individuals. That is why the new vaccine technologies are critical to treating infectious diseases and cancer. These technologies may have the antigen to present, but without a costimulatory molecule, they do not induce the desired immunogenicity. This is where proper adjuvant use becomes vital. Figure 1.11 illustrates the timeline of licensed adjuvants for human vaccines. As seen in Figure 1.11, the number of clinically available adjuvants is low compared to the number of antigens. Thus, it became increasingly urgent to discover new adjuvant to support advancement in new vaccine technologies against newly emerging infectious diseases.[72-75]

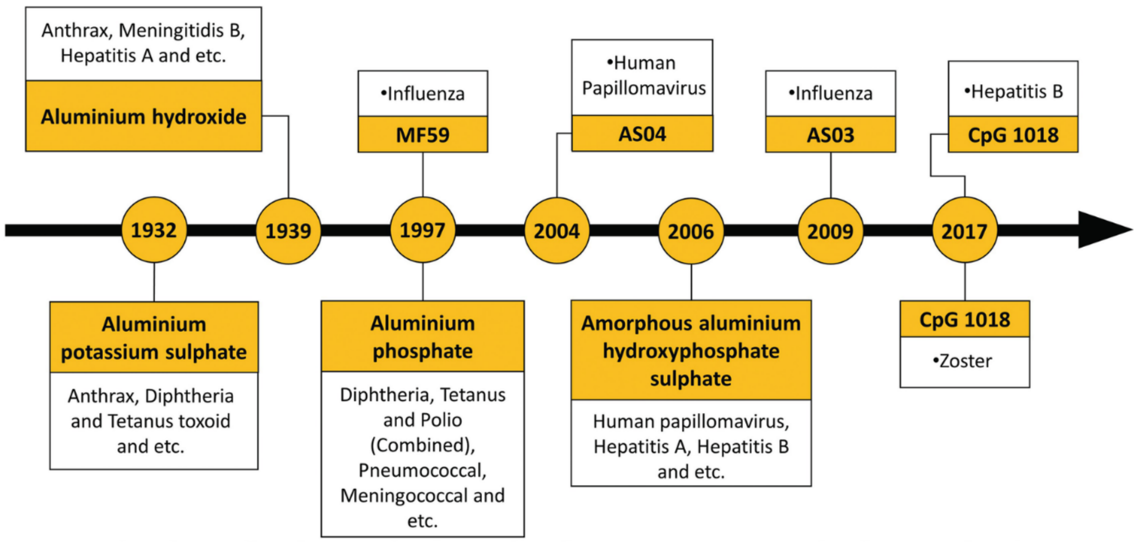

Figure 1.11. Timeline of approved adjuvants used for human vaccine.[77]

Many adjuvants present in today's world are in clinical and pre-clinical phases. In this study, we worked with three of them: K-type CpG oligonucleotide, polyinosine-polycytidylic acid, and 2,3-Cyclic guanosine monophosphate–adenosine monophosphate (CpG, poly(I:C), and CDN thereafter, respectively).

1.3.2.1 CpG ODN

TLR9 recognizes CpG motifs that are present in bacterial DNA. This motif is characterized by a central unmethylated CG dimer flanked by 3’ pyrimidines and 5’ purines. TLR9 is expressed in both B cells and plasmacytoid dendritic cells (pDCs). Recognition of CpG DNA by TLR9 is depicted in Figure 1.6. To summarize, TLR9 activation by CpG recognition leads to the production of proinflammatory cytokines as well as Type I IFNs. This increases the possibility of a more effective presentation of antigen to T cell, which is followed by an increased chance of B cell exposure to antigen. Since TLR9 activation is pivotal in both cellular and humoral immune responses, four distinct classes of the motif are found to mimic these effects: D-type, C-type, P-type, and B- type (K-type). [77,79]

D-type contains palindromic sequences leading to stem-loop structure. Unlike bacterial CpG DNA, it does not affect B cells, but it aids plasmacytoid dendritic cells to mature and induce the secretion of IFNα. This type of CpG ODN remains in the early endosome and interacts with MyD88/IRF-7 complexes inducing the IFNα secretion. C-type ODN contains palindromic sequences, like D-type, enabling it to form dimers or stem-loop structures and consists of phosphorothioate (PS) nucleotides. It can interact with TLR9 in both early and late endosomes. Thus, it induces IFNα production in pDCs and IL-6 secretion in B cells. Due to double palindromes, P-type ODN forms hairpins and concatemer and induces the highest type I IFN response among CpG ODNs. [77,78]

K-type ODN has a prolonged in-vivo half-life due to having phosphorothioate backbone enhancing nuclease resistance. It triggers pDC differentiation for secretion of TNFα and triggers B cell proliferation and IgM secretion. It has been used in clinical trials. K-type CpG ODN favors Th1 biased response. Thus, it supports the activation of NK cells, enhances the cross-priming of CD8+ cytotoxic T cells, and improves robust antibody response. Extensive studies revealed its potential to enhance mucosal immunity and alter the T cell response towards Th1, enhancing cytotoxic lymphocyte response and antibody production. [78,79]

1.3.2.2 Poly(I:C)

One virus-related danger signal is double-stranded RNA. It is recognized by TLR3, and unlike TLR9, its expression of TLR3 is more widely spread, making it a great candidate for vaccination. Even though TLR3 is not expressed in pDCs, TLR3-expressing cells vary greatly from monocyte-derived macrophages to HeLa cells and intestinal epithelial cells. This wide range is both advantage and disadvantage for human use since it may cause autoimmunity and overstimulation of the immune system. Ds-RNA formed during viral replication is recognized by RLR family members such as MDA-5 and RIG-I, leading to the production of Type I IFN as well as proinflammatory cytokines. Several TLR3 ligands, such as Poly(I:C), PIKA and NexaVant (NVT), are under clinical investigation for human use. Some studies revealed that poly(I:C) induces MDA-dependent Type I IFN secretion in non-hematopoietic cells like hepatocytes, essential for DC maturation, NK cell activation, and robust CD4+ T cell immunity. Hence, poly (I:C) is a noteworthy candidate for vaccines to augment Th1-biased immunity and activate innate cells. [80-83]

1.3.2.3 2,3-cGAMP

Pathogenic or aberrant DNA molecules are recognized by cGAS as danger signals since double-stranded DNA is found either within the nucleus or within mitochondria in eukaryotic cells. Upon recognition by cGAS, it promotes the synthesis of 2′3′-cyclic GMP–AMP followed by activation of STING on the ER membrane as illustrated in Figure 1.6. ın response to this activation, several transcription factors are activated to start the transcription of type-I interferon and interferon-stimulated genes (ISG). Several studies suggested that STING, but not cGAS, has an essential part in the eradication of viral infection. As vaccine adjuvant, intradermal injections of CDN, when combined with saponin, enhanced the duration of immune response and protection against the 2009 H1N1 influenza pandemic. Another study showed that chitosan, a naturally occurring adjuvant, induces a Th1-skewed immune response and activates dendritic cells through the activation of cGAS-STING. Thus, all together, these suggest CDN could be a promising adjuvant for vaccines. [85-89]

1.4 Aim and Outline of the Study

The SARS-CoV-2 pandemic first emerged as an outbreak in late 2019 in Wuhan, China. With high transmissibility and an increase in death, scientists worldwide tried to find a treatment. During this process, it was observed that finding a platform that is easy to edit, produce, and cost-efficient and inducing the appropriate immune response for the current and future pandemics is necessary. Approved vaccines and the ones in the clinical trials mainly include only the spike protein of SARS-CoV-2 or its pre-fusion stable version as an antigen. However, new variants have been formed due to high transmissibility. The effectiveness and neutralizing antibody levels of already developed vaccines against the infection have declined with these new variants since the mutations happened on spike protein. This pandemic has also revealed another missing part in immunology: adjuvant. The number of licensed adjuvants is limited for human use, and many antigens can be produced; this limited number of adjuvants narrow the possibilities for clearance of the virus.

Our VLP-58-1023-Al-K3 SARS-CoV-2 vaccine produced strong cellular and humoral immunity, and its most prominent difference from others is it is made up of all four structural proteins of SARS-CoV-2 adjuvanted with CpG and Alum. It is currently being tested in Phase II-III clinical trials. In this study, in addition to CpG ODN, a TLR9 agonist, we aimed to test the efficacy of other adjuvants and their dual and triple combinations to reveal their potential for clinical use. The additional adjuvants were poly(I:C) and a member of cyclic dinucleotides 2,3-cGAMP (CDN hereafter), which are TLR3 and STING agonists, respectively. In this study, we investigated the humoral immunity of C57BL/6 mice in response to the injection of a mixture of VLP with single, dual, or triple adjuvant combinations.

In this context, VLP is mixed with three different adjuvants as single, dual, or triple combinations. Then, these mixtures are given to a group of seven mice intraperitoneally, as mentioned in Section 2.2.1. These mixtures were injected into mice on days 0, 15, and 71, so three injections were performed. The blood from the tail vein of the animal is collected on days 14, 28, 42, 70, 84. The sera of these animals were used for immunogenicity assays like ELISA. Two weeks after the third injection, we collected spleens of animals to measure T cell response with antigen recall assay. We measured humoral and cellular immune responses. ELISA results implicated that VLP combined with CpG plus Poly(I:C) and VLP combined with all three adjuvants induced high levels of total IgG levels against RecS. When compared with placebo and only VLP injected groups, groups injected with VLP adjuvanted with single CpG and poly(I:C), dually with CpG+poly(I:C), CpG+CDN and triple with CpG+poly(I:C)+CDN induces significant IgG2c levels while showing no difference in the IgG1 levels. When checked for the Th1 response by the ratio of IgG2c to IgG1, four groups did not show a Th1-skewed response: placebo, only VLP, VLP adjuvanted with CDN, and VLP adjuvanted with poly(I:C) with CDN injected groups. As a result of the antigen recall assay, only one group showed the expected cytokine profile: VLP combined with triple adjuvants. It shows the expected Th1-biased cytokine profile. This study shows that poly(I:C) and CpG has the potential as vaccine adjuvants as single and/or dual.

CHAPTER 2

MATERIALS AND METHODS

2.1 Materials

2.1.1 Cell Culture Reagents

RPMI medium (5% FBS) was prepared using HEPES buffer, RPMI, non-essential amino acid, sodium pyruvate, heat-inactivated Fetal Bovine serum, and penicillin-streptomycin. Cells were frozen with 10% (v/v) Dimethyl sulfoxide (DMSO) (AppliChem, Germany).

2.1.2 ELISA Reagents

Recombinant proteins and secondary antibodies used in ELISA are given in Table 2.1.

Table 2.1 Recombinant proteins, antibodies, and ELISA reagents used in this study.

Product	Company	Catalog number	Working Concentration
Delta+ RBD Protein	IBG, Turkey	N/A	0.5 µg/ml
Homemade Recombinant SARS-CoV-2 Spike Protein	Bilkent University, Turkey	N/A	5 µg/ml

Goat Anti-Mouse IgG-AP	Southern Biotech, USA	1030-04	1:1000 dilution
Goat Anti-Mouse IgG1-AP	Southern Biotech, USA	1070-04	1:1000 dilution
Mouse IL17a ELISA BASIC Kit (ALP)	Mabtech, Sweden	3521-1A-20	CoatinG: 1 μg/ml Biotin: 1:1000
Anti-mouse IFNγ Coating	Mabtech, Sweden	3321-1A-20	Coating: 2 μg/ml Biotin: 1:1000
Anti-mouse IL4 Coating	Mabtech, Sweden	3311-1A-20	Coating: 2 μg/ml Biotin: 1:1000
Goat Anti-Mouse IgG2c-AP	Southern Biotech, USA	1079-04	1:1000 dilution
SARS-CoV-2 SMNO Peptide Pool	Mabtech, Sweden	3622-1	N/A
Virus-like Particles	Bilkent University, Turkey	N/A	2 μg/well
Streptavidin ALP	Mabtech, Sweden	3310-8	
PNPP Tablets	Thermo Fisher Scientific, USA	34047	1 tablet / 5 ml
Substrate Buffer 5X	Thermo Fisher Scientific, USA	34064	1 ml/plate
Bovine Serum Albumin (BSA)	Capricorn, Germany	BSA-1T	N/A
Sodium Chloride (NaCl)	Isolab, Germany	7647-14-5	N/A
Potassium Chloride (KCl)	Merck, Germany	1.04936.1000	N/A

Potassium Phosphate Monobasic (KH_2PO_4)	Sigma Aldrich, USA	7778-77-0	N/A
Sodium phosphate dibasic dihydrate ($Na_2HPO_4.2H_2O$)	Sigma Aldrich, USA	10028-24-7	N/A
Tween-20	VWR, USA	97062-332	N/A

2.1.3 Ligands

TLR ligands and a STING pathway's ligand, their relative signaling pathways, and working concentrations are listed in Table 2.2.

Table 2.2 Ligands, their relative signaling pathways, and concentrations used in the study.

Ligand Name	Company	Catalog Number	Working Concentration	Signaling Pathway
K3-type CpG ODN	RiboBio	--	30 µg/ml	TLR9
p(I:C)	Invivogen, USA	tlrp-picw	50 µg/ml	TLR3
2’3’-cGAMP	Invivogen, USA	tlrl-nacga23s	5 µg/ml	STING

2.2 Methods

2.2.1 Immunization Studies

All animal studies were conducted with the approval of the animal ethics committee of Bilkent University. Nine vaccine combinations were designed, and one group was assigned as the placebo group (Table 2.3). Groups of male mice (C57BL/6, 6–8 weeks old) were intraperitoneally (i.p.)

injected with 200 µl VLP (5 µg/mouse) formulated with CpG (30 µg /mouse), cyclic dinucleotide (2',3'- cGAMP) (5 µg/mouse) and polyinosinic: polycytidylic acid (poly(I:C)) (50 µg/mouse) on days 15, 29 and 71. Each group had seven animals in the cage at the beginning.

2.2.1.1 Collection of Sera

Mice were bled on days 14, 28, 42, 70, 84. The blood was collected from the tail vein of the animals. About 300 µl of blood were collected in BD microtainer SST blood collection tubes. Only clean sera can be used in further studies, so the collected blood was centrifuged at 2500 x g for 10 minutes. Fresh sera were collected at 0.6 ml Eppendorf tubes and stored at -20°C.

Table 2.3. Animal groups and formulation of vaccine injected into each group for three doses.

Animal Group	Vaccine Formulation
Group 1	PBS
Group 2	Only VLP
Group 3	VLP+CpG
Group 4	VLP+pIC
Group 5	VLP+CDN
Group 6	VLP+CpG+pIC
Group 7	VLP+CpG+CDN
Group 8	VLP+CDN+pIC
Group 9	VLP+CpG+pIC+CDN

2.2.2 Cell Culture

2.2.2.1 Splenocyte Isolation

Spleens were removed from euthanized mice. These spleens were mashed with the plunger end of a 2 ml syringe. After splenocytes were washed twice with 2% FBS which contains complete RPMI media, they were centrifuged at 300 x g for 5 minutes and resuspended with 1 ml 10% FBS containing complete RPMI media. The suspension was taken into flow cytometry to count. 15×10^6 cells/ ml was frozen in 10% DMSO-FBS solution.

2.2.2.2 Stimulation of Splenocyte with VLPs

Splenocytes isolated from C57BL/6 were seeded at 4×10^6 cell/ml on 96-well cell culture plates and stimulated 5 µg/ml VLP or cells were unstimulated. After stimulation for 72 h, supernatant was collected for ELISA analysis of IFN-g, IL4, IL17A secretion.

2.2.3 ELISA

2.2.3.1 IgG ELISA

Maxi binding semi-hydrophobic enzyme-linked immunosorbent assay (ELISA) plates (SPL Life Sciences, Korea) were coated with 50 µl/well in-house recombinant 6p-Spike (0.5 µg/ml) and nucleocapsid (20 µg/ml), commercial recombinant RBD (1 µg/ml), and inactive SARS-CoV-2 virus (5 µg/ml) in PBS at 4°C overnight. The plates were washed five times (3 minutes intervals) with PBS-Tween (0.05%, PBS-T), washed with dH_2O, and then blocked for 3 hours using 200 µl/well (5% BSA- PBS- T solution). Following subsequent washing, 50X diluted mice sera were serially diluted 4X with 5% BSA in PBS-Tween (0.05%, PBS-T) into wells. ALP conjugated anti-mouse IgG (Southern Biotech, USA), anti-mouse IgG1 (Southern Biotech, USA), and anti-mouse IgG2c (Southern Biotech, USA) antibodies were plated at a 1000 X dilution. For the development of the plates, p-nitrophenyl phosphate (PNPP, Thermo, USA) substrate solution (50 µl/well) was added according to the manufacturer's instructions. Consecutive optical density values were measured at 405 nm with a microplate reader (Molecular Devices, USA) for 5 hours.

2.2.3.2 Cytokine ELISA

After stimulating cells with the stimulants indicated in section 2.2.2.2, the plates were centrifuged at 600 x g for 5 minutes, and supernatants were transferred into new plates. Maxi binding semi-hydrophobic enzyme-linked immunosorbent assay (ELISA) plates (SPL Life Sciences, Korea) were coated with anti-cytokine monoclonal antibodies by adding antibodies diluted in 1X PBS at 50 µl/well and incubated overnight at 4^{o}C. After overnight incubation, the wells were blocked with 200 µl blocking buffer (5% BSA, 0.05% Tween-20 in 1X PBS) for 2 hours at room temperature. Plates were washed four times at 3 minutes intervals with wash buffer (0.05% PBS-T) and two times with dH_2O. Then, the supernatants and serially diluted standards were added into wells at 50 µl/well and incubated overnight at 4^{o}C. The plates were washed as described earlier. Biotinylated anti-cytokine monoclonal antibodies that are diluted in blocking buffer were added into the wells at 50 µl/well and incubated for 2 hours at room temperature, followed by a washing step mentioned earlier. Streptavidin-Alkaline Phosphatase (SA-ALP) was 1000 X diluted in blocking buffer and added into wells as 50 µl/well to be incubated for 1 hour at room temperature. After incubation, the plates were washed as described previously. PNPP solution was added as 50 µl/well, which was prepared according to the manufacturer's protocol. Consecutive optical density values were measured at 405 nm with a microplate reader (Molecular Devices, USA) until the recombinant cytokine standards reached saturation. The concentrations of the unknowns were calculated based on the standard curve drawn by the standard values.

2.2.4 Statistical Analysis

One-way ANOVA with Kruskal-Wallis and mixed-effect analysis were employed to determine the significance of the difference among groups (GraphPad Prism version 9, San Diego, California). The statistically significant values were determined as P value below 0.05.

CHAPTER 3

RESULTS

3.1 In vivo Studies

3.1.1 Immunization of C57BL/6 Mice

In order to test the immune potency of VLP combined with three distinct adjuvants individually and their combinations as dual and triple, seven male C57BL/6 mice/immunization group were injected with three doses of the mixtures of vaccines. The first group was a placebo group where they received 200 μL PBS as a vaccine while the second group got 200 μl of 5 μg VLP/animal. The third, fourth, and fifth groups were injected with 200 μl of VLP combined individually with 30 μg CpG, 50 μg polyinosinic: polycytidylic acid (poly(I:C)), and 5 μg cyclic dinucleotide (2',3'-cGAMP) per animal respectively. The sixth, seventh and eighth groups received 200 μl of 5 μg of VLP dually combined with 30 μg CpG+ 50 μg poly(I:C), 30 μg CpG+ 5 μg CDN, and 50 μg poly(I:C)+ 5 μg CDN per mice, respectively. Three injection doses were performed on days 0, 15, and 71. The mice were bled from the tail vein five times to collect the serum. The first bleeding was done 14 days after the primary injection. The second bleeding corresponds to 14 days after the booster injection. The third and fourth bleedings were performed one month and two months after the booster injection. The fifth and last bleeding was done two weeks after the third injection.

3.1.2 Humoral Immune Responses

3.1.2.1 Total IgG Titers of Immunized Mice against Recombinant Spike

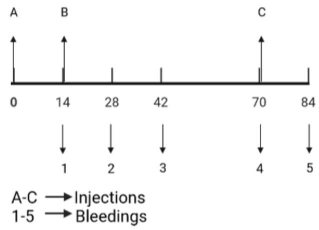

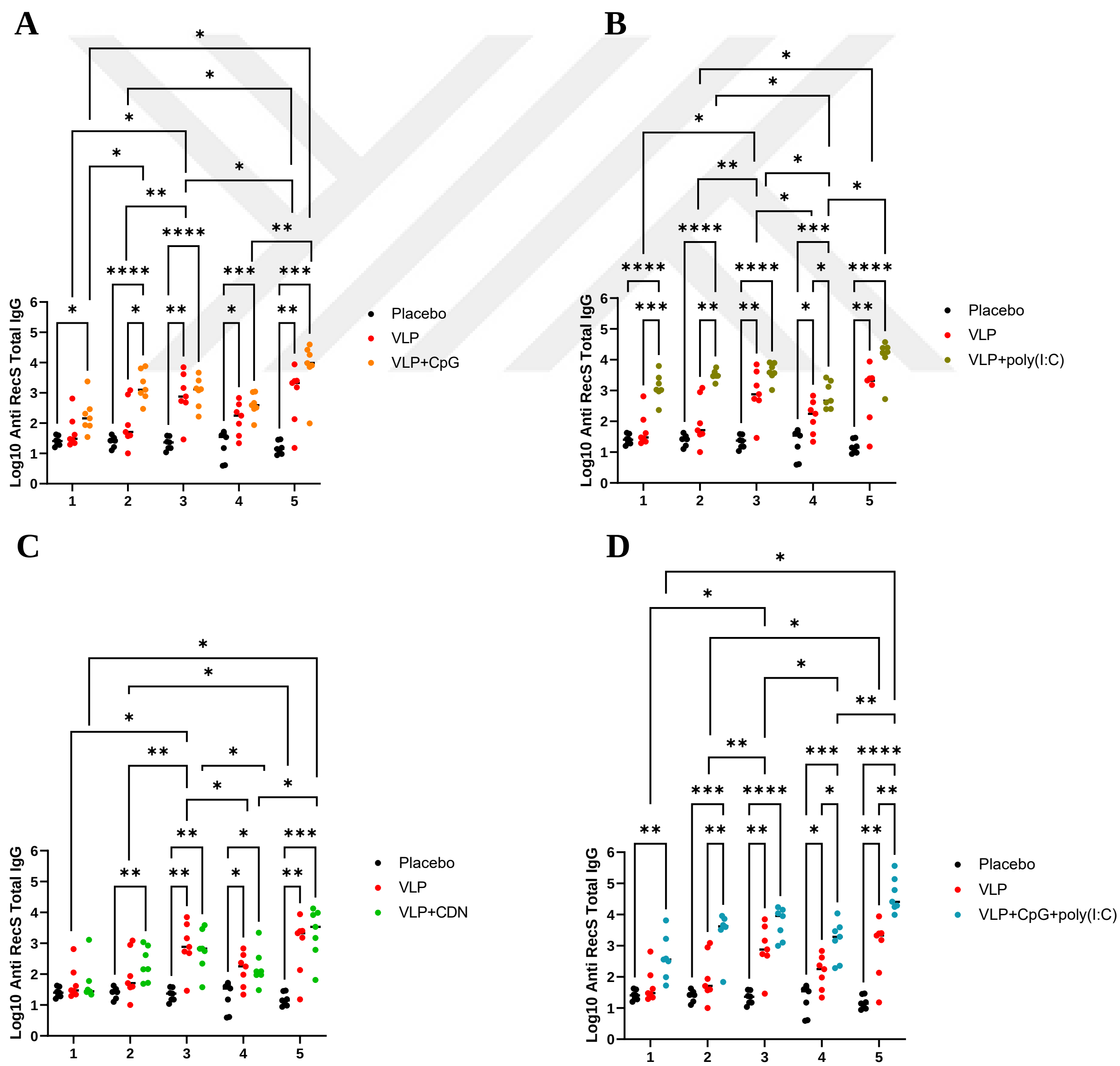

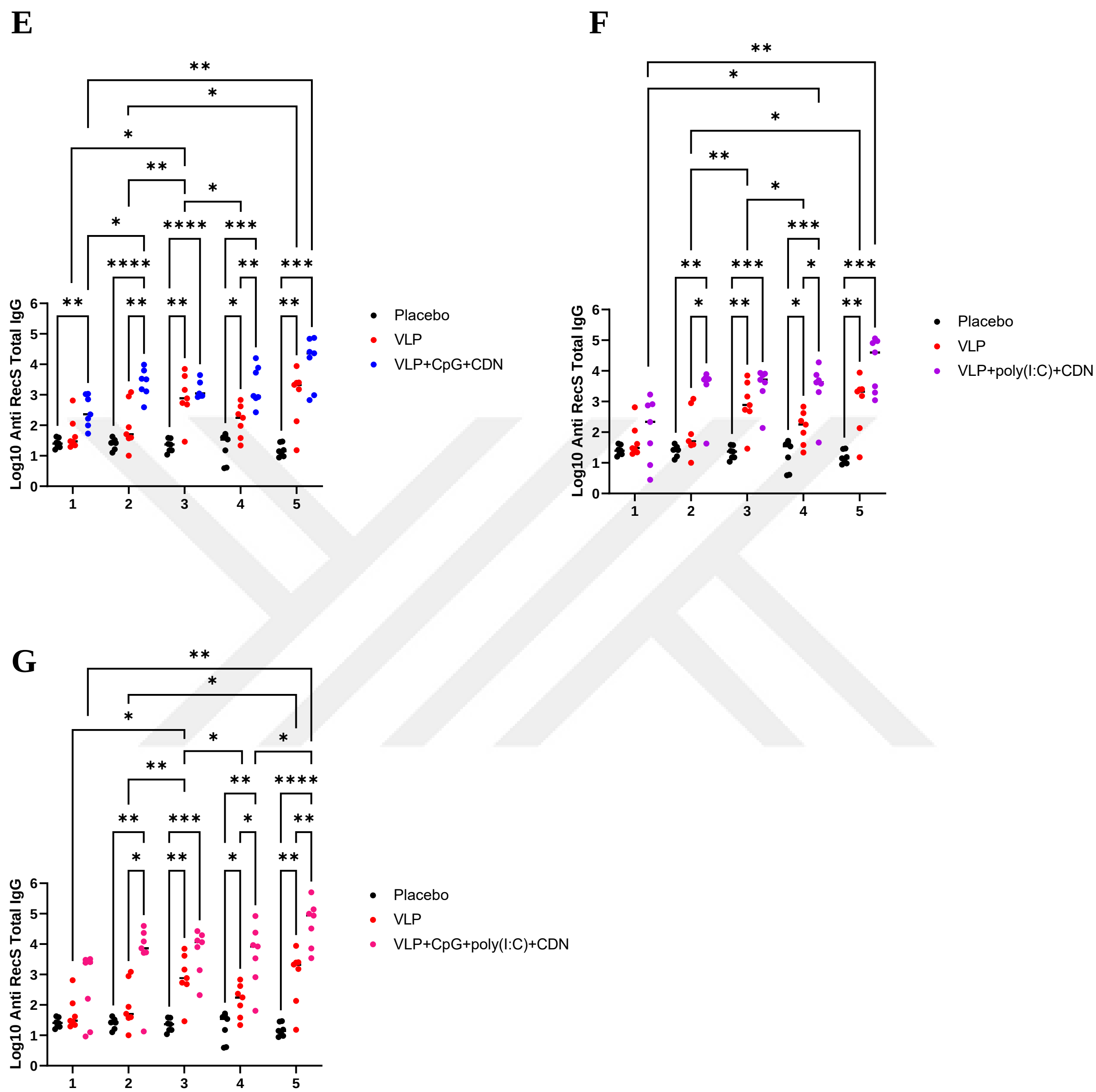

Figure 3.1. Immunogenicity comparison of VLP with single, dual or triple adjuvant combinations with K-type CpG ODN, poly(I:C), and 2,3-cGAMP over time against in-house recombinant trimeric Spike protein. Cellular immune response comparison of male C57BL/6 mice (n=7/group) immunized with placebo, VLP only and VLP with A) individual adjuvant CpG; B) individual adjuvant poly(I:C); C) individual adjuvant CDN; D) combinations of CpG and poly(I:C); E) combinations of CpG and 2,3-cGAMP; F) combinations of CDN and poly(I:C); G) combinations of CpG and poly(I:C) and CDN. Groups were compared with one-way ANOVA with

mixed-effect analysis. *P < 0.05, **P < 0.01, ***P <0 .001, ****P <0 .0001. Numbers on the x-axis represents the bleedings.

We wanted to evaluate the immune response augmented after each vaccination. To measure the levels of humoral response, total IgG, IgG1, and IgG2c levels are measured against the main two immunogens, which are RBD and Spike parts of the virus. These two parts are the most important ones in the evasion of host immunity; that is why the mutations happen primarily on their genes affecting tertiary structure of those parts. Figure 3.1 summarizes the total IgG levels of all nine groups and their comparison to placebo and only VLP-injected groups against RecS. When Figure 3.1 A, B, and C compared, it can be said that the anti-S specific IgG responses of all the adjuvant receiving groups wane off over time whereas only VLP receiving group have a stable profile in terms of antibody response against RecS after the second injection. Thus, Adjuvants alone do not provide significant Anti-S total IgG response as opposed to VLP alone group.

When it comes to dual and triple adjuvant groups which are in Figure 3.1 D to G, contrary to VLP alone anti-S specific IgG response does not wane off for all adjuvant combination groups after the second injection. Upon the third injection strongest immune induction is seen in the CpG+poly(I:C) combination receiving group which is followed by triple adjuvant group. The weakest immune induction is seen in both CpG+CDN and poly(I:C)+CDN, equally. So, Dual adjuvant and triple adjuvant combinations significantly boost anti-S response compared to VLP alone group.

3.1.2.2 IgG1 and IgG2c Titers of Immunized Mice against Recombinant Spike

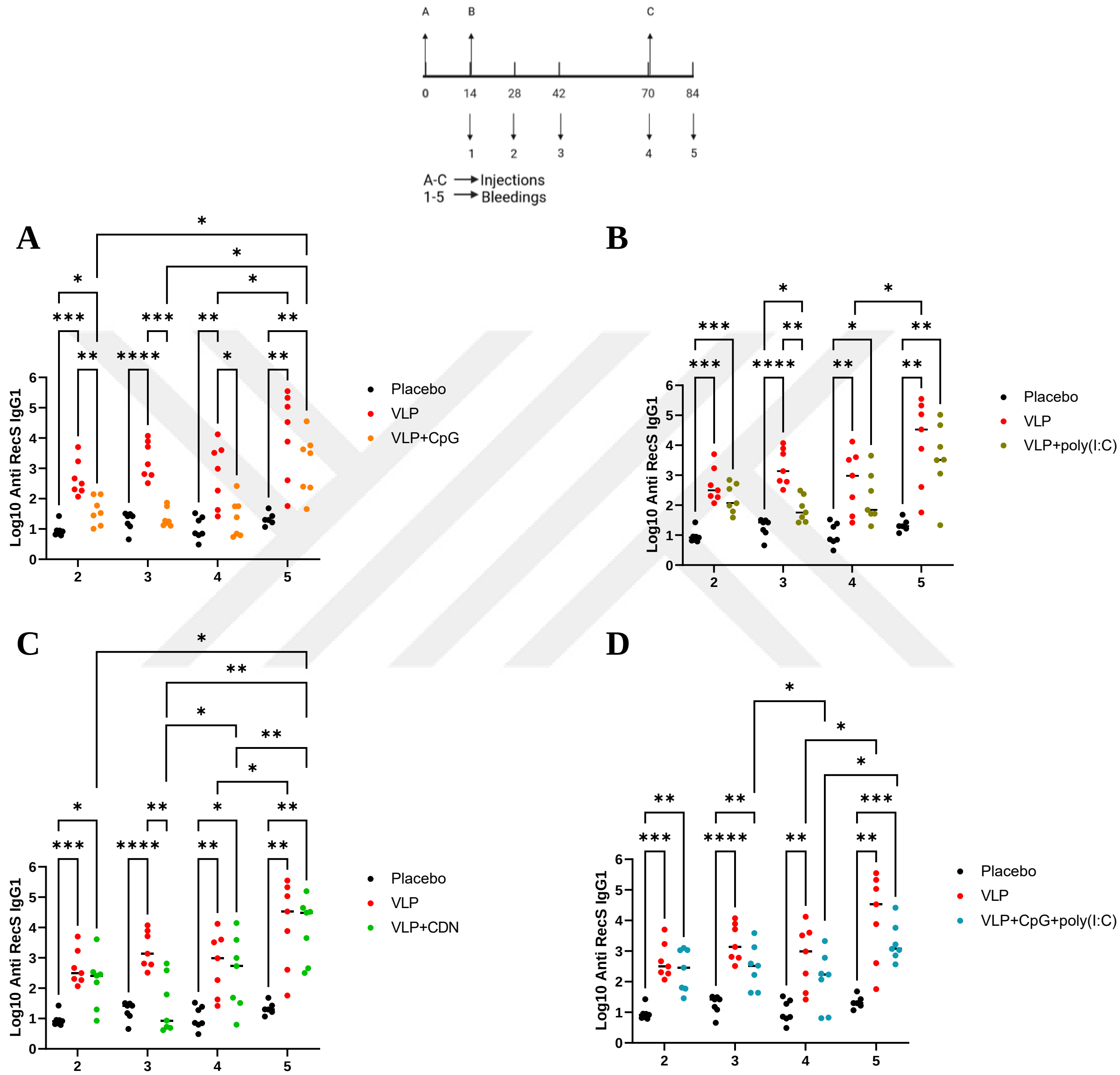

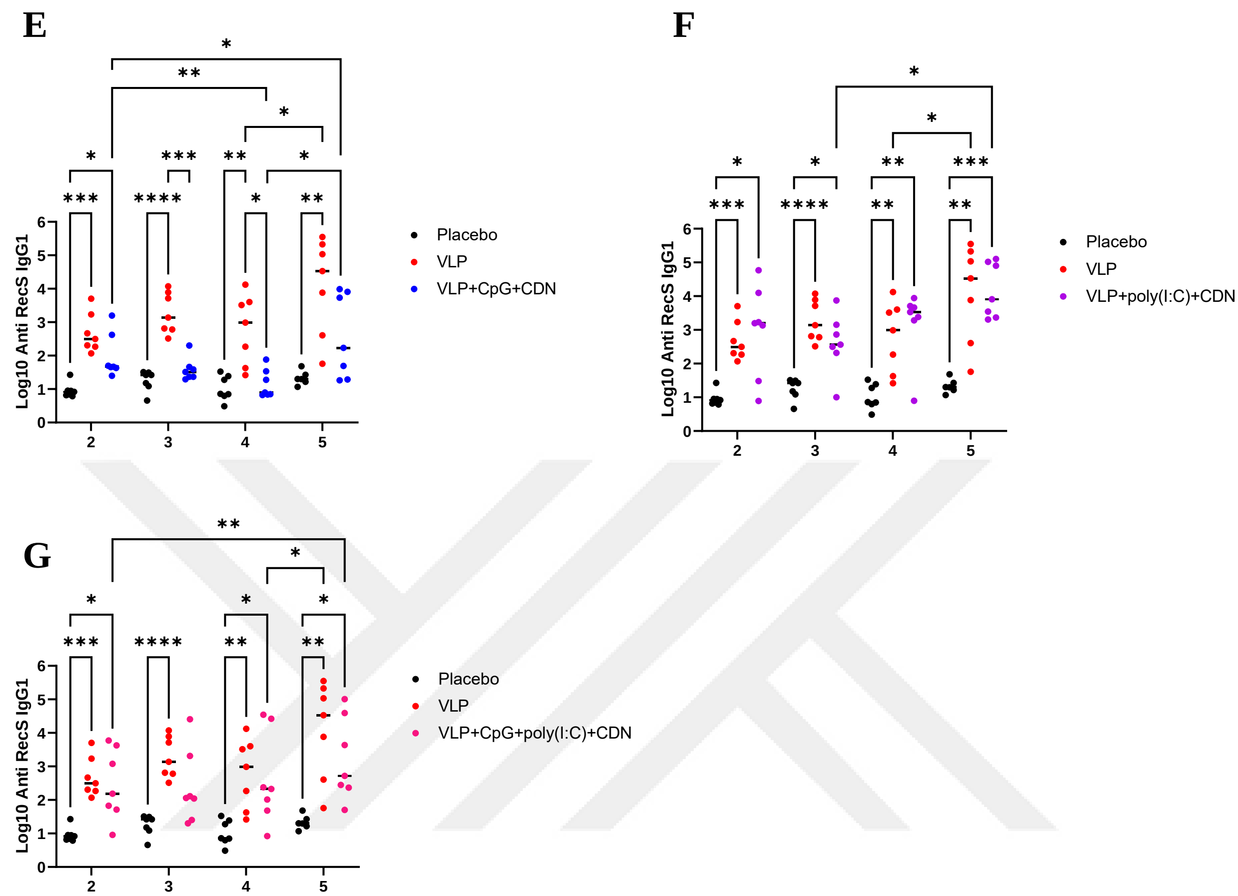

Figure 3.2. IgG1 comparison of VLP with single, dual, or triple adjuvant combinations with K-type CpG ODN, poly(I:C), and CDN over time against in-house recombinant trimeric Spike protein. IgG1 value comparison of male C57BL/6 mice (n=7/group) immunized with placebo, VLP only, and VLP with **A)** individual adjuvant CpG; **B)** individual adjuvant poly(I:C); C) individual adjuvant CDN; D) combinations of CpG and poly(I:C); E) combinations of CpG and 2,3-cGAMP; F) combinations of CDN and poly(I:C); G) combinations of CpG and poly(I:C) and CDN. Groups were compared with one-way ANOVA with mixed-effect analysis. *P < 0.05, **P < 0.01, ***P <0 .001, ****P <0 .0001. Numbers on the x-axis represents the bleedings.

To understand the immunogenicity and efficacy of the vaccine combinations, we performed ELISA to measure the IgG1 and IgG2c values against RecS. Figure 3.2 illustrates the IgG1 values of the injection groups compared with placebo and only VLP injected groups and a comparison of each group over time. Since the adjuvant utilized in the study induces Th1 response in the recipient. After the second injection, anti-S IgG1 responses of single adjuvant injected groups wane off over time contrary to VLP alone group. CDN injected group showed the strongest immune induction two weeks after the third immunization while CpG and poly(I:C) groups showed the weakest induction albeit weaker then only VLP receiving group. Hence, single adjuvants, as expected, do not augment IgG1 specific immune response against RecS compared to VLP alone group.

Figure 3.2 D to G summarizes the anti-S IgG1 responses of dual and triple adjuvant groups. Dual and triple adjuvant groups show a decremental response after the second injection in contrast to only VLP group. These low responses led to an increment in the dual and triple adjuvant groups in the following order from most potent to least: poly(I:C)+CDN, CpG+poly(I:C)+CDN, CpG+CDN, CpG+poly(I:C). However, the increment for any group was weaker than only VLP injected group. As a conclusion, it can be said that dual and triple adjuvant use in VLP vaccine does not induce significantly high IgG1 levels against RecS.

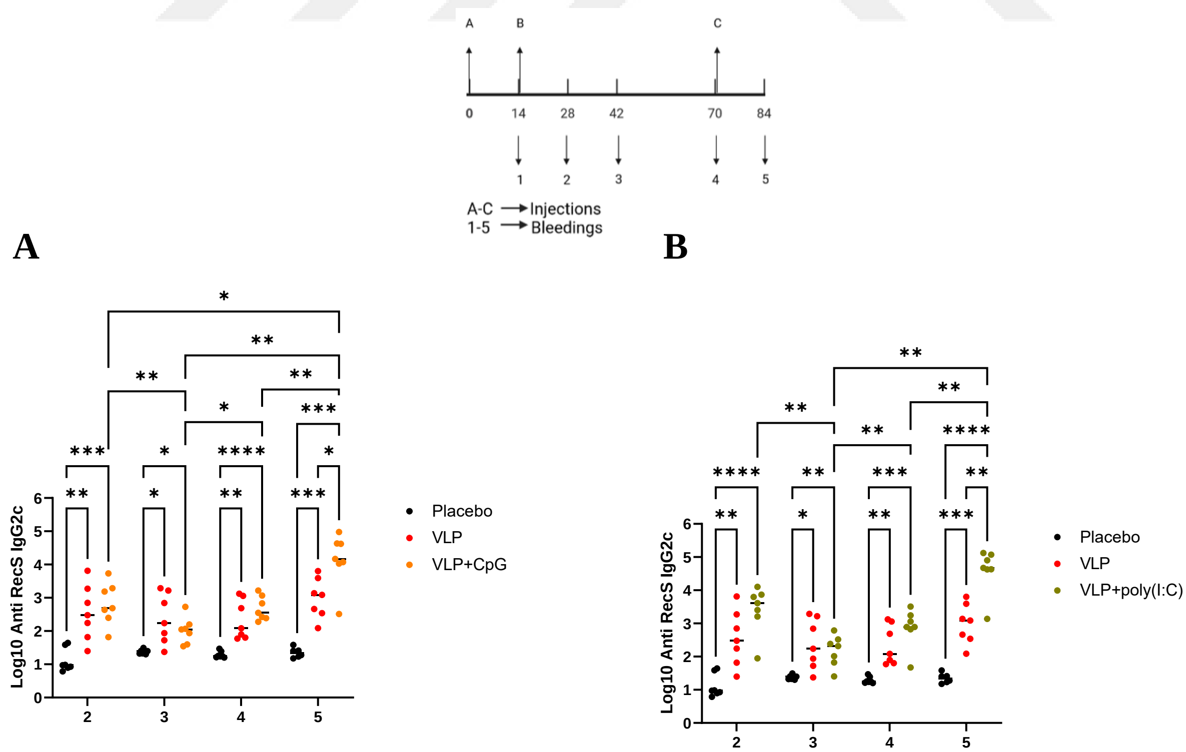

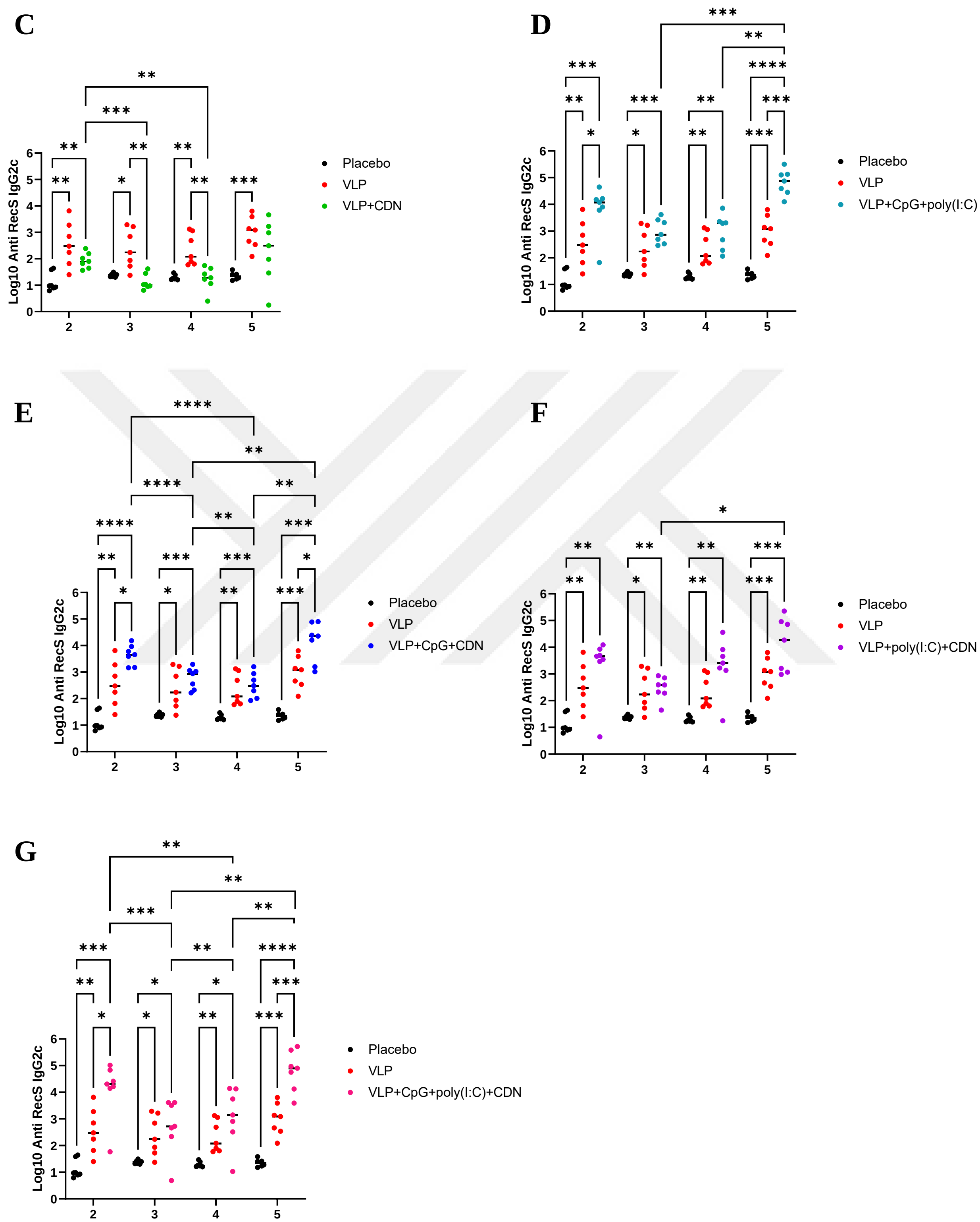
C
D
E
F
G
Log10 Anti RecS IgG2c
Placebo
VLP
VLP+CDN
VLP+CpG+poly(I:C)
VLP+CpG+CDN
VLP+poly(I:C)+CDN
VLP+CpG+poly(I:C)+CDN

Figure 3.3. IgG2c comparison of VLP with single, dual, or triple adjuvant combinations with K-type CpG ODN, poly(I:C), and CDN over time against in-house recombinant trimeric Spike protein. IgG2c value comparison of male C57BL/6 mice (n=7/group) immunized with placebo, VLP only, and VLP with A) individual adjuvant CpG; B) individual adjuvant poly(I:C); C) individual adjuvant CDN; D) combinations of CpG and poly(I:C); E) combinations of CpG and 2,3-cGAMP; F) combinations of CDN and poly(I:C); G) combinations of CpG and poly(I:C) and CDN. Groups were compared with one-way ANOVA with mixed-effect analysis. *P < 0.05, **P < 0.01, ***P <0 .001, ****P <0 .0001. Numbers on the x-axis represents the bleedings.

Figure 3.3 demonstrates IgG2c levels secreted in each injection group and their comparison after each injection. for single adjuvant groups it can be said that there is no distinct difference among VLP and single adjuvant groups with respect to anti-S IgG2c levels after the second injection. Upon immunization for the third time, individually CpG and poly(I:C) injected groups illustrate most potent profile, followed by only VLP group. The least potent one is CDN group. Thus, Individually CpG and poly(I:C) formulated with VLP induces significantly high IgG2c levels against RecS compared to VLP alone group.

Anti-S specific IgG2c responses of dual and triple adjuvant groups depicts a downward trend as the only VLP group on the days following the second injection. This trend is altered by the third time immunization. The most potent groups are triple adjuvant and the dual combination of CpG and poly(I:C) groups. They are followed by CpG+CDN group and then the least potent one is poly(I:C)+CDN group among these combinations. As a result, we can say that adjuvant combinations either dual or triple augmented substantially high IgG2c levels against RecS compared to only VLP group.

3.1.2.3 Total IgG Titers of Immunized Mice against Delta^{+} RBD

Due to being the binding region and enhancing the entry, we measured and compared total IgG levels over time via ELISA against Delta+ RBD. In Figure 3.4, anti-RBD IgG response of only VLP group wanes off while that response of all the single adjuvant groups persists after the second injection. The third injection resulted the most potent response in poly(I:C) and CpG groups, equally. CDN group follows these two groups. Thus, CpG and poly(I:C) groups induce comparable anti-RBD specific IgG to that of VLP alone group. Dual and triple adjuvant combinations demonstrate a similar pattern to single adjuvant groups after the second injection. strongest immune induction is seen in CpG+poly(I:C) group and the rest was lower than this group and equal. So, adjuvant combinations do not provide a selective advantage over VLP alone group against Delta+ RBD.

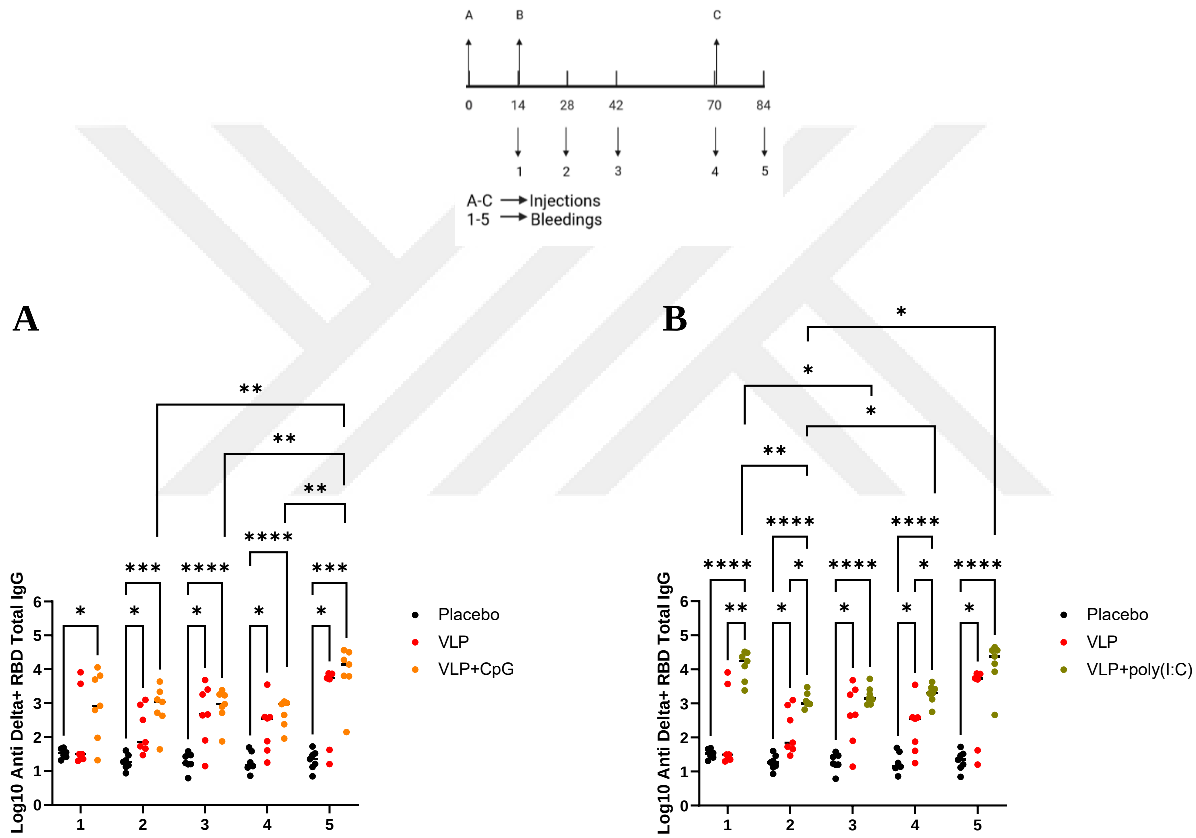

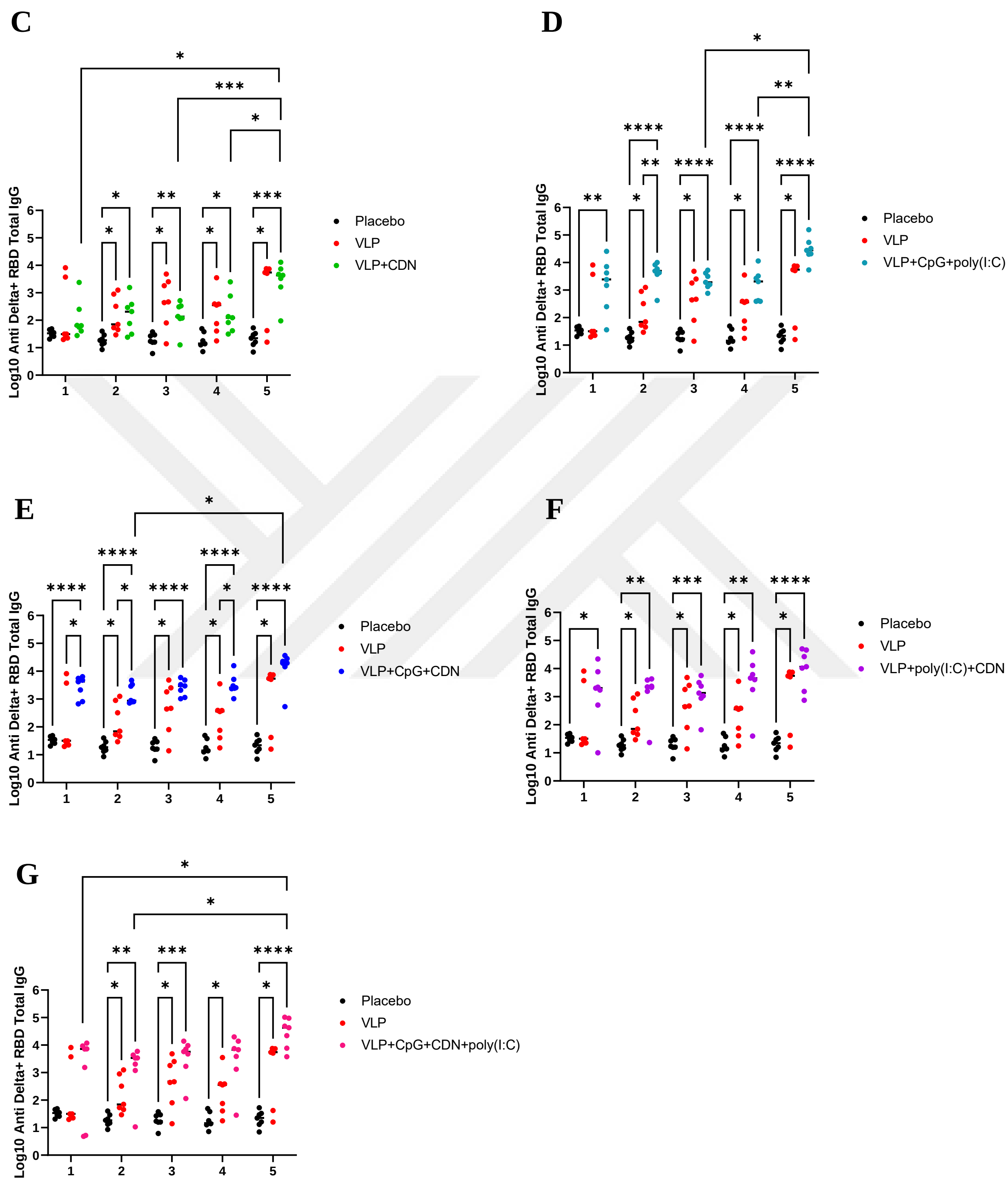

Figure 3.4. Immunogenicity comparison of VLP with single, dual, or triple adjuvant combinations over time against Delta⁺ RBD protein. Cellular immune response comparison of male C57BL/6 mice (n=7/group) immunized with placebo, VLP only and VLP with A) individual

adjuvant CpG; B) individual adjuvant poly(I:C); C) individual adjuvant CDN; D) combinations of CpG and poly(I:C); E) combinations of CpG and 2,3-cGAMP; F) combinations of CDN and poly(I:C); G) combinations of CpG and poly(I:C) and CDN. Groups were compared with one-way ANOVA with mixed-effect analysis. *P < 0.05, **P < 0.01, ***P <0 .001, ****P <0 .0001. Numbers on the x-axis represents the bleedings.

3.1.2.4 IgG1 and IgG2c Titers of Immunized Mice against Delta^{+} RBD

To determine the tendency of the T cell response, we measured IgG1 and IgG2c values of the animal groups. Figure 3.5 illustrates the anti-RBD specific IgG1 responses of all immunized groups and their comparison to placebo and VLP only groups. For single adjuvant groups and only VLP group (depicted in Figure 3.5A-C), anti-RBD specific IgG1 responses are more or less equal after the second time of immunization. Third injection led to the CDN be the most potent group, followed by poly(I:C) and the least potent was CpG group. Single adjuvants, as expected, do not augment IgG1 specific immune response against Delta+ RBD compared to VLP alone group since these adjuvants are Th1-inducing adjuvants. The responses of dual and triple adjuvant groups are not better than the only VLP group on the days following the second injection. Upon the third injection, poly(I:C)+CDN is more potent than CpG+poly(I:C) which has higher potency than both CpG+CDN and CpG+poly(I:C)+CDN groups albeit weaker than VLP alone group.

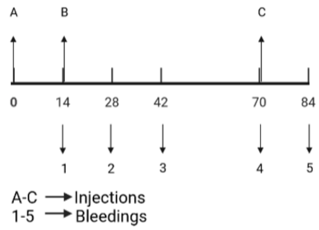
A
B
C
0
14
28
42
70
84
1
2
3
4
5
A-C → Injections
1-5 → Bleedings

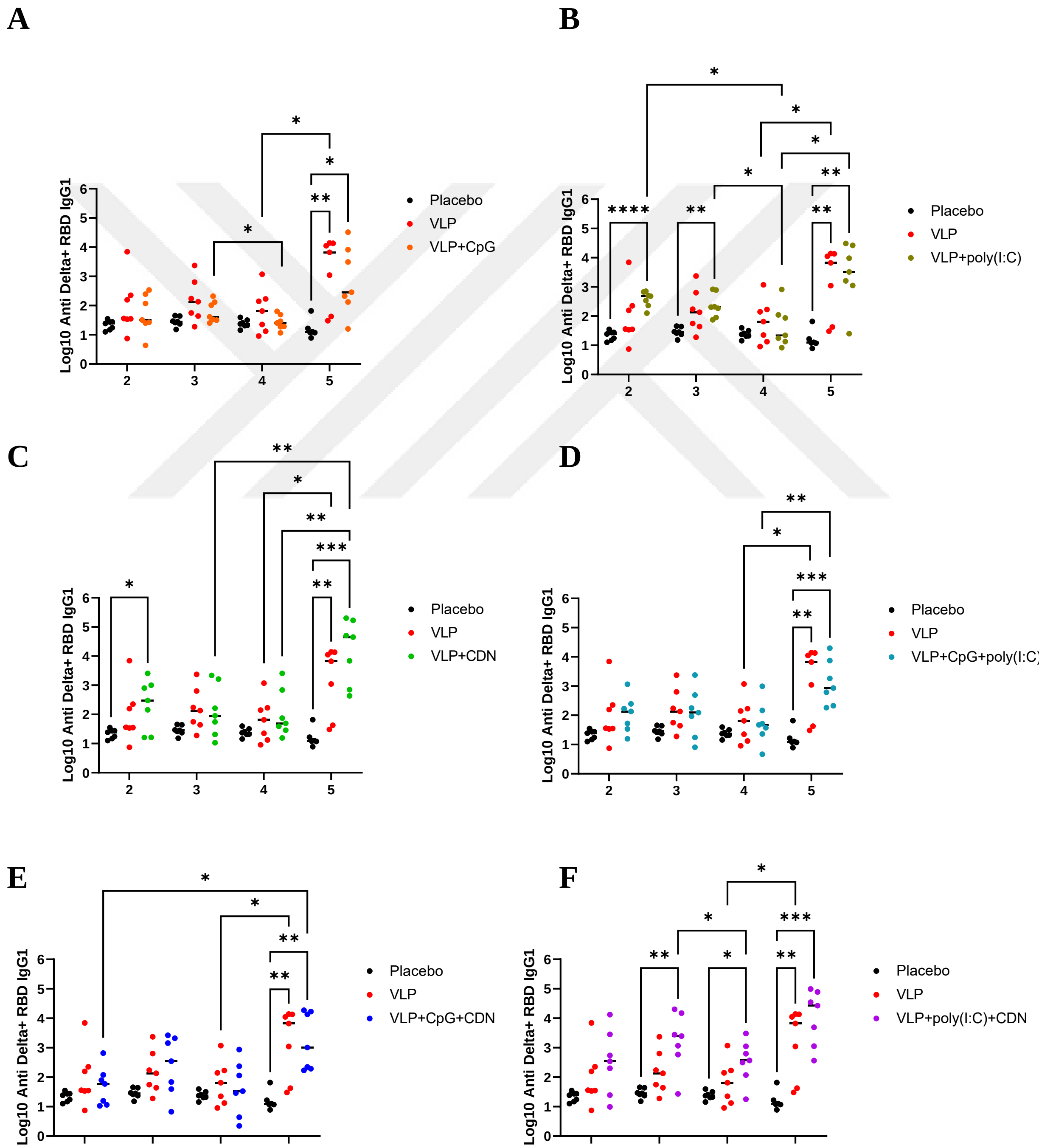
A
B
C
D
E
F
Log10 Anti Delta+ RBD IgG1
Placebo
VLP
VLP+CpG
VLP+poly(I:C)
VLP+CDN
VLP+CpG+poly(I:C)
VLP+CpG+CDN
VLP+poly(I:C)+CDN

G

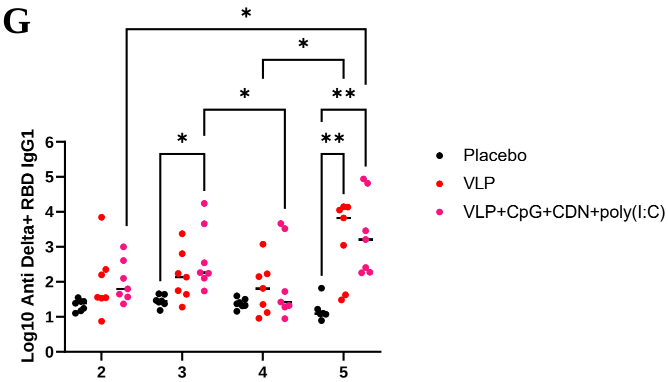

Figure 3.5. IgG1 comparison of VLP with single, dual, or triple adjuvant combinations with K-type CpG ODN, poly(I:C), and CDN over time against Delta$^+$ RBD protein. IgG1 value comparison of male C57BL/6 mice (n=7/group) immunized with placebo, VLP only, and VLP with A) individual adjuvant CpG; B) individual adjuvant poly(I:C); C) individual adjuvant CDN; D) combinations of CpG and poly(I:C); E) combinations of CpG and 2,3-cGAMP; F) combinations of CDN and poly(I:C); G) combinations of CpG and poly(I:C) and CDN. Groups were compared with one-way ANOVA with mixed-effect analysis. *P < 0.05, **P < 0.01, ***P <0 .001, ****P <0 .0001. Numbers on the x-axis represents the bleedings.

IgG2c produced by the vaccination groups against Delta+ RBD is shown in Figure 3.6. Anti-RBD specific IgG2c responses of single adjuvant groups do not wane off contrary to only VLP group on the days following the second injection. The most potent group is CpG group followed by poly(I:C) and the least potent group is CDN. So, CpG and poly(I:C) formulated with VLP show significantly high IgG2c levels against Delta+ RBD. The dual and triple adjuvants produced a response that did not wane off over time after second injection. The most potent group is triple adjuvant group. It is followed by the dual combination of CpG and poly(I:C) and CpG+CDN group and then the least potent one is poly(I:C)+CDN group among these combinations. As a result, adjuvant combinations (dual or triple) augmented substantially high IgG2c levels against RBD compared to VLP alone.

.

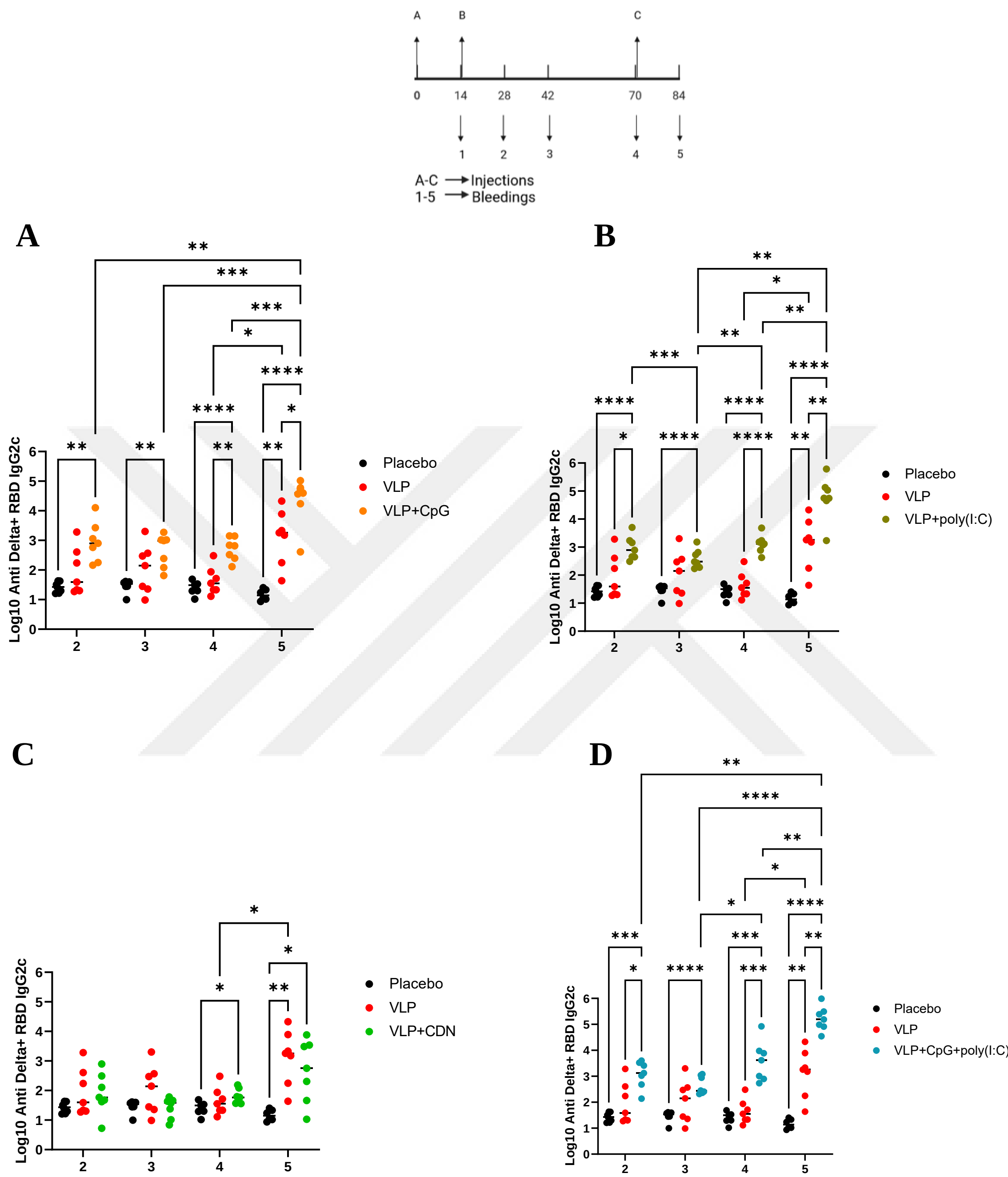
A
B
C
0
14
28
42
70
84
1
2
3
4
5
A-C → Injections
1-5 → Bleedings
A
B
C
D
Log10 Anti Delta+ RBD IgG2c
Placebo
VLP
VLP+CpG
VLP+poly(I:C)
VLP+CDN
VLP+CpG+poly(I:C)

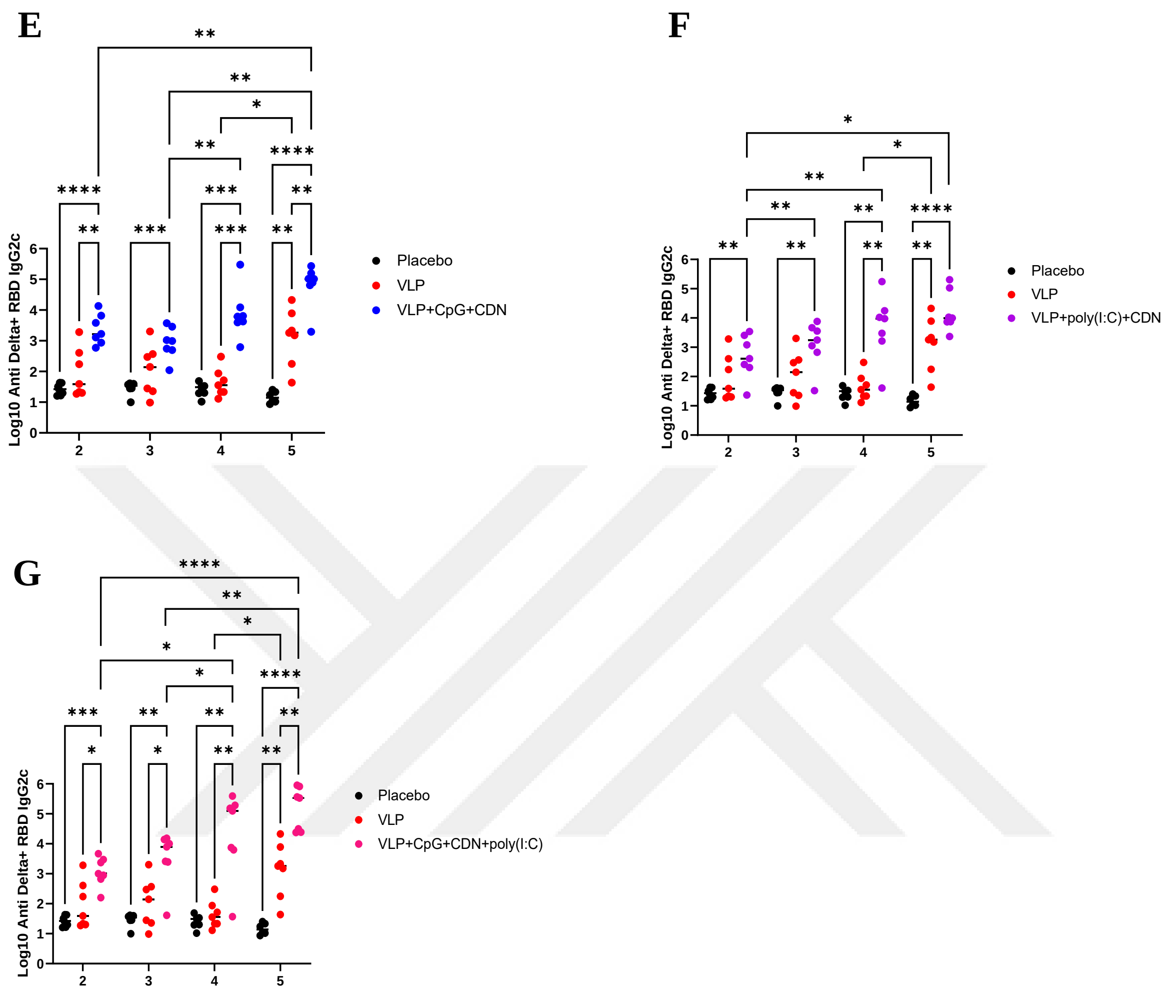

Figure 3.6. IgG2c comparison of VLP with single, dual or triple adjuvant combinations with K-type CpG ODN, poly(I:C), and CDN over time against Delta^{+} RBD protein. IgG2c value comparison of male C57BL/6 mice (n=7/group) immunized with placebo, VLP only, and VLP with A) individual adjuvant CpG; B) individual adjuvant poly(I:C); C) individual adjuvant CDN; D) combinations of CpG and poly(I:C); E) combinations of CpG and 2,3-cGAMP; F) combinations of CDN and poly(I:C); G) combinations of CpG and poly(I:C) and CDN. Groups were compared with one-way ANOVA with mixed-effect analysis. *P < 0.05, **P < 0.01, ***P <0 .001, ****P <0 .0001. Numbers on the x-axis represents the bleedings.

3.1.2.5 Evaluation Ratio of IgG2c over IgG1 of Immunized Mice against Recombinant Spike and Delta+ RBD

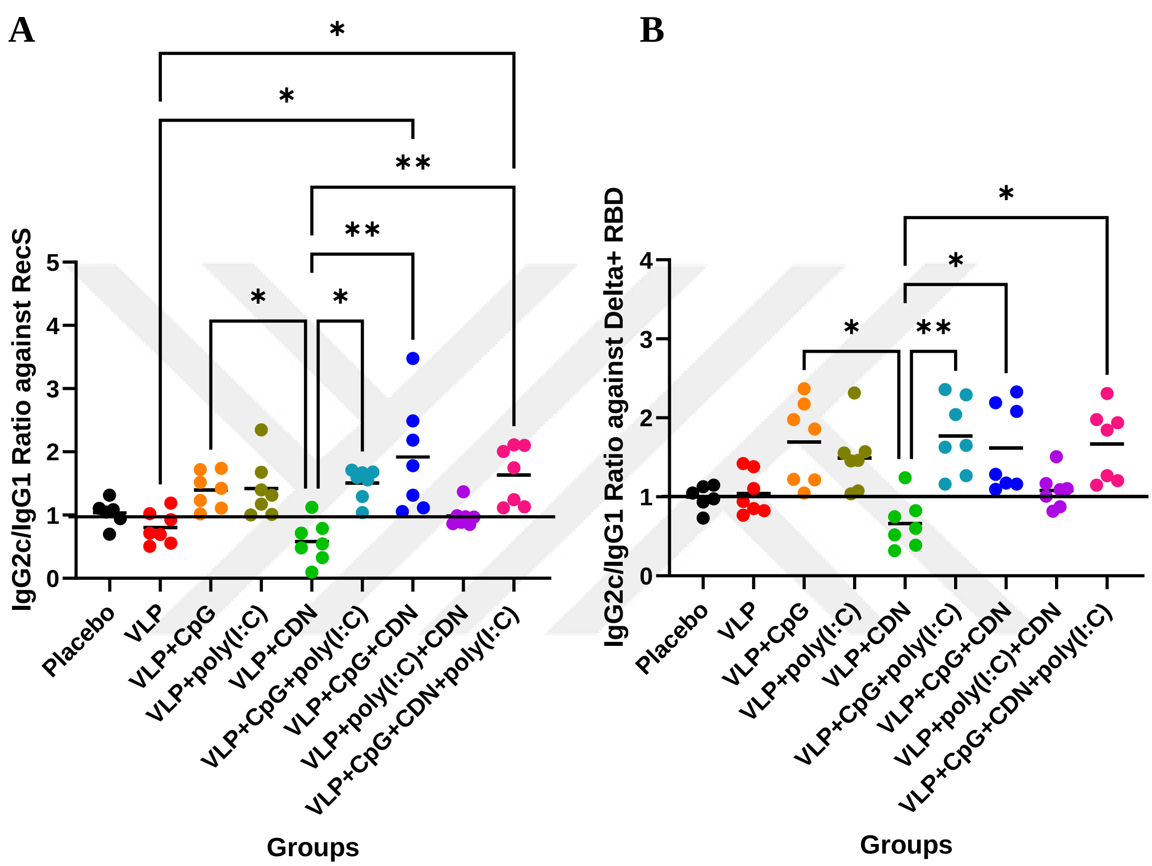

Figure 3.7. Th1 responses of the groups of mice injected with VLP with single, dual or triple adjuvant combinations with K-type CpG ODN, poly(I:C), and CDN and their comparison among themselves against in-house recombinant trimeric Spike and Delta+ RBD protein two weeks after third dose. IgG2c to IgG1 ratio of each injection group compared with others against (A) in-house recombinant trimeric Spike and (B) Delta+ RBD protein. Groups were compared with one-way ANOVA with Kruskal-Wallis test. *P < 0.05, **P < 0.01, ***P <0 .001, ****P <0 .0001.

To assess the tendency in the vaccination groups, we calculated the ratio of IgG2c to IgG1 of each mouse in each group. Figure 3.7 shows these ratios against RecS (A) and Delta+ RBD (B). In the right part of the figure, the placebo and VLP+CDN+ poly(I:C) injected groups have a Th1 ratio close to 1, while only VLP injected and VLP+ CDN injected groups tend to show Th2 biased profile. Even though the remaining groups have ratios higher than 1, the ratios of VLP+ CpG+ CDN and VLP+ CpG+ CDN+poly(I:C) injected groups are significantly high compared to only the VLP-injected group of mice.

Figure 3.7B illustrates the ratio of IgG2c levels to IgG1 levels against Delta+ RBD. Herein, we see a similar pattern for placebo, only VLP injected, and VLP+ CDN injected groups in Figure 3.7A. However, there is no significant difference between the adjuvant-used groups and placebo and only VLP injected groups.

3.2 In vitro Studies

3.2.1 Evaluation of IFNγ, IL17A and IL-4 Producing Splenocytes with Antigen Recall Assay

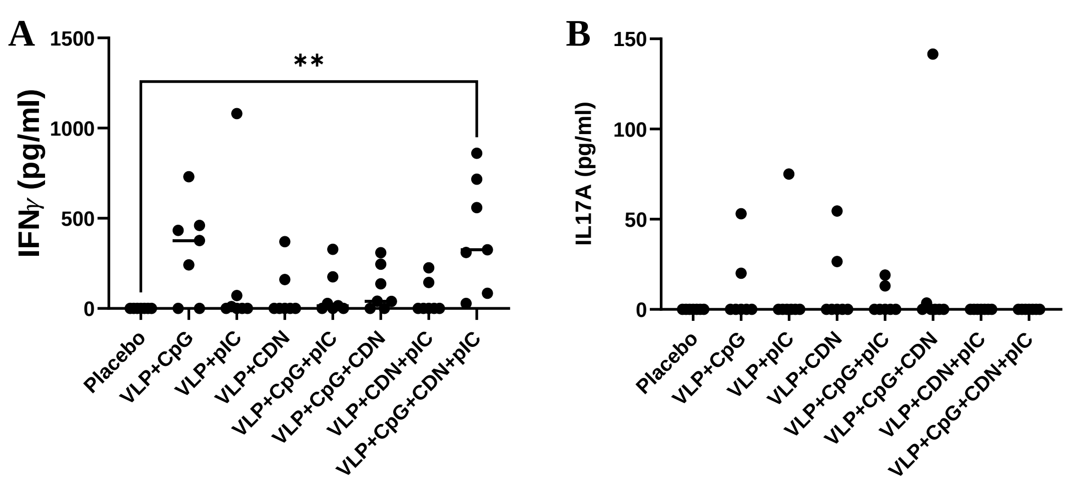

Figure 3.8. The Antigen Recall Assay using immunized mice spleen cells to assess IFNγ and IL-17A secretion by ELISA. Spleen cells were incubated with VLP (0.5ug/well) for 48 hours, and A) secreted IFNγ and B) secreted IL-17A amounts compared among groups. Vaccinated

groups were compared with one-way ANOVA followed by the Kruskal-Wallis test for multiple comparisons. *$P < 0.05$, **$P < 0.01$, ***$P <0 .001$, ****$P <0 .0001$.

CD4+ T cells are differentiated into a variety of effector subtypes. Their functions vary from activating B cells, cytotoxic T cells, and nonimmune cells as well as suppressing immune reactions. Th1, Th2, and Th17 are the main subsets of the helper T cells. While Th1 is known to produce IFNγ and IL12, which is responsible for cellular immunity to control intracellular microorganisms, IL4, IL5, and IL13 are the main products of Th2 cells, which is necessary for humoral immunity against extracellular pathogens.[21]

To investigate the polarization of the T helper cells, the antigen-recall assay is conducted with splenocytes of the immunized mice against IFNγ, IL4, and IL17A. 400.000 spleen cells are seeded to each well in 250 ul of culture media and incubated with 0.5 ug VLP antigen for 72 hours. Upon completion of this duration, secreted IFNγ, IL4, and IL17A levels were measured by cytokine ELISA. The results of these ELISAs are represented in Figure 3.8.

On the left panel, there is the only difference between placebo-received groups and VLP+CpG+CDN+pIC injected group. As expected, we did not see any difference in IL4 (shown in the Appendix, Figure A33). As seen on the right panel, there is no significant difference in Th-17 produced among injection groups. When all the results are combined, the VLP+CpG+CDN+pIC combination is the best adjuvant combination to generate a Th1-biased response.

CHAPTER 4

DISCUSSION

The SARS-CoV-2 emerged in late 2019 in Wuhan and, a couple of months later, was announced as a pandemic by WHO. It led to 767.726.861 cases and 6.948.764 deaths as of July 5th, 2023. High transmissibility and increased deaths generated an urgent need for therapeutic ways to treat and protect from COVID-19. The virus is an enveloped positive-sense single-stranded RNA virus and belongs to the *betacoronavirus* subfamily of the *Coronaviridae* family. Although the best protection method for a viral disease is vaccination, studies took time. Until the first vaccine was approved, antiviral drugs such as lopinavir/ritonavir and remdesivir were given to COVID-19 patients. Because of the high transmission of the virus, many variants have emerged. Among these, the ones increasing the transmission, infectivity, or evading of the immune system become VUM, VOC, or VOI. These mutations mainly occur in the Spike protein of the virus, which creates the bridge for the cell entry that happens by binding to ACE2. Nevertheless, approved vaccines as well as the ones in the clinical and pre-clinical trials, mostly use either spike, RBD, or prefusion stabilized spike as antigen, although the virus has another three structural proteins: namely envelope (E), membrane (M), and nucleocapsid (N).

Many vaccine platforms have been used to develop an efficient immune response to fight pathogens. Among those, the most effective platforms are in the whole-pathogen vaccines: inactive virus vaccine and live-attenuated virus. However, this bears a danger of virus reversion to its virulence which makes them unfit for immunocompromised individuals. When these are taken into consideration, the VLP platform stands out since its structure resembles the natural form of the virus while not containing any genetic material of the virus that may cause virulence. VLPs can contain one or more structural proteins of the pathogen, and due to their virus-like structure, they can induce robust cellular and humoral immune responses. The only downside of the VLP platform is that proper adjuvant use is essential as opposed to whole-pathogen vaccines, which mimic natural viral infection without an adjuvant. Thus, adjuvant choice is as important as the choice of vaccine platform.

VLP-58-1023-Al-K3 SARS-COV-2 vaccine is developed in our laboratory and is in Phase II/III clinical trials. VLP is chosen as a vaccine platform because of the advantages as mentioned earlier. In VLP-58-1023-Al-K3, all four structural proteins of the virus (S, M, E, N) are included to not lose as much effectiveness in augmenting immune response because of mutations in spike protein. Studies have shown that the inclusion of membrane and nucleocapsid proteins of the virus in vaccine formulation enhances the immune response by activating T cells. Most approved vaccines possess prefusion stabilized spike protein as antigen since this pre-fusion resulted in high protection and stronger antibody titers. Throughout the study, we used HexaPro (6p) VLP as previous studies indicated that because of its more stable pre-fusion structure, it induces stronger immunity and neutralizing antibody compared to 2p-prefused variants in mice and hamsters. VLP used in this thesis is used for the vaccine candidate, which is in phase II clinical trials and yields better humoral and cellular immunity.

Literature search points out VLP platform enhances the induction of a more robust immune response than subunit vaccines. This study shows that VLP alone is a Th2-promoting antigen. However, the choice of adjuvant determines whether the vaccine produces the desired immune response. In addition to classical adjuvant Alum, VLP is adjuvanted with CpG K3 to induce TLR9 activation and skew the response towards Th1. However, there is a limited number of adjuvants for human use as opposed to the existence of several platforms for antigen presentation. Herein, we attempted to test the efficacy of other adjuvants and their combinations to reveal their possible clinical use. The additional adjuvants were poly (I:C), and CDN, which are TLR3 and STING agonist, respectively. To find out their potential as adjuvants for clinical usage in future pandemics, nine (9) groups of male mice (C57BL/6, 6-8 weeks old) were intraperitoneally injected three times with mixtures of VLP vaccine using a variety of adjuvant single, dual or triple combinations of CpG ODN, CDN, and poly(I:C). many studies have indicated the necessity for the third dose of vaccine for protein vaccines to produce more robust and higher levels of protective immunity. The tail vein blood was collected on days 14, 28, 14, 28, 42, 70, and 84 to assess the secreted antibody levels against recombinant spike protein and delta+ receptor binding domain of the SARS-CoV-2 virus.

All injection groups except for the placebo group received 5 ug HexaPro VLP/animal. Three groups received VLP formulated individually with CpG, poly(I:C), and CDN. Another three groups are vaccinated with VLP combined with dual adjuvants as CpG+poly(I:C), CpG+CDN and CDN+poly(I:C). The last group is immunized with VLP formulated with triple adjuvants. Evaluation of anti-spike IgG levels resulted that only VLP immunization is not enough to induce an immune response, unlike immunization with individual CpG and poly(I:C). CpG combined with poly(I:C) and CDN separately, worked synergistically to induce a humoral response. Upon the second injection, the placebo and only VLP groups did not yield any significant antibody production, whereas the remaining groups displayed a rise in antibody levels. Two months after the second injection, only VLP receiving group enhanced the IgG levels, and the ones immunized with VLP adjuvanted with CDN individually, dual or triple showed no change in their antibody levels, whereas the remaining groups are in line with the literature, which supports this decline in IgG production. Anti-spike antibody titers significantly increased after the third immunization in groups injected with VLP formulated with individually CpG, poly(I:C), and CDN; VLP combined with CpG+ poly(I:C) and triple adjuvants. We can draw the conclusion from these results that CDN might work antagonistically with CpG and poly(I:C) separately when injected for the third time. Overall, formulizing HexaPro VLP with a combination of CpG and poly(I:C) as well as a combination of CpG, poly(I:C), and CDN induce a more robust humoral response in male C57BL/6 mice. Many studies emphasize the importance of TLR3 involvement in protecting against SARS-CoV-2 infection, and our study confirms this one more time.

To understand the specificity of the humoral response, we measured the IgG1 and IgG2c levels of these immunization groups against the spike protein of the virus. All groups showed high levels of IgG1 after both the second and third doses. However, none of these increases have significant meaning compared to placebo and only VLP-injected groups. However, IgG1 levels by themselves do not give an idea about the vaccine's efficiency. Depending on the species, anti-spike IgG2c antibody levels should be measured to be able to have an idea of the subsets and their relative contribution to the total IgG levels. IgG2c levels of the groups which are immunized with VLP formulated with a combination of CpG and poly(I:C); the combination of CpG and CDN and triple adjuvants mounted significantly upon the second injection. Two weeks after the third injection, two additional groups followed the same pattern of immune response: VLP adjuvanted individually with poly(I:C) and CpG. Thus, Addition of Th1-promoting adjuvants confers skewed Th1 response.

As mentioned earlier, Th1 cells secrete IL-2, IFNγ and TNF-α, which mounts an immune response against intracellular pathogen but also involved in autoimmune disease. Th2 subset, on the other hand, mediate immune response against extracellular parasites and causes allergy and inflammatory asthmatic disease in extreme production by secreting IL-4, IL-5 and IL-13. Thus, the balance between Th1 and Th2 cytokines have vital role in response to infections so as studies suggest. In vaccination studies, the polarization of the Th response is a key aspect. After vaccination, it is suggested that ratio of Th1 to Th2 should be higher than 1 to have an efficient and robust immune response. Consequently, the ratio of IgG2c over IgG1 is calculated for each group to assess the tendency of the response. Placebo group and Group 8 which is immunized with VLP adjuvanted with both poly(I:C) and CDN posed a balanced Th response which is ratio of Th1 to Th2 is around 1. Group 2 which is immunized with only VLP and Group 5 receiving VLP combined with CDN polarizes response towards Th2 while the remaining groups skews the response as required for an effective vaccine formulation. Only VLP is not enough to get an efficient response and adjuvanting VLP vaccine with CDN creates the same effect as only VLP group, resulted in an

Th2-skewed response. Also, the balanced response of the group immunized with VLP adjuvanted with poly(I:C) and CDN imply that they work antagonistically while mounting an immune response. This can be used to manage or cancel out toxicity created by poly(I:C) adjuvant usage. Cytokine profile of the injection groups was measured by recall assay. The result showed that no significant IL4 or IL17 A response augmented while only the group which is vaccinated with VLP combined triple adjuvants CpG, poly(I:C) and CDN induced desired cytokine profile by secretion of significant amount of IFNγ. All together these results suggest that combining CpG, poly(I:C) and CDN as adjuvant would yield desired efficient immune response for a vaccine. Anti-RecS and anti-RBD responses persist over time when adjuvants are included in the final formulation.

Survival of any virus depends on either on its capability to evade immune system or high transmissibility. Several variants of SARS-CoV-2 have been emerging. That is why COVID-19 vaccine should be effective to other variants as well as origin to some extent until a vaccine developed against that newly emerged variant. Consequently, effectiveness of these vaccine against Delta+ variant was evaluated by ELISA. Anti-Delta+ total IgG levels were not significant enough from both placebo and the group immunized with only VLP two weeks after the first injection. However, three groups induced significantly higher humoral immune response than placebo and the group immunized with only VLP upon the second injection: individual poly(I:C) adjuvanted and combination of CpG and poly(I:C) and combination of CpG and CDN adjuvanted groups. The groups immunized with VLP adjuvanted with individually poly(I:C) and adjuvanted with combination of CpG and CDN were still posing significantly higher immune responses against Delta+ RBD even two months after the second injection. However, the third injection did not yield the same pattern. the last injection induced so high levels of anti-Delta+ RBD IgG that the other injection groups could not induce significant levels of humoral response. Anti-Delta+ IgG1 levels, in Figure 3.5, shows no significant difference among the groups, which is not applicable to IgG2c. Figure 3.6 depicts the groups which produced robust immune response which are groups immunized with VLP adjuvanted with individual CpG and poly(I:C); with combination of CpG and poly(I:C); with combination of CpG and CDN; and combination of all three adjuvants.

Tendency of the helper T cell is measured by calculating ratios of IgG1 levels to IgG2c for each adjuvanted injection group. Figure 3.7B illustrate the results of those ratios. It can be said that usage of CDN does not yield desired immune response for vaccination and its effect was balanced by use of poly(I:C). However, placebo, only VLP injected groups and that adjuvanted with a combination of poly(I:C) and CDN induced a balanced immune response, and the remaining groups generated Th1-skewed one against Delta+ RBD. All together, we can say that VLP vaccine which is formulized with individual CpG and poly(I:C); with combination of CpG and poly(I:C); with combination of CpG and CDN; and combination of all three adjuvants could bear a potential for vaccine against Delta+ variant.

This study is a little demonstration of how different adjuvants can be useful tools for vaccine given individually or in combination. CpG is an accepted adjuvant by FDA and it has been already used in Hepatitis B vaccine. However, it does not yield the required profile in this study by itself; that is, it needs another adjuvant. Alum is used to form the desired response in COVID-19 vaccine. Other adjuvant utilized in this study is poly(I:C) which is a strong immune inducer but might cause autoimmunity[70]. Since TLR3 is expressed in many cell types, the toxicity of its agonist is inevitable which has been presented by several in vivo studies. We can see that the toxicity can be reduced by the antagonist such as a CDN as this work suggest or by delivering the adjuvant with a delivery system such as in liposome as studies recommend. Instead, newly developed derivatives of poly(I:C) such as poly(ICLC) poly(IC12U) have been used as adjuvant for both infectious diseases and cancer with lower toxicity and type-I IFN production. Use of individual CDN and its dual combination with two other adjuvants did not give rise to expected immunity which is most probably due to its poor pharmacokinetic (PK) properties such as short half-life. The STING agonist employed in this study is 1st generation adjuvant. The ones with better PK profiles are called 3rd generation agonist which are shown to be effective and promising for immunotherapy in oncology and against SARS-CoV-2. Despite the result of this study, 3rd generation STING agonists can be very advantageous for vaccine development if their formulation is improved.

In several studies, it is shown that there is a correlation between use of combination of CpG and poly(I:C) and production of Nabs in animals and this combination showed promising results in

HIV studies and anti-tumor therapies. Yang and his colleagues studied combination of CpG and several CDNs. It shows similar results with the CDN utilized in this study. Instead of 2,3-cGAMP, using 2'3'-c-di-AM(PS)2 yields the desired outcome for the vaccine. When it comes to combining poly (IC) and CDN, HIV studies gives promising results which shows Th1-skewed response and efficient viral clearance. Dual combinations are studied in a triple adjuvant study in addition to already approved adjuvants such as Alum both in cancer vaccine and HIV vaccines demonstrating good profile for future use. The triple combination of these adjuvants had never been used in vaccine development against infectious diseases. We showed that these three adjuvants provide a synergistic effect against original SARS-CoV- 2 and Delta+ variant of the virus. The latter was checked against RBD domain of the virus and studies mention IgG levels against this domain is correlated with the neutralizing Ab levels of the vaccine. Thus, employing this combination of triple adjuvants and CpG+ poly(I:C) in VLP platform could have a potential for future use against infectious diseases.

The Figure 3.1 and Figure 3.4 demonstrates the combination of adjuvants inducing persistent antibody response against Spike and RBD, respectively. When calculated this corresponds to 10 months of persistent antibody response. If RBD-specific antibody response is desired, then triple adjuvant group where CDN is in the formulation should be utilized. On the other hand, anti-S response is more pronounced when CDN is not in the vaccine formulation according to results of this study. Since the future of COVID has been thought to be seasonal. This vaccine candidate can be used as a booster dose when the primary vaccination is with other approved COVID-19 vaccines. A study published recently shows that different vaccines use as primary and booster doses can induce antiviral immune response fast.[92]

For future perspective, it can be said that ACE2 transgenic mice should be immunized with these adjuvant groups and then, challenged with the live virus to see immune response upon infection. Then, virus neutralization of those challenged animals should be estimated. Other question that needs to be asked is whether the best formulation groups in this study are better than the one in the clinical trial with Alum and CpG so that adjuvant potential of these best formulations can be compared and evaluated. Another point is that other route of injections should be tried like subcutaneous and intramuscular to see which one will yield the best result. The last but not the least point is that IFNγ T cell memory should be evaluated.

CHAPTER 5

REFERENCE

1. Guo, Y. R., Cao, Q. D., Hong, Z. S., Tan, Y. Y., Chen, S. D., Jin, H. J., Tan, K. S., Wang, D. Y., & Yan, Y. (2020). The origin, transmission and clinical therapies on coronavirus disease 2019 (COVID-19) outbreak - an update on the status. *Military Medical Research*, 7(1), 11. https://doi.org/10.1186/s40779-020-00240-0
2. *WHO Coronavirus (COVID-19) Dashboard | WHO Coronavirus (COVID-19) Dashboard With Vaccination Data*. (n.d.). WHO Coronavirus (COVID-19) Dashboard | WHO Coronavirus (COVID-19) Dashboard With Vaccination Data. Retrieved 19 April, 2023, from http://covid19.who.int/
3. Frutos, R., Gavotte, L., & Devaux, C. A. (2021). Understanding the origin of COVID-19 requires to change the paradigm on zoonotic emergence from the spillover to the circulation model. Infection, genetics and evolution : *journal of molecular epidemiology and evolutionary genetics in infectious diseases*, 95, 104812. https://doi.org/10.1016/j.meegid.2021.104812
4. Zhou, P., Yang, X. L., Wang, X. G., Hu, B., Zhang, L., Zhang, W., Si, H. R., Zhu, Y., Li, B., Huang, C. L., Chen, H. D., Chen, J., Luo, Y., Guo, H., Jiang, R. D., Liu, M. Q., Chen, Y., Shen, X. R., Wang, X., Zheng, X. S., … Shi, Z. L. (2020). A pneumonia outbreak associated with a new coronavirus of probable bat origin. *Nature*, 579(7798), 270–273. https://doi.org/10.1038/s41586-020-2012-7

5. Mistry, P., Barmania, F., Mellet, J., Peta, K., Strydom, A., Viljoen, I. M., James, W., Gordon, S., & Pepper, M. S. (2022). SARS-CoV-2 Variants, Vaccines, and Host Immunity. *Frontiers in immunology*, 12, 809244. https://doi.org/10.3389/fimmu.2021.809244
6. Jackson, C. B., Farzan, M., Chen, B., & Choe, H. (2022). Mechanisms of SARS-CoV-2 entry into cells. *Nature reviews. Molecular cell biology*, *23*(1), 3–20. https://doi.org/10.1038/s41580-021-00418-x
7. Wang, M. Y., Zhao, R., Gao, L. J., Gao, X. F., Wang, D. P., & Cao, J. M. (2020). SARS-CoV-2: Structure, Biology, and Structure-Based Therapeutics Development. *Frontiers in cellular and infection microbiology*, 10, 587269. https://doi.org/10.3389/fcimb.2020.587269
8. Kim, D., Lee, J. Y., Yang, J. S., Kim, J. W., Kim, V. N., & Chang, H. (2020). The Architecture of SARS-CoV-2 Transcriptome. *Cell*, 181(4), 914–921.e10. https://doi.org/10.1016/j.cell.2020.04.011
9. Huang, Y., Yang, C., Xu, X. F., Xu, W., & Liu, S. W. (2020). Structural and functional properties of SARS-CoV-2 spike protein: potential antivirus drug development for COVID-19. *Acta pharmacologica Sinica*, 41(9), 1141–1149. https://doi.org/10.1038/s41401-020-0485-4
10. Chilamakuri, R., & Agarwal, S. (2021). COVID-19: Characteristics and Therapeutics. *Cells*, 10(2), 206. https://doi.org/10.3390/cells10020206
11. Peeling, R. W., Heymann, D. L., Teo, Y. Y., & Garcia, P. J. (2022). Diagnostics for COVID-19: moving from pandemic response to control. *Lancet* (London, England), 399(10326), 757–768. https://doi.org/10.1016/S0140-6736(21)02346-1
12. Siu, Y. L., Teoh, K. T., Lo, J., Chan, C. M., Kien, F., Escriou, N., Tsao, S. W., Nicholls, J. M., Altmeyer, R., Peiris, J. S., Bruzzone, R., & Nal, B. (2008). The M, E, and N structural proteins of the severe acute respiratory syndrome coronavirus are required for efficient assembly, trafficking, and release of virus-like particles. *Journal of virology*, 82(22), 11318–11330. https://doi.org/10.1128/JVI.01052-08
13. Zhang, Z., Nomura, N., Muramoto, Y., Ekimoto, T., Uemura, T., Liu, K., Yui, M., Kono, N., Aoki, J., Ikeguchi, M., Noda, T., Iwata, S., Ohto, U., & Shimizu, T. (2022). Structure of SARS-CoV-2 membrane protein essential for virus assembly. *Nature communications*, 13(1), 4399. https://doi.org/10.1038/s41467-022-32019-3

14. Boson, B., Legros, V., Zhou, B., Siret, E., Mathieu, C., Cosset, F. L., Lavillette, D., & Denolly, S. (2021). The SARS-CoV-2 envelope and membrane proteins modulate maturation and retention of the spike protein, allowing assembly of virus-like particles. The *Journal of biological chemistry*, 296, 100111. https://doi.org/10.1074/jbc.RA120.016175
15. Schoeman, D., & Fielding, B. C. (2019). Coronavirus envelope protein: current knowledge. *Virology journal*, 16(1), 69. https://doi.org/10.1186/s12985-019-1182-0
16. Bai, Z., Cao, Y., Liu, W., & Li, J. (2021). The SARS-CoV-2 Nucleocapsid Protein and Its Role in Viral Structure, Biological Functions, and a Potential Target for Drug or Vaccine Mitigation. *Viruses*, 13(6), 1115. https://doi.org/10.3390/v13061115
17. Chang, C. K., Hsu, Y. L., Chang, Y. H., Chao, F. A., Wu, M. C., Huang, Y. S., Hu, C. K., & Huang, T. H. (2009). Multiple nucleic acid binding sites and intrinsic disorder of severe acute respiratory syndrome coronavirus nucleocapsid protein: implications for ribonucleocapsid protein packaging. *Journal of virology*, 83(5), 2255–2264. https://doi.org/10.1128/JVI.02001-08
18. Fehr, A. R., & Perlman, S. (2015). Coronaviruses: an overview of their replication and pathogenesis. *Methods in molecular biology* (Clifton, N.J.), 1282, 1–23. https://doi.org/10.1007/978-1-4939-2438-7_1
19. Barthe, M., Hertereau, L., Lamghari, N., Osman-Ponchet, H., & Braud, V. M. (2023). Receptors and Cofactors That Contribute to SARS-CoV-2 Entry: Can Skin Be an Alternative Route of Entry?. *International journal of molecular sciences*, 24(7), 6253. https://doi.org/10.3390/ijms24076253
20. González-Vázquez, L. D., & Arenas, M. (2023). Molecular Evolution of SARS-CoV-2 during the COVID-19 Pandemic. *Genes*, 14(2), 407. https://doi.org/10.3390/genes14020407
21. Zhou, L., Chong, M. M., & Littman, D. R. (2009). Plasticity of CD4+ T cell lineage differentiation. *Immunity*, 30(5), 646–655. https://doi.org/10.1016/j.immuni.2009.05.001
22. Choi, J. Y., & Smith, D. M. (2021). SARS-CoV-2 Variants of Concern. *Yonsei medical journal*, *62*(11), 961–968. https://doi.org/10.3349/ymj.2021.62.11.961
23. Parkin, J., & Cohen, B. (2001). An overview of the immune system. *Lancet (London, England)*, *357*(9270), 1777–1789. https://doi.org/10.1016/S0140-6736(00)04904-7

24. *Innate Immunity - Molecular Biology of the Cell - NCBI Bookshelf.* (n.d.). National Center for Biotechnology Information. Retrieved June 14, 2023, from https://www.ncbi.nlm.nih.gov/books/NBK26846/
25. Jang, J. H., Shin, H. W., Lee, J. M., Lee, H. W., Kim, E. C., & Park, S. H. (2015). An Overview of Pathogen Recognition Receptors for Innate Immunity in Dental Pulp. *Mediators of inflammation*, *2015*, 794143. https://doi.org/10.1155/2015/794143
26. *Induced innate responses to infection - Immunobiology - NCBI Bookshelf.* (n.d.). National Center for Biotechnology Information. Retrieved June 14, 2023, from https://www.ncbi.nlm.nih.gov/books/NBK27122/
27. Sun, L., Wang, X., Saredy, J., Yuan, Z., Yang, X., & Wang, H. (2020). Innate-adaptive immunity interplay and redox regulation in immune response. *Redox biology*, *37*, 101759. https://doi.org/10.1016/j.redox.2020.101759
28. Chi, X., Yan, R., Zhang, J., Zhang, G., Zhang, Y., Hao, M., Zhang, Z., Fan, P., Dong, Y., Yang, Y., Chen, Z., Guo, Y., Zhang, J., Li, Y., Song, X., Chen, Y., Xia, L., Fu, L., Hou, L., Xu, J., … Chen, W. (2020). A neutralizing human antibody binds to the N-terminal domain of the Spike protein of SARS-CoV-2. *Science (New York, N.Y.)*, *369*(6504), 650–655. https://doi.org/10.1126/science.abc6952
29. Liu, L., Wang, P., Nair, M. S., Yu, J., Rapp, M., Wang, Q., Luo, Y., Chan, J. F., Sahi, V., Figueroa, A., Guo, X. V., Cerutti, G., Bimela, J., Gorman, J., Zhou, T., Chen, Z., Yuen, K. Y., Kwong, P. D., Sodroski, J. G., Yin, M. T., … Ho, D. D. (2020). Potent neutralizing antibodies against multiple epitopes on SARS-CoV-2 spike. *Nature*, *584*(7821), 450–456. https://doi.org/10.1038/s41586-020-2571-7
30. Cantuti-Castelvetri, L., Ojha, R., Pedro, L. D., Djannatian, M., Franz, J., Kuivanen, S., van der Meer, F., Kallio, K., Kaya, T., Anastasina, M., Smura, T., Levanov, L., Szirovicza, L., Tobi, A., Kallio-Kokko, H., Österlund, P., Joensuu, M., Meunier, F. A., Butcher, S. J., Winkler, M. S., … Simons, M. (2020). Neuropilin-1 facilitates SARS-CoV-2 cell entry and infectivity. *Science (New York, N.Y.)*, *370*(6518), 856–860. https://doi.org/10.1126/science.abd2985
31. *Scientific Brief: SARS-CoV-2 Transmission* | CDC. (2020, February 11). Centers for Disease Control and Prevention. https://www.cdc.gov/coronavirus/2019-ncov/science/science-briefs/sars-cov-2-transmission.html

32. Zhang, H. P., Sun, Y. L., Wang, Y. F., Yazici, D., Azkur, D., Ogulur, I., Azkur, A. K., Yang, Z. W., Chen, X. X., Zhang, A. Z., Hu, J. Q., Liu, G. H., Akdis, M., Akdis, C. A., & Gao, Y. D. (2023). Recent developments in the immunopathology of COVID-19. *Allergy*, *78*(2), 369–388. https://doi.org/10.1111/all.15593
33. Sharma, A., Ahmad Farouk, I., & Lal, S. K. (2021). COVID-19: A Review on the Novel Coronavirus Disease Evolution, Transmission, Detection, Control and Prevention. *Viruses*, *13*(2), 202. https://doi.org/10.3390/v13020202
34. Gusev, E., Sarapultsev, A., Solomatina, L., & Chereshnev, V. (2022). SARS-CoV-2-Specific Immune Response and the Pathogenesis of COVID-19. *International journal of molecular sciences*, *23*(3), 1716. https://doi.org/10.3390/ijms23031716
35. Hasan, A., Paray, B. A., Hussain, A., Qadir, F. A., Attar, F., Aziz, F. M., Sharifi, M., Derakhshankhah, H., Rasti, B., Mehrabi, M., Shahpasand, K., Saboury, A. A., & Falahati, M. (2021). A review on the cleavage priming of the spike protein on coronavirus by angiotensin-converting enzyme-2 and furin. *Journal of biomolecular structure & dynamics*, *39*(8), 3025–3033. https://doi.org/10.1080/07391102.2020.1754293
36. *SARS-CoV-2 variants of concern as of 27 July 2023*. (2021, April 30). European Centre for Disease Prevention and Control. https://www.ecdc.europa.eu/en/covid-19/variants-concern
37. Kawai, T., & Akira, S. (2011). Toll-like receptors and their crosstalk with other innate receptors in infection and immunity. *Immunity*, *34*(5), 637–650. https://doi.org/10.1016/j.immuni.2011.05.006
38. Kumar, H., Kawai, T., & Akira, S. (2011). Pathogen recognition by the innate immune system. *International reviews of immunology*, *30*(1), 16–34. https://doi.org/10.3109/08830185.2010.529976
39. Tyrkalska, S. D., Martínez-López, A., Pedoto, A., Candel, S., Cayuela, M. L., & Mulero, V. (2023). The Spike protein of SARS-CoV-2 signals via Tlr2 in zebrafish. *Developmental and comparative immunology*, *140*, 104626. https://doi.org/10.1016/j.dci.2022.104626
40. Shirato, K., & Kizaki, T. (2021). SARS-CoV-2 spike protein S1 subunit induces pro-inflammatory responses via toll-like receptor 4 signaling in murine and human macrophages. *Heliyon*, *7*(2), e06187. https://doi.org/10.1016/j.heliyon.2021.e06187
41. Zheng, M., Karki, R., Williams, E. P., Yang, D., Fitzpatrick, E., Vogel, P., Jonsson, C. B., & Kanneganti, T. D. (2021). TLR2 senses the SARS-CoV-2 envelope protein to produce

inflammatory cytokines. *Nature immunology*, *22*(7), 829–838. https://doi.org/10.1038/s41590-021-00937-x

42. Bortolotti, D., Gentili, V., Rizzo, S., Schiuma, G., Beltrami, S., Strazzabosco, G., Fernandez, M., Caccuri, F., Caruso, A., & Rizzo, R. (2021). TLR3 and TLR7 RNA Sensor Activation during SARS-CoV-2 Infection. *Microorganisms*, *9*(9), 1820. https://doi.org/10.3390/microorganisms9091820
43. Shen, J., Fan, J., Zhao, Y., Jiang, D., Niu, Z., Zhang, Z., & Cao, G. (2023). Innate and adaptive immunity to SARS-CoV-2 and predisposing factors. *Frontiers in immunology*, *14*, 1159326. https://doi.org/10.3389/fimmu.2023.1159326
44. Diamond, M. S., & Kanneganti, T. D. (2022). Innate immunity: the first line of defense against SARS-CoV-2. *Nature immunology*, *23*(2), 165–176. https://doi.org/10.1038/s41590-021-01091-0
45. Hosseini, A., Hashemi, V., Shomali, N., Asghari, F., Gharibi, T., Akbari, M., Gholizadeh, S., & Jafari, A. (2020). Innate and adaptive immune responses against coronavirus. *Biomedicine & pharmacotherapy = Biomedecine & pharmacotherapie*, *132*, 110859. https://doi.org/10.1016/j.biopha.2020.110859
46. Karki, R., & Kanneganti, T. D. (2022). Innate immunity, cytokine storm, and inflammatory cell death in COVID-19. *Journal of translational medicine*, *20*(1), 542. https://doi.org/10.1186/s12967-022-03767-z
47. Bonilla, F. A., & Oettgen, H. C. (2010). Adaptive immunity. *The Journal of allergy and clinical immunology*, *125*(2 Suppl 2), S33–S40. https://doi.org/10.1016/j.jaci.2009.09.017
48. Pishesha, N., Harmand, T. J., & Ploegh, H. L. (2022). A guide to antigen processing and presentation. *Nature reviews. Immunology*, *22*(12), 751–764. https://doi.org/10.1038/s41577-022-00707-2
49. Gutcher, I., & Becher, B. (2007). APC-derived cytokines and T cell polarization in autoimmune inflammation. *The Journal of clinical investigation*, *117*(5), 1119–1127. https://doi.org/10.1172/JCI31720
50. Kumar, B. V., Connors, T. J., & Farber, D. L. (2018). Human T Cell Development, Localization, and Function throughout Life. *Immunity*, *48*(2), 202–213. https://doi.org/10.1016/j.immuni.2018.01.007

51. Coffman R. L. (2006). Origins of the T(H)1-T(H)2 model: a personal perspective. *Nature immunology*, *7*(6), 539–541. https://doi.org/10.1038/ni0606-539
52. McGhee J. R. (2005). The world of TH1/TH2 subsets: first proof. *Journal of immunology (Baltimore, Md. : 1950)*, *175*(1), 3–4. https://doi.org/10.4049/jimmunol.175.1.3
53. Raphael, I., Nalawade, S., Eagar, T. N., & Forsthuber, T. G. (2015). T cell subsets and their signature cytokines in autoimmune and inflammatory diseases. *Cytokine*, *74*(1), 5–17. https://doi.org/10.1016/j.cyto.2014.09.011
54. Raphael, I., Nalawade, S., Eagar, T. N., & Forsthuber, T. G. (2015). T cell subsets and their signature cytokines in autoimmune and inflammatory diseases. *Cytokine*, *74*(1), 5–17. https://doi.org/10.1016/j.cyto.2014.09.011
55. Berger A. (2000). Th1 and Th2 responses: what are they?. *BMJ (Clinical research ed.)*, *321*(7258), 424. https://doi.org/10.1136/bmj.321.7258.424
56. Schijns, V., Majhen, D., van der Ley, P., Thakur, A., Summerfield, A., Berisio, R., Nativi, C., Fernández-Tejada, A., Alvarez-Dominguez, C., Gizurarson, S., Zamyatina, A., Molinaro, A., Rosano, C., Jakopin, Ž., Gursel, I., & McClean, S. (2021). Rational Vaccine Design in Times of Emerging Diseases: The Critical Choices of Immunological Correlates of Protection, Vaccine Antigen and Immunomodulation. *Pharmaceutics*, *13*(4), 501. https://doi.org/10.3390/pharmaceutics13040501
57. Hua, Z., & Hou, B. (2013). TLR signaling in B-cell development and activation. *Cellular & molecular immunology*, *10*(2), 103–106. https://doi.org/10.1038/cmi.2012.61
58. Jordan S. C. (2021). Innate and adaptive immune responses to SARS-CoV-2 in humans: relevance to acquired immunity and vaccine responses. *Clinical and experimental immunology*, *204*(3), 310–320. https://doi.org/10.1111/cei.13582
59. Primorac, D., Vrdoljak, K., Brlek, P., Pavelić, E., Molnar, V., Matišić, V., Erceg Ivkošić, I., & Parčina, M. (2022). Adaptive Immune Responses and Immunity to SARS-CoV-2. *Frontiers in immunology*, *13*, 848582. https://doi.org/10.3389/fimmu.2022.848582
60. Strategic Advisory Group of Experts on Immunization. (n.d.). World Health Organization (WHO). Retrieved June 11, 2023, from https://www.who.int/groups/strategic-advisory-group-of-experts-on-immunization/covid-19-materials
61. Fernandes, Q., Inchakalody, V. P., Merhi, M., Mestiri, S., Taib, N., Moustafa Abo El-Ella, D., Bedhiafi, T., Raza, A., Al-Zaidan, L., Mohsen, M. O., Yousuf Al-Nesf, M. A., Hssain,

A. A., Yassine, H. M., Bachmann, M. F., Uddin, S., & Dermime, S. (2022). Emerging COVID-19 variants and their impact on SARS-CoV-2 diagnosis, therapeutics and vaccines. *Annals of medicine*, *54*(1), 524–540. https://doi.org/10.1080/07853890.2022.2031274

62. Fiolet, T., Kherabi, Y., MacDonald, C. J., Ghosn, J., & Peiffer-Smadja, N. (2022). Comparing COVID-19 vaccines for their characteristics, efficacy and effectiveness against SARS-CoV-2 and variants of concern: a narrative review. *Clinical microbiology and infection : the official publication of the European Society of Clinical Microbiology and Infectious Diseases*, *28*(2), 202–221. https://doi.org/10.1016/j.cmi.2021.10.005
63. Li, M., Wang, H., Tian, L., Pang, Z., Yang, Q., Huang, T., Fan, J., Song, L., Tong, Y., & Fan, H. (2022). COVID-19 vaccine development: milestones, lessons and prospects. *Signal transduction and targeted therapy*, *7*(1), 146. https://doi.org/10.1038/s41392-022-00996-y
64. Li, Y. D., Chi, W. Y., Su, J. H., Ferrall, L., Hung, C. F., & Wu, T. C. (2020). Coronavirus vaccine development: from SARS and MERS to COVID-19. *Journal of biomedical science*, *27*(1), 104. https://doi.org/10.1186/s12929-020-00695-2
65. Vitiello, A., Ferrara, F., Troiano, V., & La Porta, R. (2021). COVID-19 vaccines and decreased transmission of SARS-CoV-2. *Inflammopharmacology*, *29*(5), 1357–1360. https://doi.org/10.1007/s10787-021-00847-2
66. Castro Dopico, X., Ols, S., Loré, K., & Karlsson Hedestam, G. B. (2022). Immunity to SARS-CoV-2 induced by infection or vaccination. *Journal of internal medicine*, *291*(1), 32–50. https://doi.org/10.1111/joim.13372
67. COVID-19 vaccine tracker and landscape. (n.d.). World Health Organization (WHO). Retrieved July 11, 2023, from https://www.who.int/publications/m/item/draft-landscape-of-covid-19-candidate-vaccines
68. Bayani, F., Hashkavaei, N. S., Arjmand, S., Rezaei, S., Uskoković, V., Alijanianzadeh, M., Uversky, V. N., Ranaei Siadat, S. O., Mozaffari-Jovin, S., & Sefidbakht, Y. (2023). An overview of the vaccine platforms to combat COVID-19 with a focus on the subunit vaccines. *Progress in biophysics and molecular biology*, *178*, 32–49. https://doi.org/10.1016/j.pbiomolbio.2023.02.004
69. Nooraei, S., Bahrulolum, H., Hoseini, Z. S., Katalani, C., Hajizade, A., Easton, A. J., & Ahmadian, G. (2021). Virus-like particles: preparation, immunogenicity and their roles as

nanovaccines and drug nanocarriers. *Journal of nanobiotechnology*, *19*(1), 59. https://doi.org/10.1186/s12951-021-00806-7

70. Yilmaz, I. C., Ipekoglu, E. M., Bulbul, A., Turay, N., Yildirim, M., Evcili, I., Yilmaz, N. S., Guvencli, N., Aydin, Y., Gungor, B., Saraydar, B., Bartan, A. G., Ibibik, B., Bildik, T., Baydemir, İ., Sanli, H. A., Kayaoglu, B., Ceylan, Y., Yildirim, T., Abras, I., … Gursel, M. (2022). Development and preclinical evaluation of virus-like particle vaccine against COVID-19 infection. *Allergy*, *77*(1), 258–270. https://doi.org/10.1111/all.15091
71. Kalyoncu, S., Yilmaz, S., Kuyucu, A. Z., Sayili, D., Mert, O., Soyturk, H., Gullu, S., Akinturk, H., Citak, E., Arslan, M., Taskinarda, M. G., Tarman, I. O., Altun, G. Y., Ozer, C., Orkut, R., Demirtas, A., Tilmensagir, I., Keles, U., Ulker, C., Aralan, G., … Inan, M. (2023). Process development for an effective COVID-19 vaccine candidate harboring recombinant SARS-CoV-2 delta plus receptor binding domain produced by Pichia pastoris. *Scientific reports*, *13*(1), 5224. https://doi.org/10.1038/s41598-023-32021-9
72. Underwood, E., Dunkle, L. M., Madhi, S. A., Gay, C. L., Heath, P. T., Kotloff, K. L., Smith, K., Chau, G., Galbiati, S., McGarry, A., Woo, W., Cho, I., Alves, K., Áñez, G., Bennett, C., Shinde, V., Fries, L., Mallory, R. M., Glenn, G. M., & Toback, S. (2023). Safety, efficacy, and immunogenicity of the NVX-CoV2373 vaccine. *Expert review of vaccines*, *22*(1), 501–517. https://doi.org/10.1080/14760584.2023.2218913
73. Pulendran, B., S Arunachalam, P., & O'Hagan, D. T. (2021). Emerging concepts in the science of vaccine adjuvants. *Nature reviews. Drug discovery*, *20*(6), 454–475. https://doi.org/10.1038/s41573-021-00163-y
74. Tom, J. K., Albin, T. J., Manna, S., Moser, B. A., Steinhardt, R. C., & Esser-Kahn, A. P. (2019). Applications of Immunomodulatory Immune Synergies to Adjuvant Discovery and Vaccine Development. *Trends in biotechnology*, *37*(4), 373–388. https://doi.org/10.1016/j.tibtech.2018.10.004
75. Shi, S., Zhu, H., Xia, X., Liang, Z., Ma, X., & Sun, B. (2019). Vaccine adjuvants: Understanding the structure and mechanism of adjuvanticity. *Vaccine*, *37*(24), 3167–3178. https://doi.org/10.1016/j.vaccine.2019.04.055
76. Del Giudice, G., Rappuoli, R., & Didierlaurent, A. M. (2018). Correlates of adjuvanticity: A review on adjuvants in licensed vaccines. *Seminars in immunology*, *39*, 14–21. https://doi.org/10.1016/j.smim.2018.05.001

77. Firdaus, F. Z., Skwarczynski, M., & Toth, I. (2022). Developments in Vaccine Adjuvants. *Methods in molecular biology (Clifton, N.J.), 2412*, 145–178. https://doi.org/10.1007/978-1-0716-1892-9_8
78. Bode, C., Zhao, G., Steinhagen, F., Kinjo, T., & Klinman, D. M. (2011). CpG DNA as a vaccine adjuvant. *Expert review of vaccines*, *10*(4), 499–511. https://doi.org/10.1586/erv.10.174
79. Kayraklioglu, N., Horuluoglu, B., & Klinman, D. M. (2021). CpG Oligonucleotides as Vaccine Adjuvants. *Methods in molecular biology (Clifton, N.J.)*, *2197*, 51–85. https://doi.org/10.1007/978-1-0716-0872-2_4
80. Klinman, D. M., Klaschik, S., Sato, T., & Tross, D. (2009). CpG oligonucleotides as adjuvants for vaccines targeting infectious diseases. *Advanced drug delivery reviews*, *61*(3), 248–255. https://doi.org/10.1016/j.addr.2008.12.012
81. Zhao, T., Cai, Y., Jiang, Y., He, X., Wei, Y., Yu, Y., & Tian, X. (2023). Vaccine adjuvants: mechanisms and platforms. *Signal transduction and targeted therapy*, *8*(1), 283. https://doi.org/10.1038/s41392-023-01557-7
82. Desmet, C. J., & Ishii, K. J. (2012). Nucleic acid sensing at the interface between innate and adaptive immunity in vaccination. *Nature reviews. Immunology*, *12*(7), 479–491. https://doi.org/10.1038/nri3247
83. Martins, K. A., Bavari, S., & Salazar, A. M. (2015). Vaccine adjuvant uses of poly-IC and derivatives. *Expert review of vaccines*, *14*(3), 447–459. https://doi.org/10.1586/14760584.2015.966085
84. Hafner, A. M., Corthésy, B., & Merkle, H. P. (2013). Particulate formulations for the delivery of poly(I:C) as vaccine adjuvant. *Advanced drug delivery reviews*, *65*(10), 1386–1399. https://doi.org/10.1016/j.addr.2013.05.013
85. Guerrero Manriquez, G. G., & Tuero, I. (2021). Adjuvants: friends in vaccine formulations against infectious diseases. *Human vaccines & immunotherapeutics*, *17*(10), 3539–3550. https://doi.org/10.1080/21645515.2021.1934354
86. Blest, H. T. W., & Chauveau, L. (2023). cGAMP the travelling messenger. *Frontiers in immunology*, *14*, 1150705. https://doi.org/10.3389/fimmu.2023.1150705

87. Su, M., Zheng, J., Gan, L., Zhao, Y., Fu, Y., & Chen, Q. (2022). Second messenger 2'3'-cyclic GMP-AMP (2'3'-cGAMP): Synthesis, transmission, and degradation. *Biochemical pharmacology*, *198*, 114934. https://doi.org/10.1016/j.bcp.2022.114934
88. Shang, M., Lu, K., Guan, W., Cao, S., Ren, M., & Zhou, C. (2022). 2',3'-Cyclic GMP-AMP Dinucleotides for STING-Mediated Immune Modulation: Principles, Immunotherapeutic Potential, and Synthesis. *ChemMedChem*, *17*(2), e202100671. https://doi.org/10.1002/cmdc.202100671
89. Kato, K., Omura, H., Ishitani, R., & Nureki, O. (2017). Cyclic GMP-AMP as an Endogenous Second Messenger in Innate Immune Signaling by Cytosolic DNA. *Annual review of biochemistry*, *86*, 541–566. https://doi.org/10.1146/annurev-biochem-061516-044813
90. Al-Jighefee, H. T., Najjar, H., Ahmed, M. N., Qush, A., Awwad, S., & Kamareddine, L. (2021). COVID-19 Vaccine Platforms: Challenges and Safety Contemplations. *Vaccines*, *9*(10), 1196. https://doi.org/10.3390/vaccines9101196
91. Hennessy, C., & McKernan, D. P. (2021). Anti-Viral Pattern Recognition Receptors as Therapeutic Targets. *Cells*, *10*(9), 2258. https://doi.org/10.3390/cells10092258
92. Kuriyama, K., Murakami, K., Masuda, T., Sugiura, K., Sakui, S., Schuring, R. P., & Mori, M. (2023). Immunogenicity and safety of a single booster dose of NVX-CoV2373 (TAK-019) in healthy Japanese adults who had previously received a primary series of COVID-19 mRNA vaccine: Primary analysis report of a phase 3 open-label trial. *Vaccine*, *41*(25), 3763–3771. https://doi.org/10.1016/j.vaccine.2023.05.001
93. Lu, R., Zhao, X., Li, J., Niu, P., Yang, B., Wu, H., Wang, W., Song, H., Huang, B., Zhu, N., Bi, Y., Ma, X., Zhan, F., Wang, L., Hu, T., Zhou, H., Hu, Z., Zhou, W., Zhao, L., Chen, J., … Tan, W. (2020). Genomic characterisation and epidemiology of 2019 novel coronavirus: implications for virus origins and receptor binding. *Lancet (London, England)*, *395*(10224), 565–574. https://doi.org/10.1016/S0140-6736(20)30251-8
94. Jocher, G., Grass, V., Tschirner, S. K., Riepler, L., Breimann, S., Kaya, T., Oelsner, M., Hamad, M. S., Hofmann, L. I., Blobel, C. P., Schmidt-Weber, C. B., Gokce, O., Jakwerth, C. A., Trimpert, J., Kimpel, J., Pichlmair, A., & Lichtenthaler, S. F. (2022). ADAM10 and ADAM17 promote SARS-CoV-2 cell entry and spike protein-mediated lung cell fusion. *EMBO reports*, *23*(6), e54305. https://doi.org/10.15252/embr.202154305

CHAPTER 6

APPENDIX

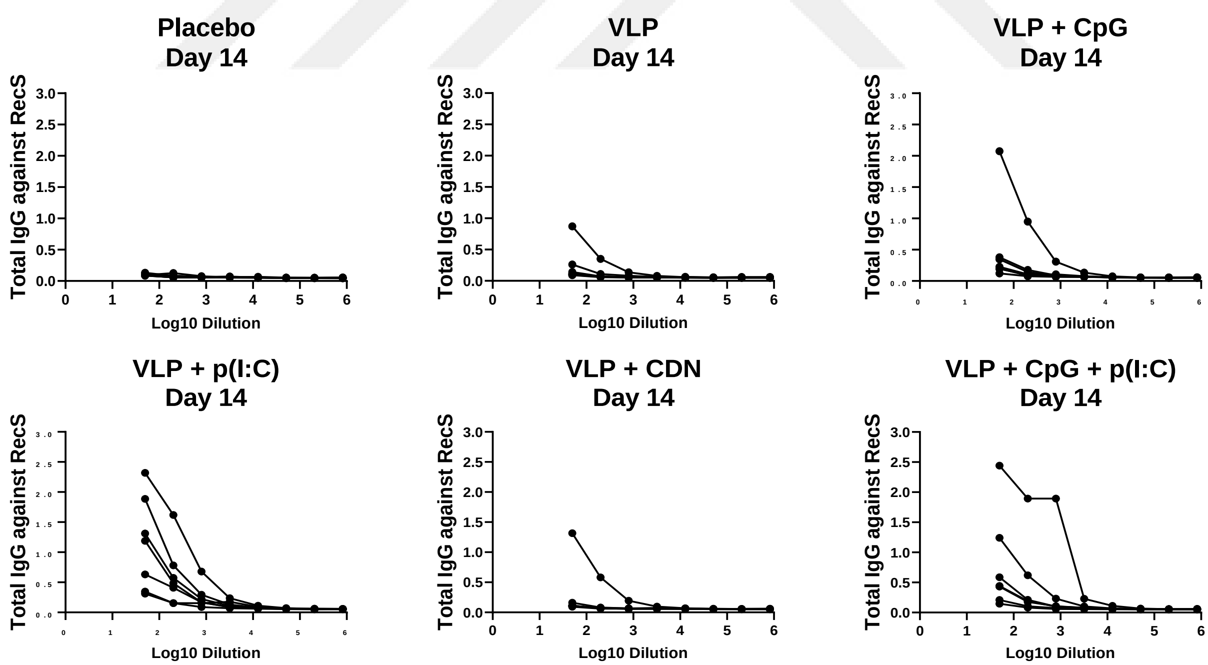

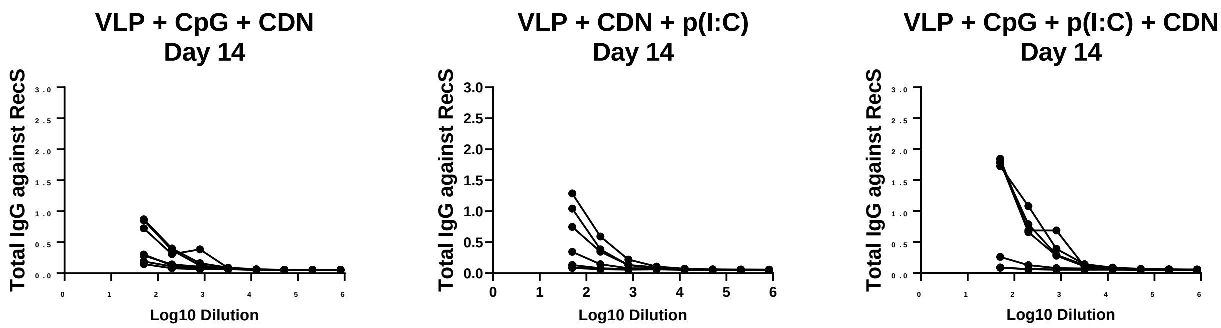

Figure A.1. IgG responses of the mice injected with VLP with single, dual or triple adjuvant combinations with K-type CpG ODN, poly(I:C), and 2,3-cGAMP two weeks after the first injection against in-house recombinant trimeric Spike protein. Each graph represents one group of mice injected with the corresponding vaccine combination.

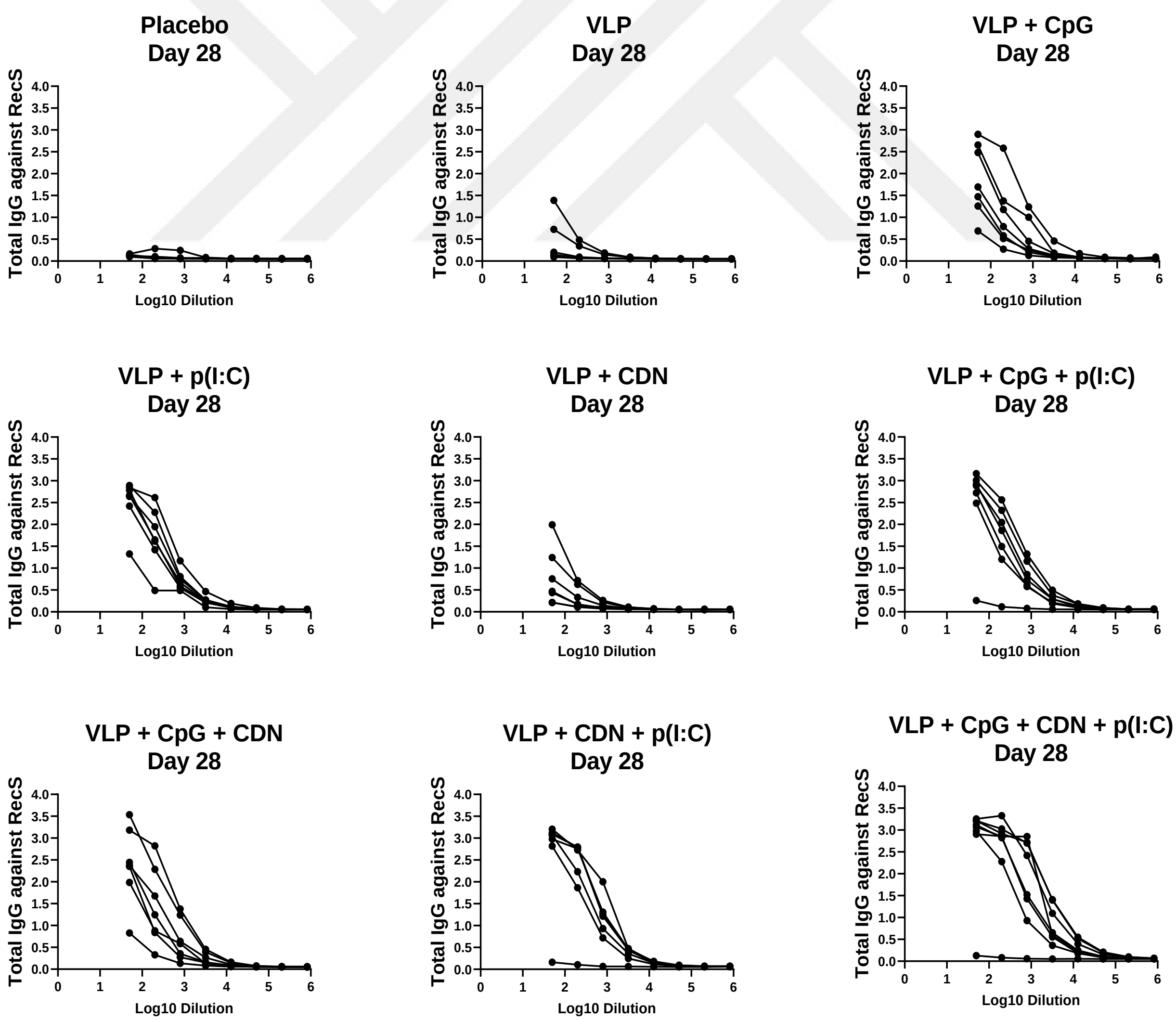

Figure A.2. Total IgG responses of the mice injected with VLP with single, dual or triple adjuvant combinations with K-type CpG ODN, poly(I:C), and 2,3-cGAMP two weeks after the second injection against in-house recombinant trimeric Spike protein. Each graph represents one group of mice injected with the corresponding vaccine combination.

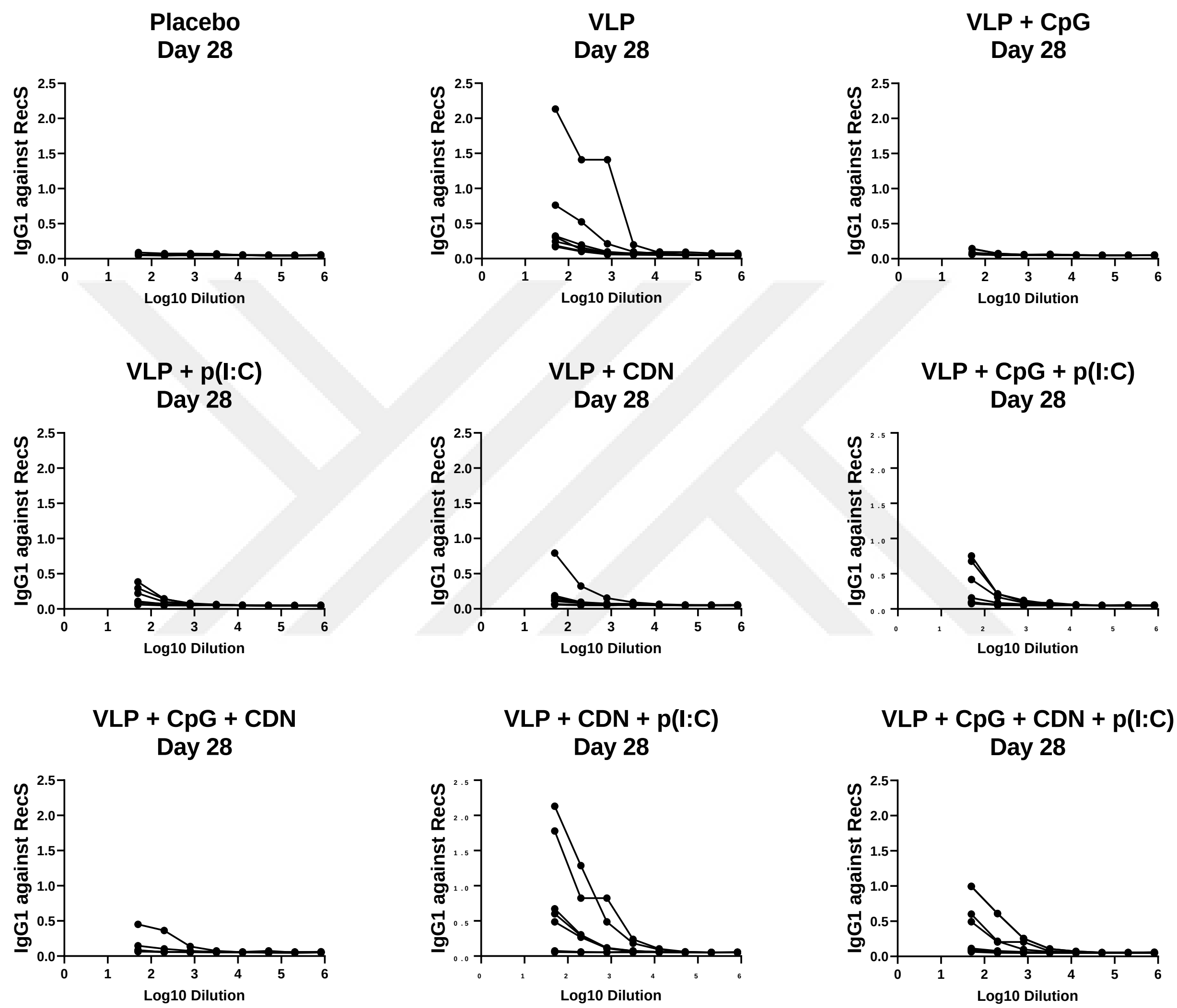

Figure A.3. IgG1 responses of the mice injected with VLP with single, dual or triple adjuvant combinations with K-type CpG ODN, poly(I:C), and 2,3-cGAMP two weeks after the second injection against in-house recombinant trimeric Spike protein. Each graph represents one group of mice injected with the corresponding vaccine combination.

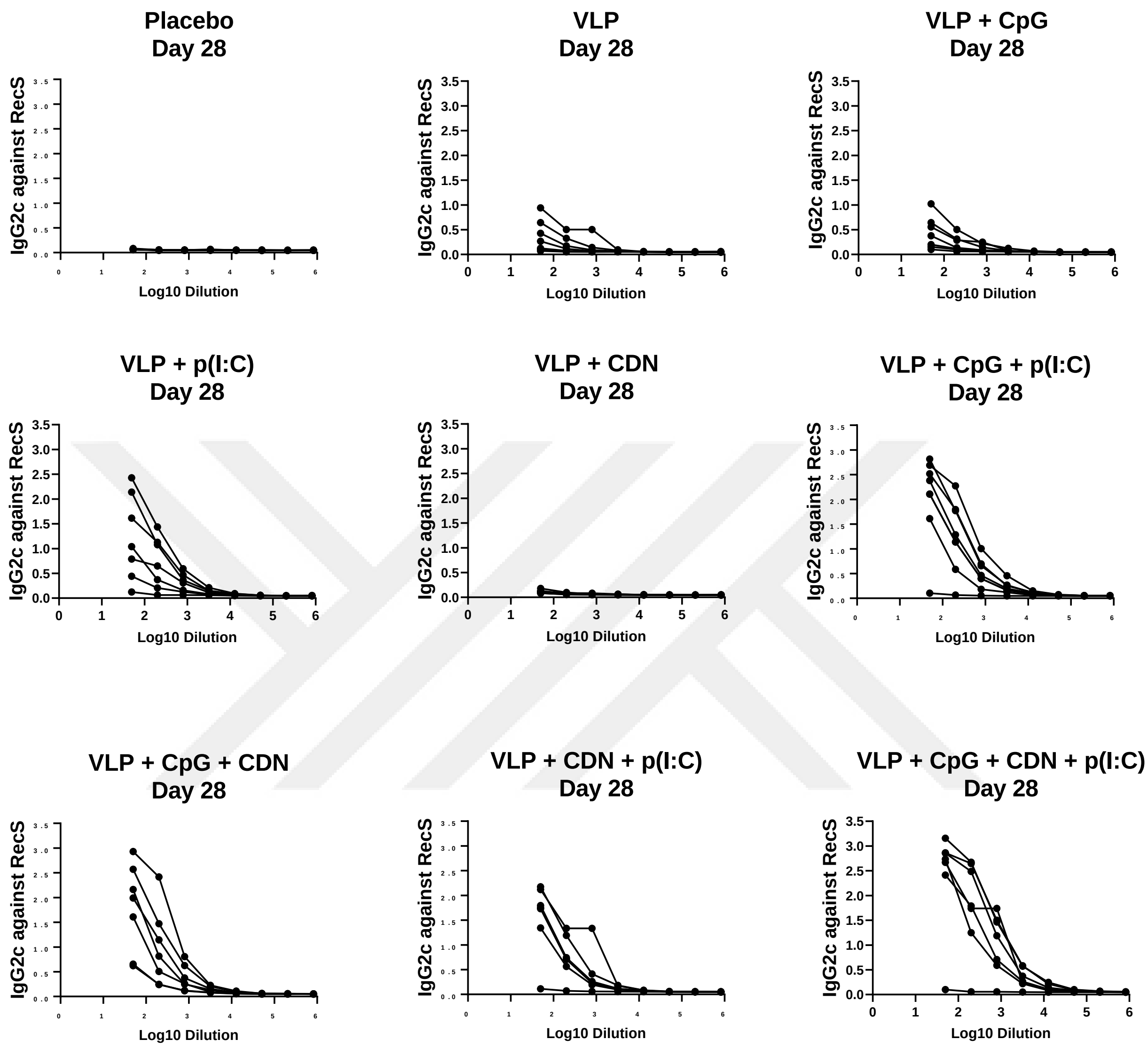

Figure A.4. IgG2c responses of the mice injected with VLP with single, dual or triple adjuvant combinations with K-type CpG ODN, poly(I:C), and 2,3-cGAMP two weeks after the second injection against in-house recombinant trimeric Spike protein. Each graph represents one group of mice injected with the corresponding vaccine combination.

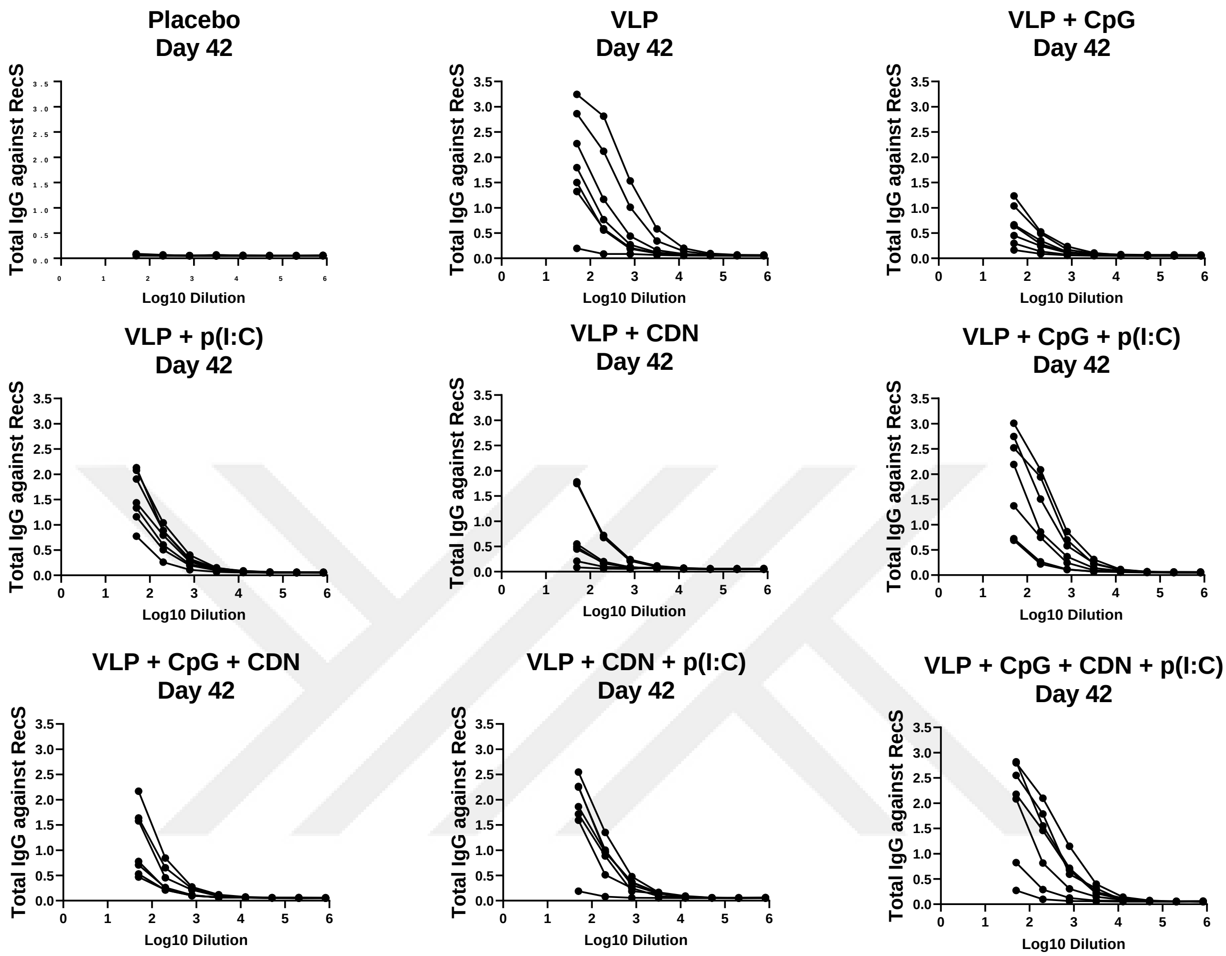

Figure A.5. Total IgG responses of the mice injected with VLP with single, dual or triple adjuvant combinations with K-type CpG ODN, poly(I:C), and 2,3-cGAMP four weeks after the second injection against in-house recombinant trimeric Spike protein. Each graph represents one group of mice injected with the corresponding vaccine combination.

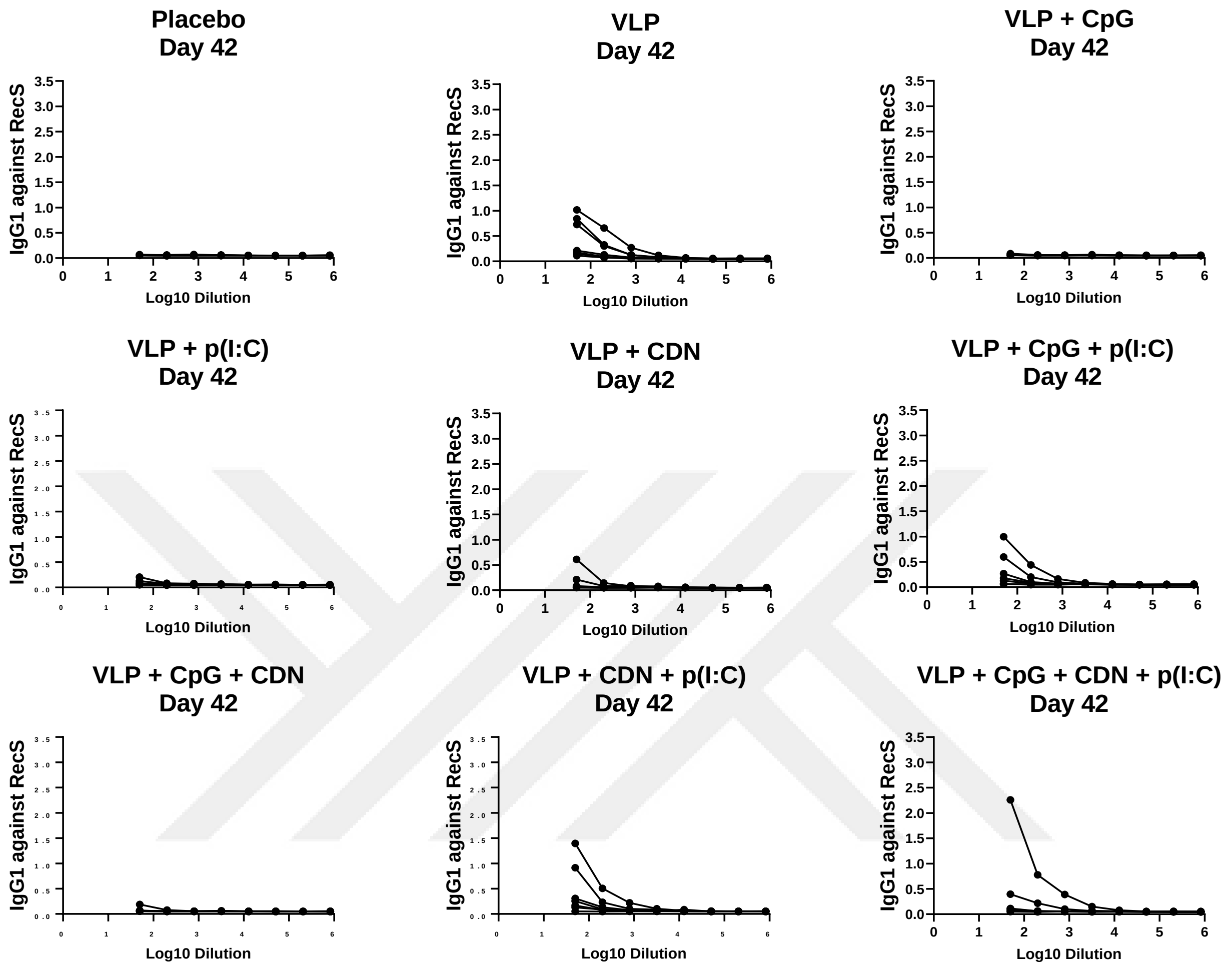

Figure A.6. IgG1 responses of the mice injected with VLP with single, dual or triple adjuvant combinations with K-type CpG ODN, poly(I:C), and 2,3-cGAMP four weeks after the second injection against in-house recombinant trimeric Spike protein. Each graph represents one group of mice injected with the corresponding vaccine combination.

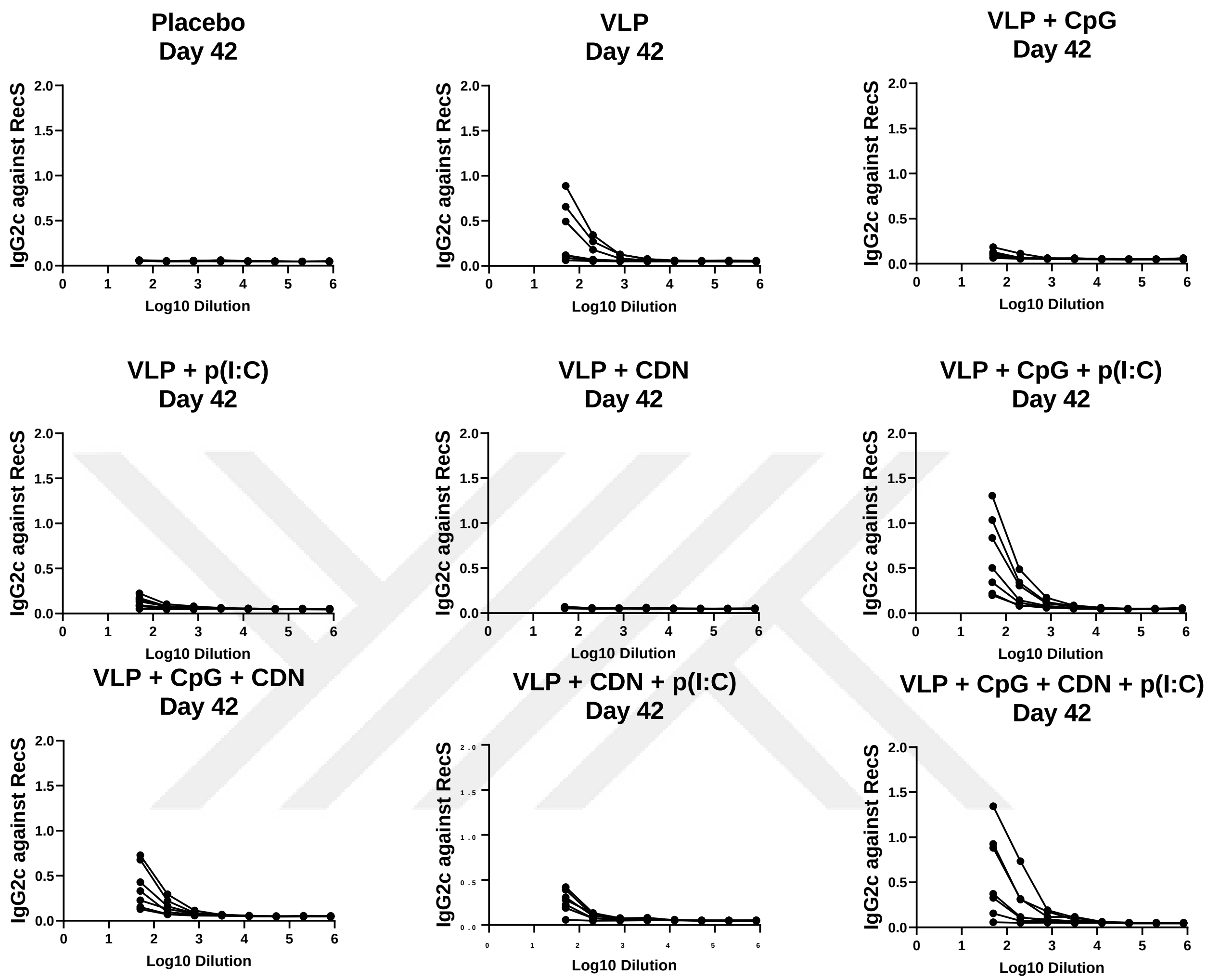

Figure A.7. IgG1 responses of the mice injected with VLP with single, dual or triple adjuvant combinations with K-type CpG ODN, poly(I:C), and 2,3-cGAMP four weeks after the second injection against in-house recombinant trimeric Spike protein. Each graph represents one group of mice injected with the corresponding vaccine combination.

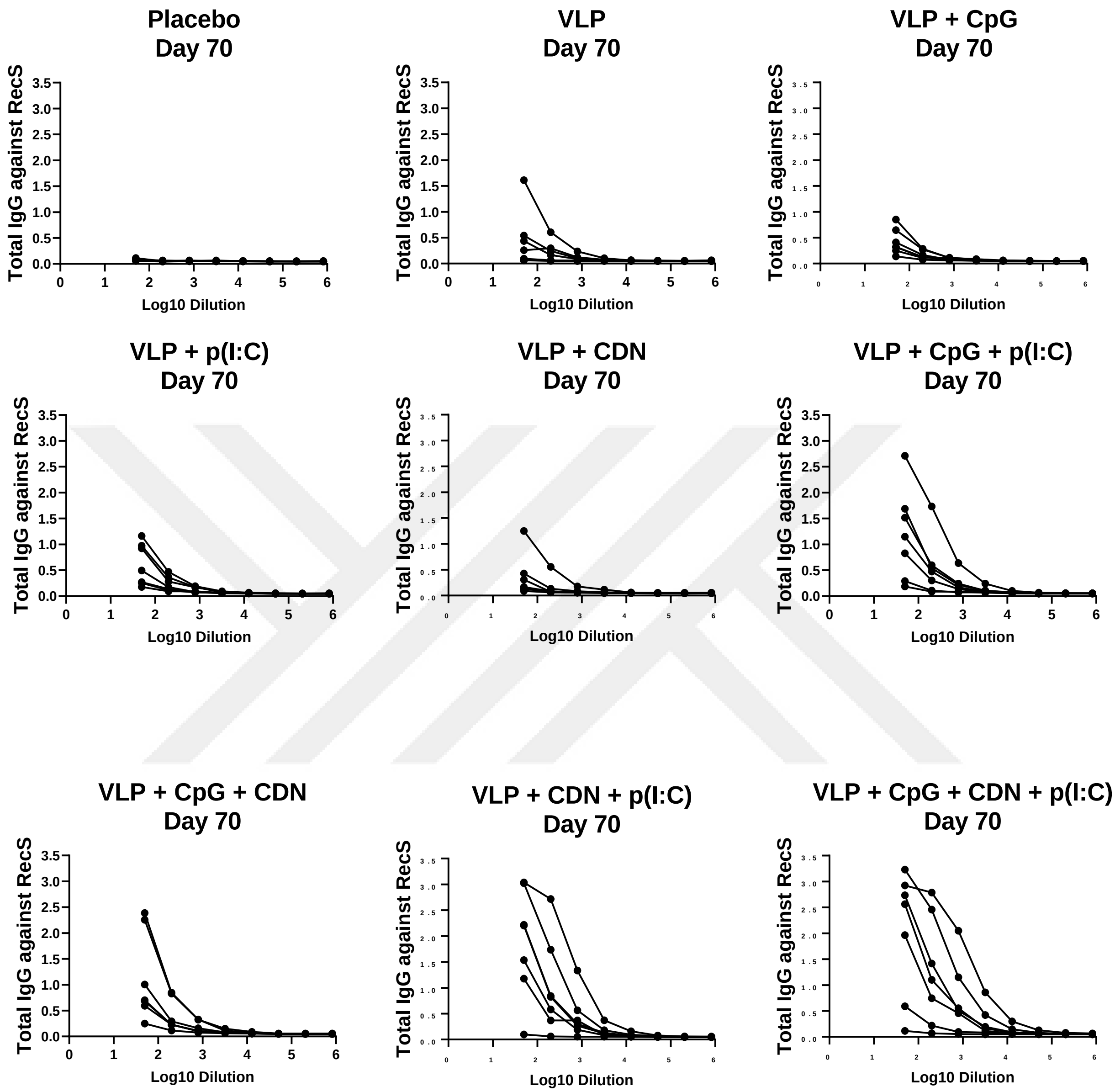

Figure A.8. Total IgG responses of the mice injected with VLP with single, dual or triple adjuvant combinations with K-type CpG ODN, poly(I:C), and 2,3-cGAMP two months after the second injection against in-house recombinant trimeric Spike protein. Each graph represents one group of mice injected with the corresponding vaccine combination.

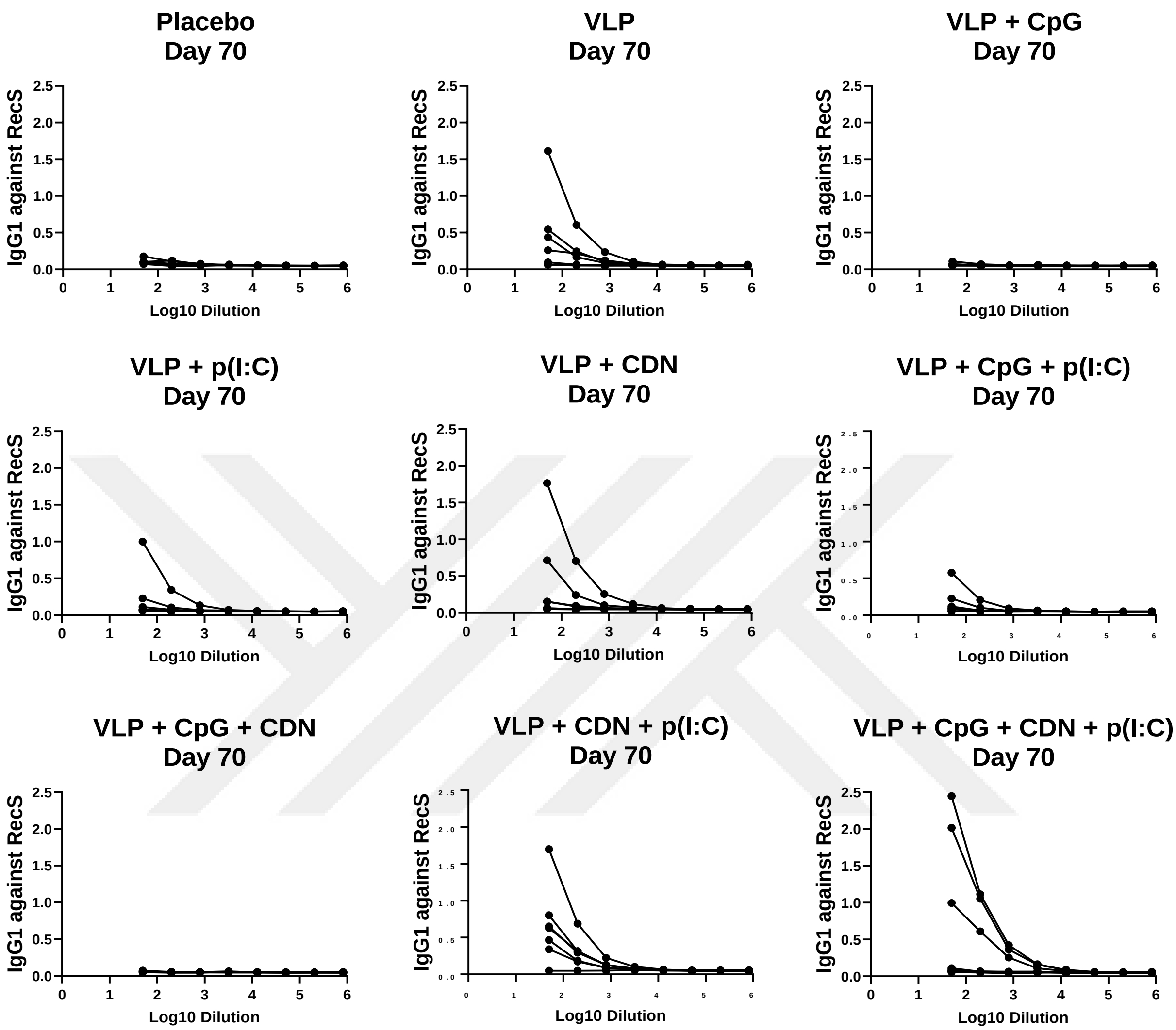

Figure A.9. IgG1 responses of the mice injected with VLP with single, dual or triple adjuvant combinations with K-type CpG ODN, poly(I:C), and 2,3-cGAMP two months after the second injection against in-house recombinant trimeric Spike protein. Each graph represents one group of mice injected with the corresponding vaccine combination.

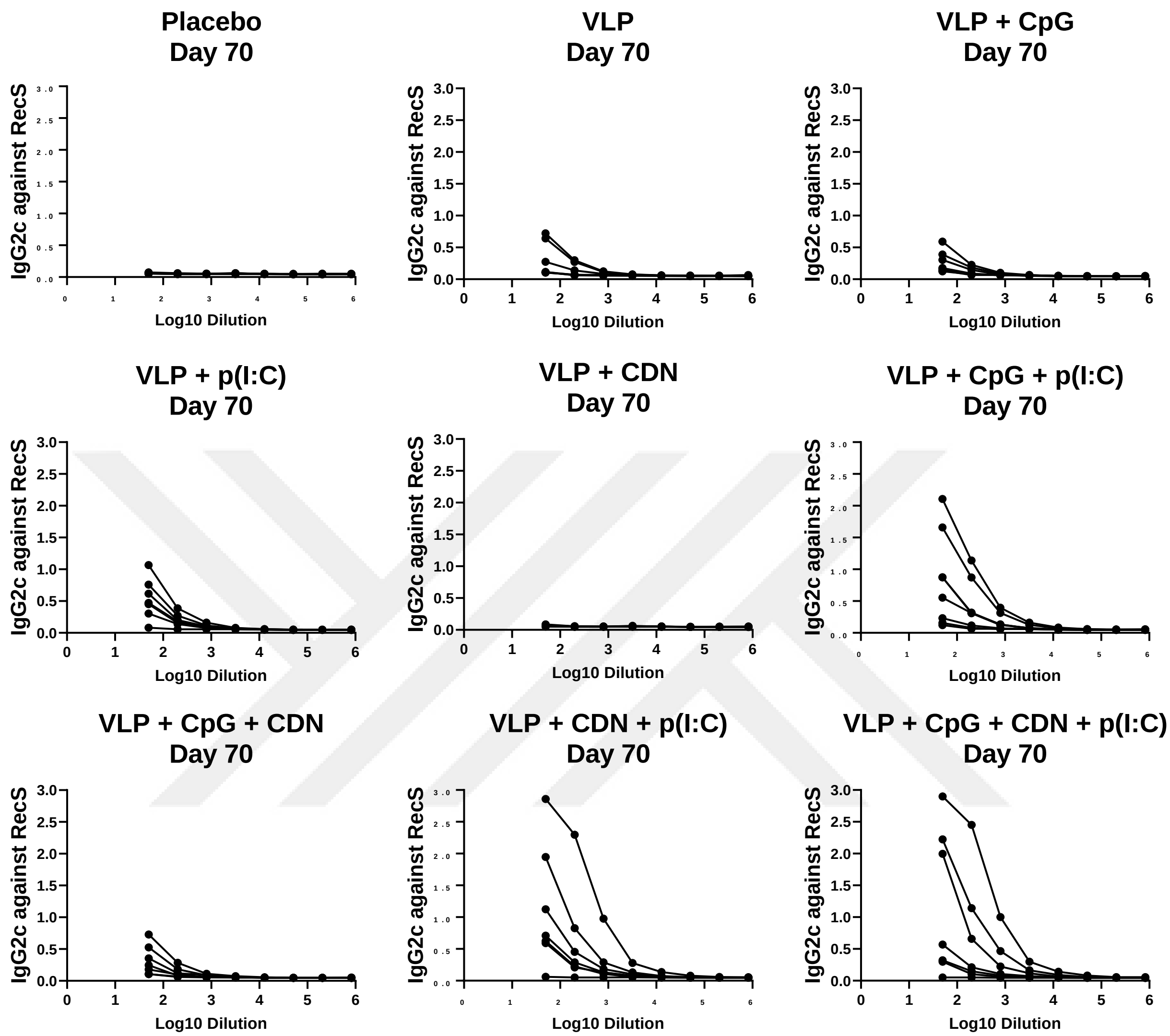

Figure A.10. IgG2c responses of the mice injected with VLP with single, dual or triple adjuvant combinations with K-type CpG ODN, poly(I:C), and 2,3-cGAMP two months after the second injection against in-house recombinant trimeric Spike protein. Each graph represents one group of mice injected with the corresponding vaccine combination.

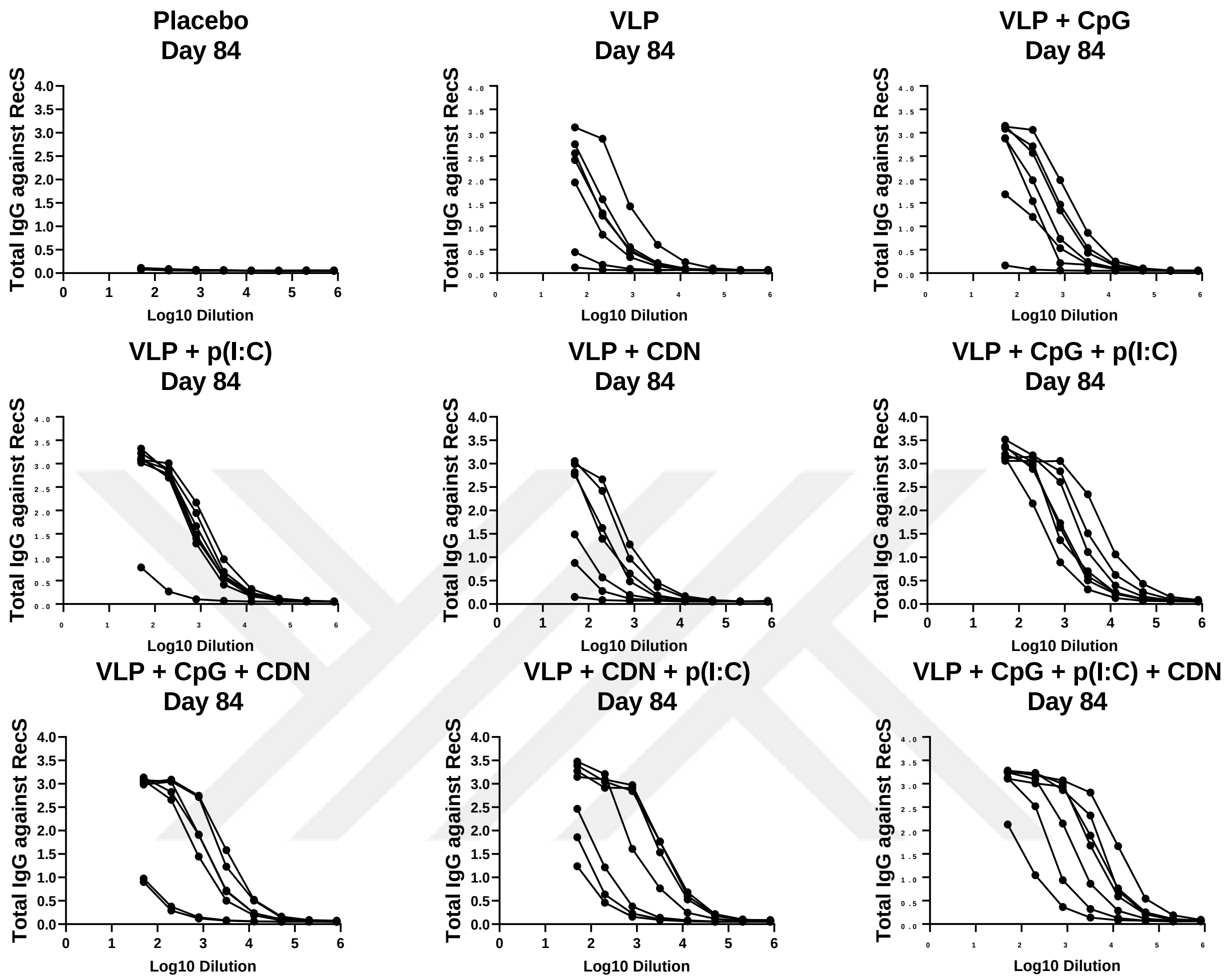

Figure A.11. Total IgG responses of the mice injected with VLP with single, dual or triple adjuvant combinations with K-type CpG ODN, poly(I:C), and 2,3-cGAMP two weeks after the third injection against in-house recombinant trimeric Spike protein. Each graph represents one group of mice injected with the corresponding vaccine combination.

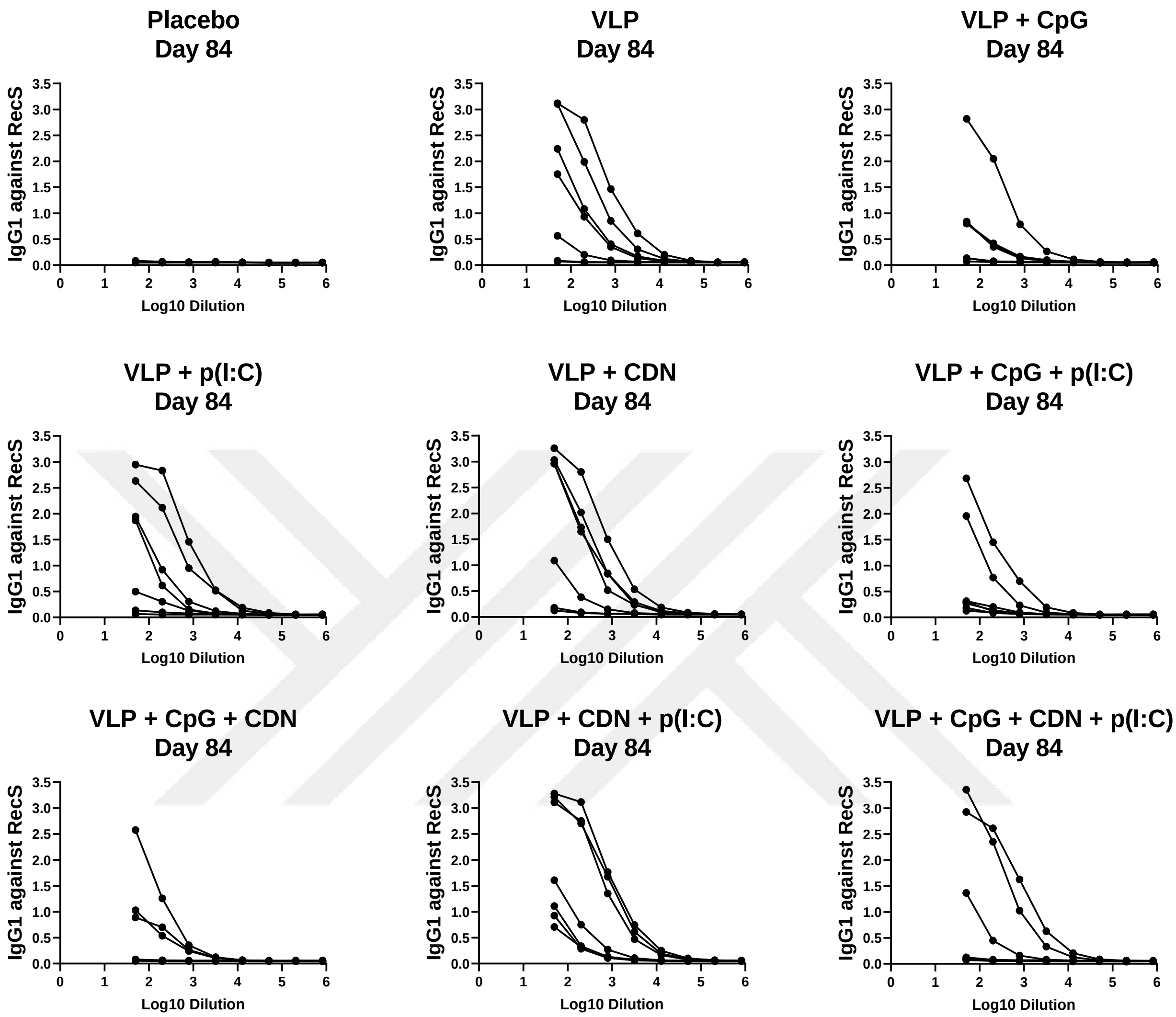

Figure A.12. IgG1 responses of the mice injected with VLP with single, dual or triple adjuvant combinations with K-type CpG ODN, poly(I:C), and 2,3-cGAMP two weeks after the third injection against in-house recombinant trimeric Spike protein. Each graph represents one group of mice injected with the corresponding vaccine combination.

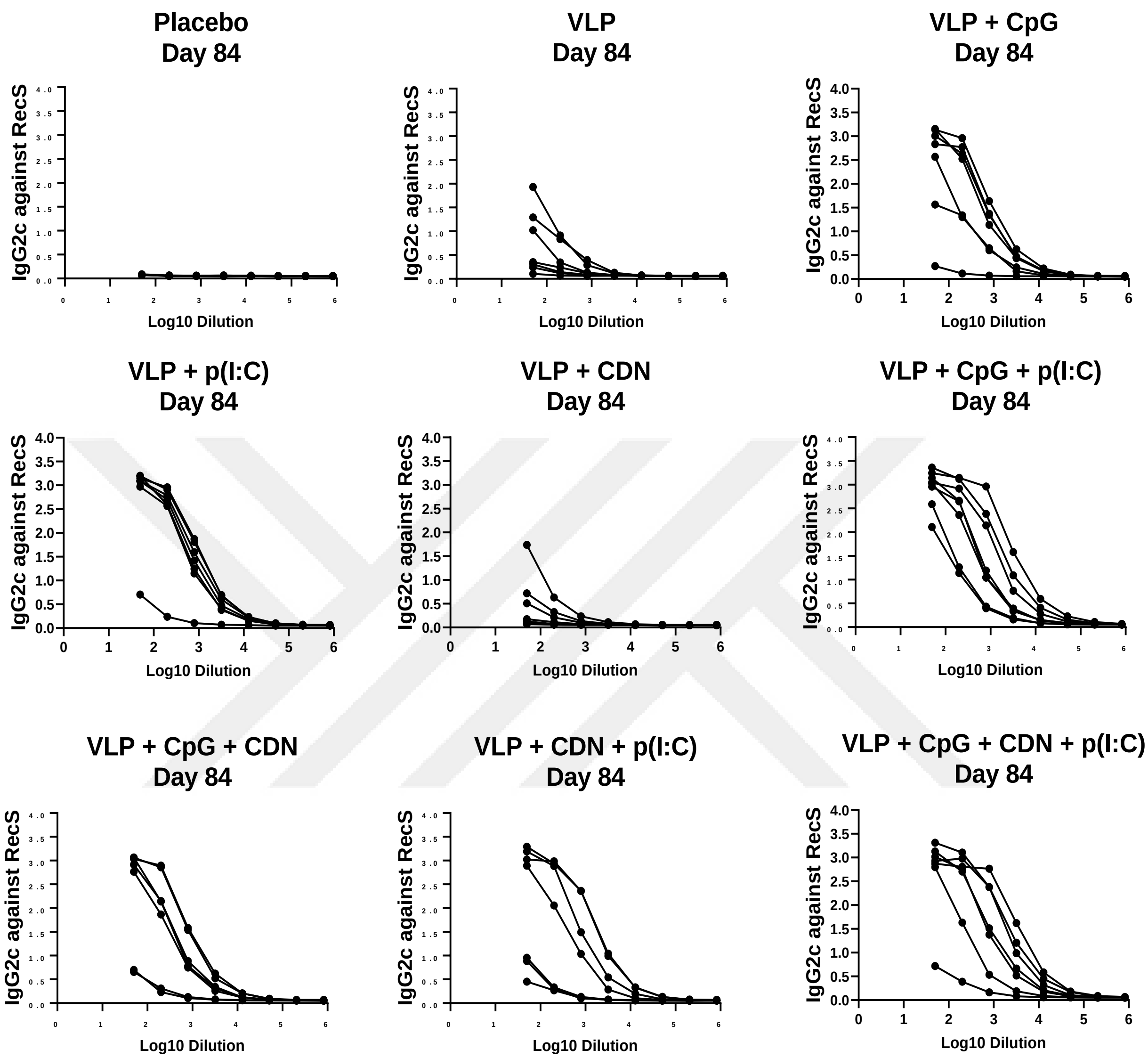

Figure A.13. IgG2c responses of the mice injected with VLP with single, dual or triple adjuvant combinations with K-type CpG ODN, poly(I:C), and 2,3-cGAMP two weeks after the third injection against in-house recombinant trimeric Spike protein. Each graph represents one group of mice injected with the corresponding vaccine combination.

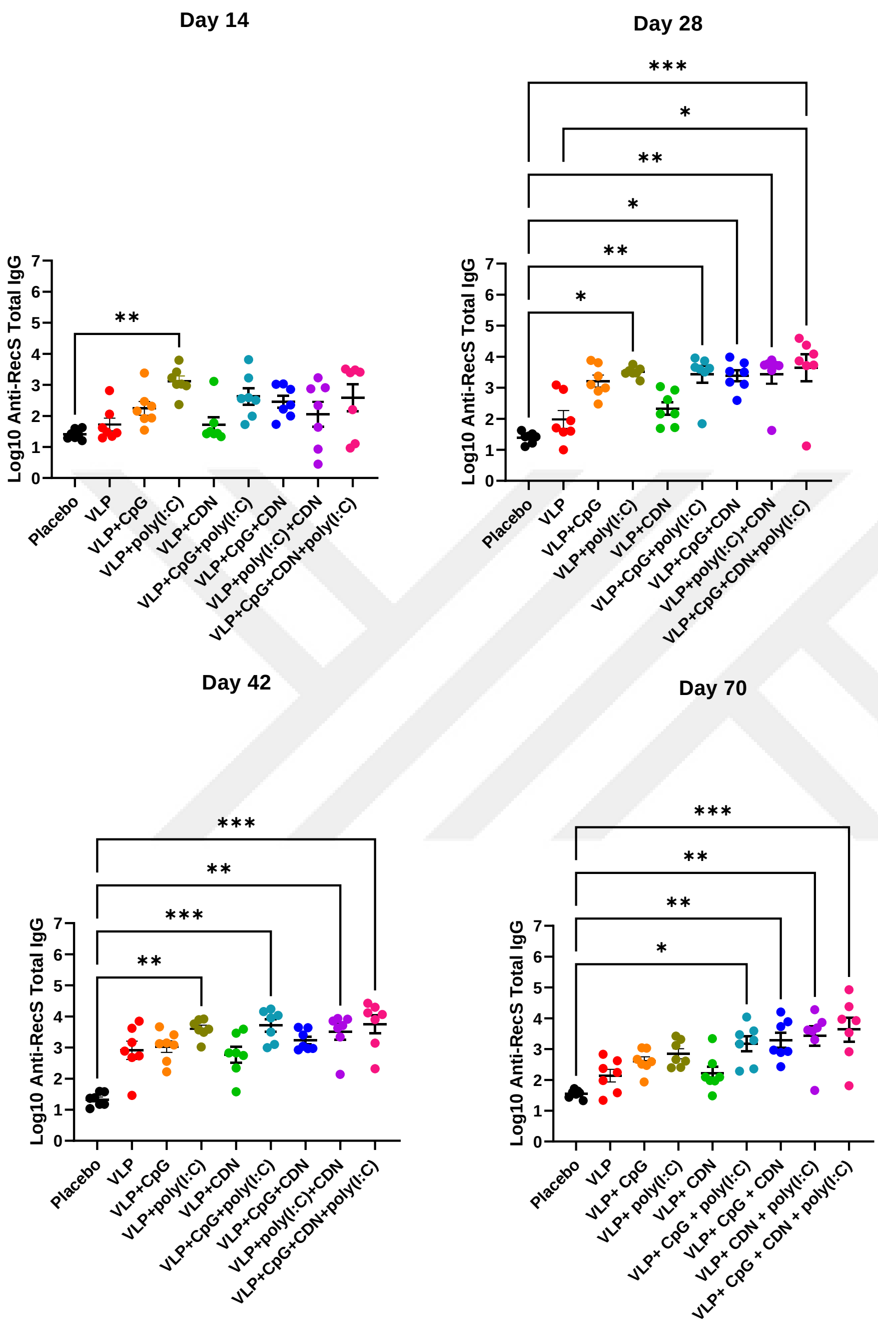
Day 14
Log10 Anti-RecS Total IgG
**
Placebo
VLP
VLP+CpG
VLP+poly(I:C)
VLP+CDN
VLP+CpG+poly(I:C)
VLP+CpG+CDN
VLP+poly(I:C)+CDN
VLP+CpG+CDN+poly(I:C)
Day 28
Log10 Anti-RecS Total IgG
***
*
**
*
**
*
Placebo
VLP
VLP+CpG
VLP+poly(I:C)
VLP+CDN
VLP+CpG+poly(I:C)
VLP+CpG+CDN
VLP+poly(I:C)+CDN
VLP+CpG+CDN+poly(I:C)
Day 42
Log10 Anti-RecS Total IgG
***
**
***
**
Placebo
VLP
VLP+CpG
VLP+poly(I:C)
VLP+CDN
VLP+CpG+poly(I:C)
VLP+CpG+CDN
VLP+poly(I:C)+CDN
VLP+CpG+CDN+poly(I:C)
Day 70
Log10 Anti-RecS Total IgG
***
**
**
*
Placebo
VLP
VLP+ CpG
VLP+ poly(I:C)
VLP+ CDN
VLP+ CpG + poly(I:C)
VLP+ CpG + CDN
VLP+ CDN + poly(I:C)
VLP+ CpG + CDN + poly(I:C)

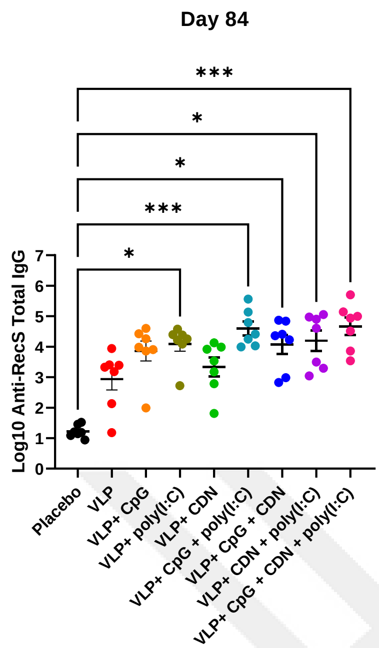

Figure A.14. Antibody responses of vaccinated male C57BL/6 mice (n=7/group) against in-house recombinant trimeric Spike Protein. Cellular immune response against homemade recombinant spike protein A) two weeks after the primary injection; B) two weeks after the booster injection; C) four weeks after the primary injection D) eight weeks after the booster injection; E) two weeks after the third dose of vaccination. Groups were compared with one-way ANOVA with Kruskal-Wallis test. P < .05, **P < .01, *P < .001, ***P < .0001.

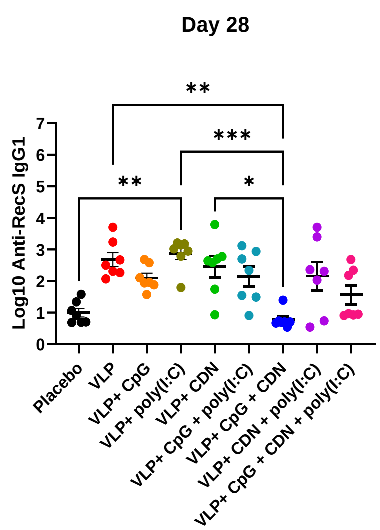

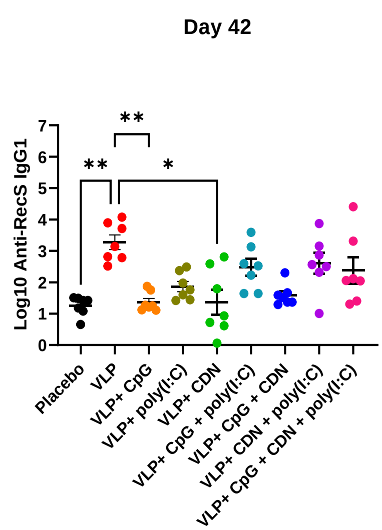

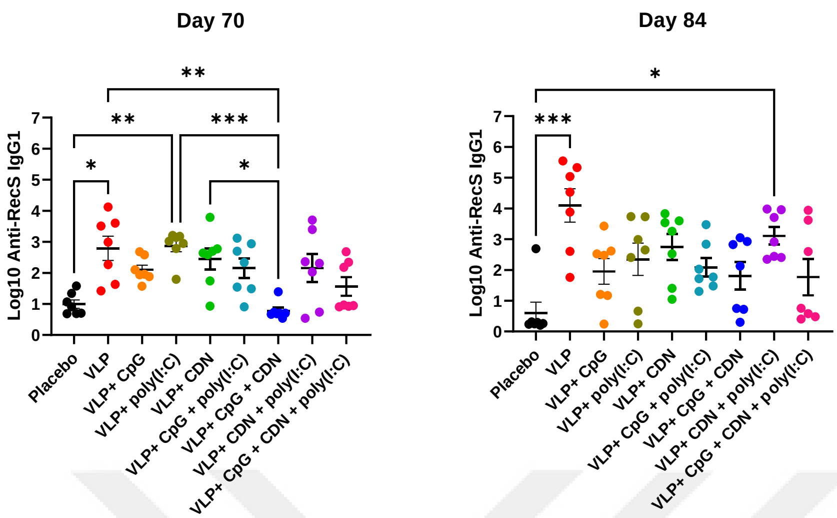

Figure A.15. IgG1 responses of vaccinated male C57BL/6 mice (n=7/group) against in-house recombinant trimeric Spike Protein. Cellular immune response against homemade recombinant spike protein A) two weeks after the booster injection; B) four weeks after the primary injection C) eight weeks after the booster injection; D) two weeks after the third vaccination dose. Groups were compared with one-way ANOVA with Kruskal-Wallis test. P < .05, **P < .01, *P < .001, ***P < .0001.

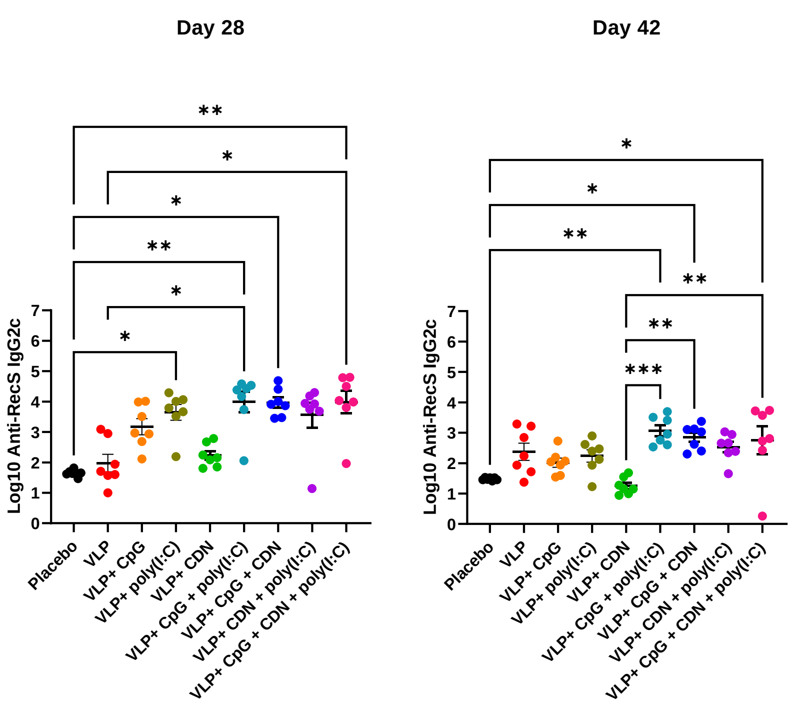

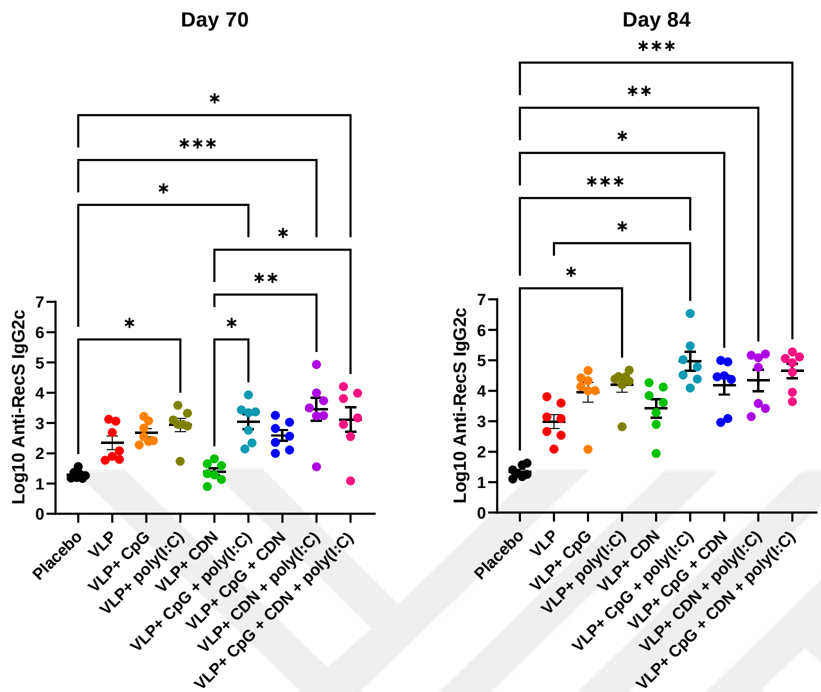

Figure A.16. IgG2c responses of vaccinated male C57BL/6 mice (n=7/group) against in-house recombinant trimeric Spike Protein. Cellular immune response against homemade recombinant spike protein A) two weeks after the booster injection; B) four weeks after the primary injection C) eight weeks after the booster injection; D) two weeks after the third vaccination dose. Groups were compared with one-way ANOVA with Kruskal-Wallis test. P < .05, **P < .01, *P < .001, ***P < .0001.

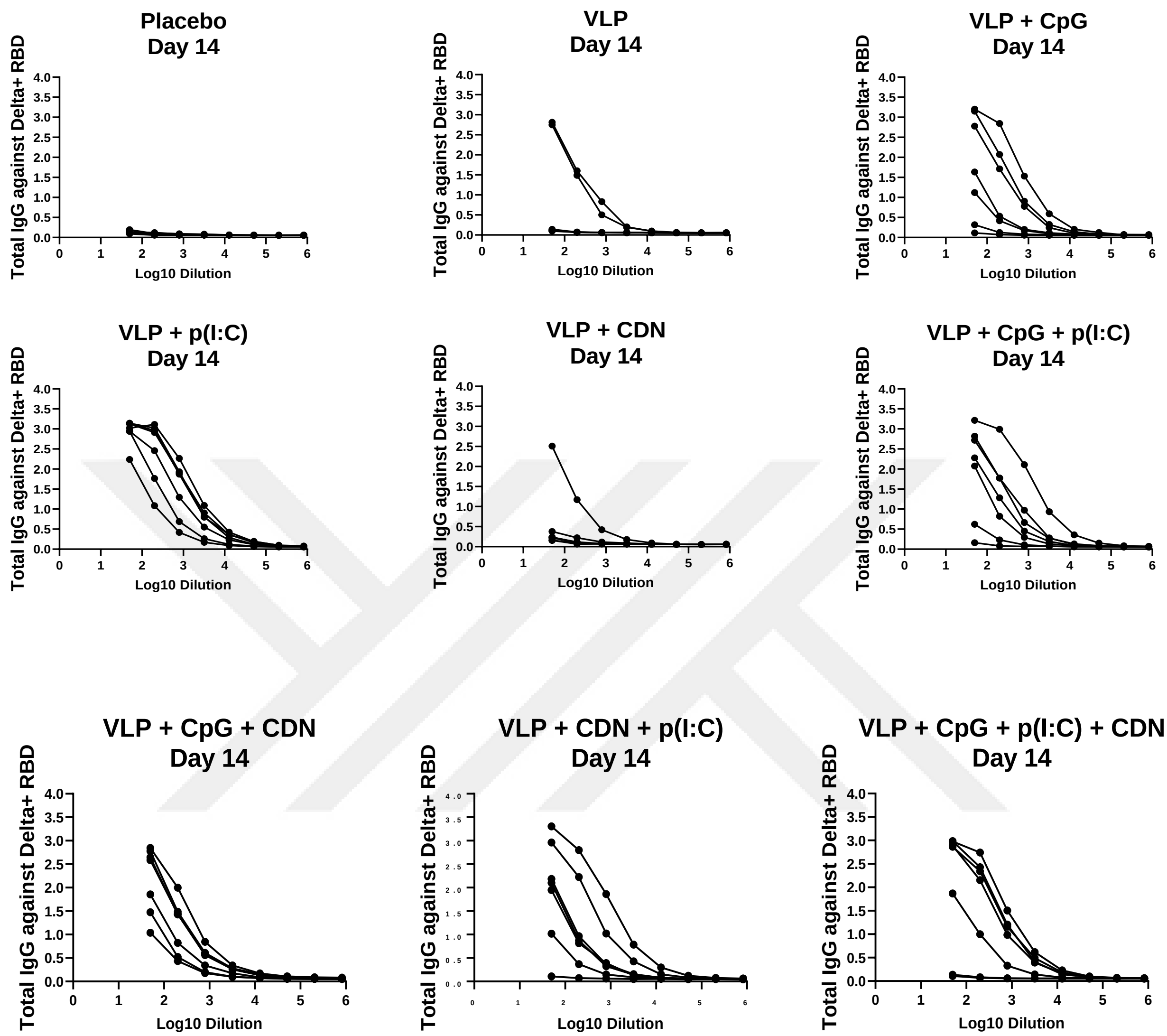

Figure A.17. Total IgG responses of the mice injected with VLP with single, dual or triple adjuvant combinations with K-type CpG ODN, poly(I:C), and 2,3-cGAMP two weeks after the first injection against Delta+ RBD protein. Each graph represents one group of mice injected with the corresponding vaccine combination.

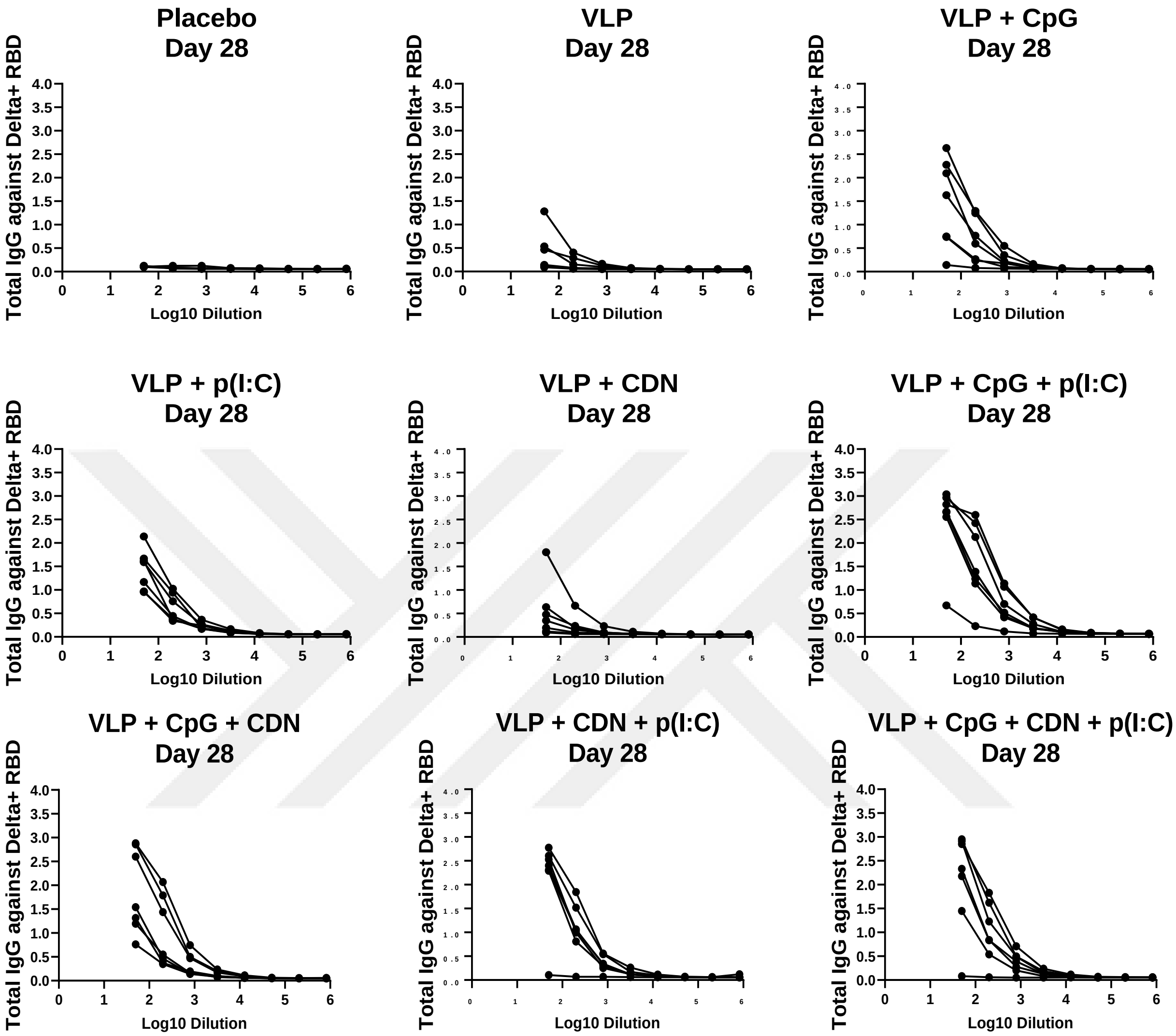

Figure A.18. Total IgG responses of the mice injected with VLP with single, dual or triple adjuvant combinations with K-type CpG ODN, poly(I:C), and 2,3-cGAMP two weeks after the second injection against Delta+ RBD protein. Each graph represents one group of mice injected with the corresponding vaccine combination.

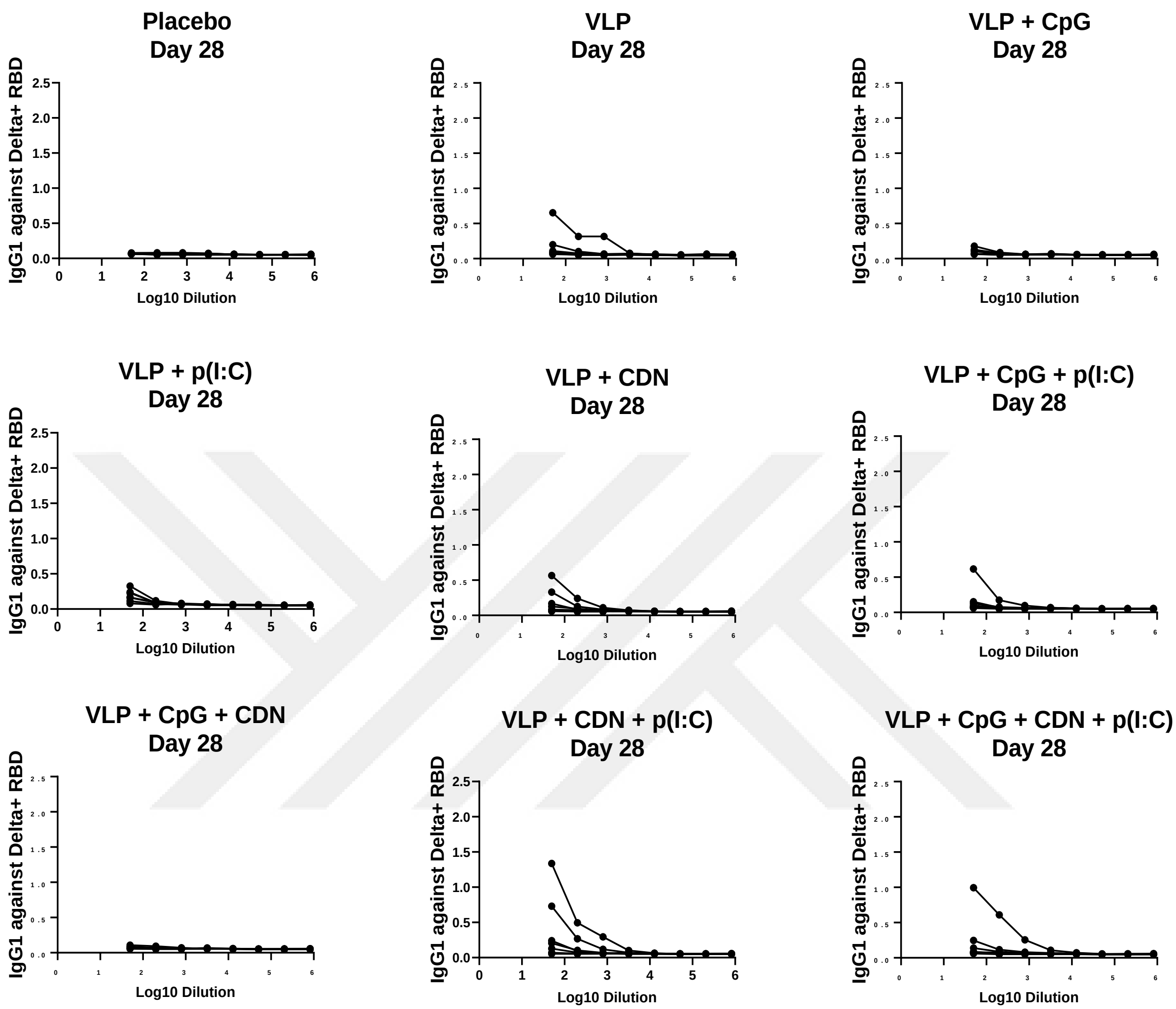

Figure A.19. IgG1 responses of the mice injected with VLP with single, dual or triple adjuvant combinations with K-type CpG ODN, poly(I:C), and 2,3-cGAMP two weeks after the second injection against Delta+ RBD protein. Each graph represents one group of mice injected with the corresponding vaccine combination.

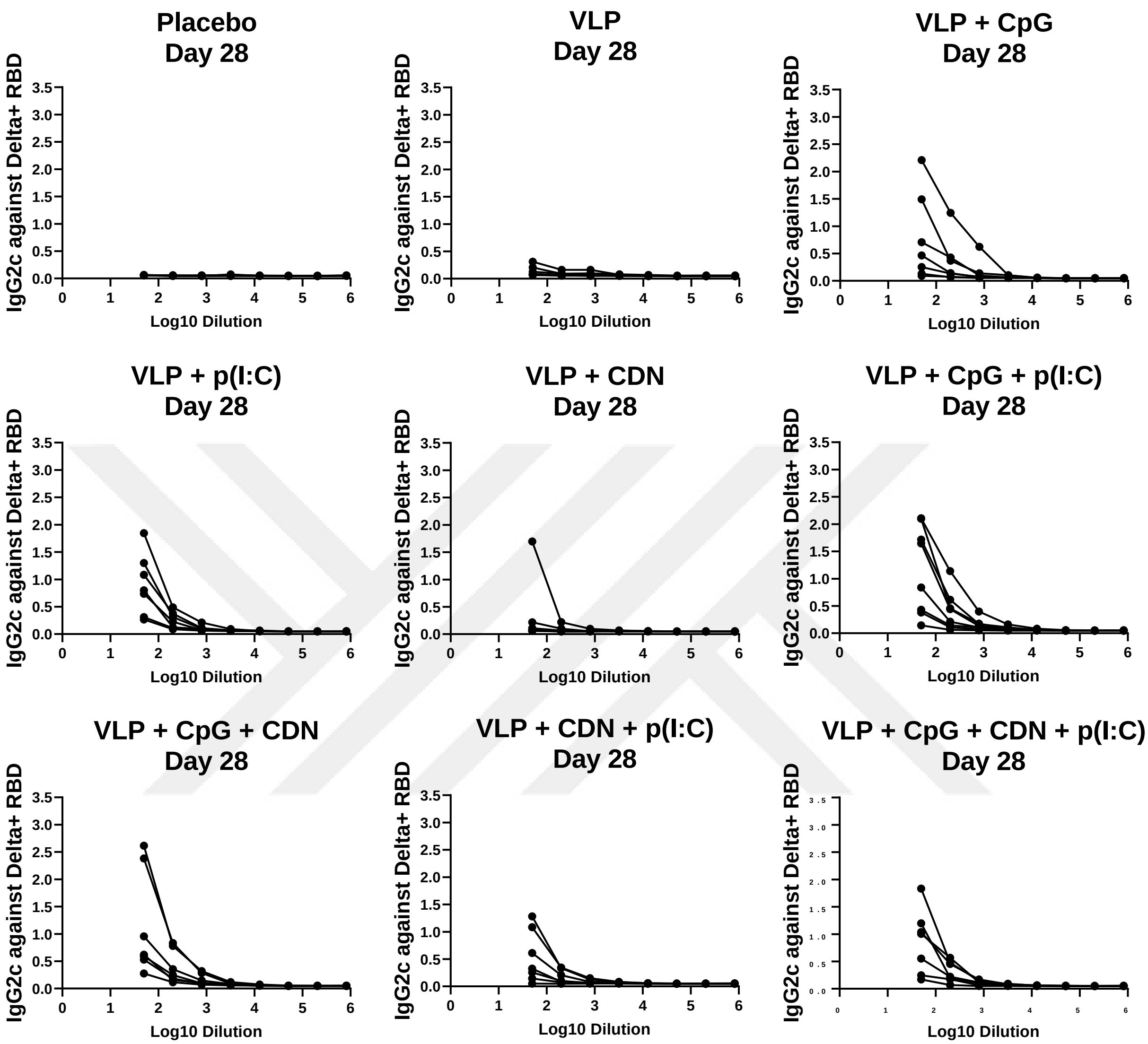

Figure A.20. IgG2c responses of the mice injected with VLP with single, dual or triple adjuvant combinations with K-type CpG ODN, poly(I:C), and 2,3-cGAMP two weeks after the second injection against Delta+ RBD protein. Each graph represents one group of mice injected with the corresponding vaccine combination.

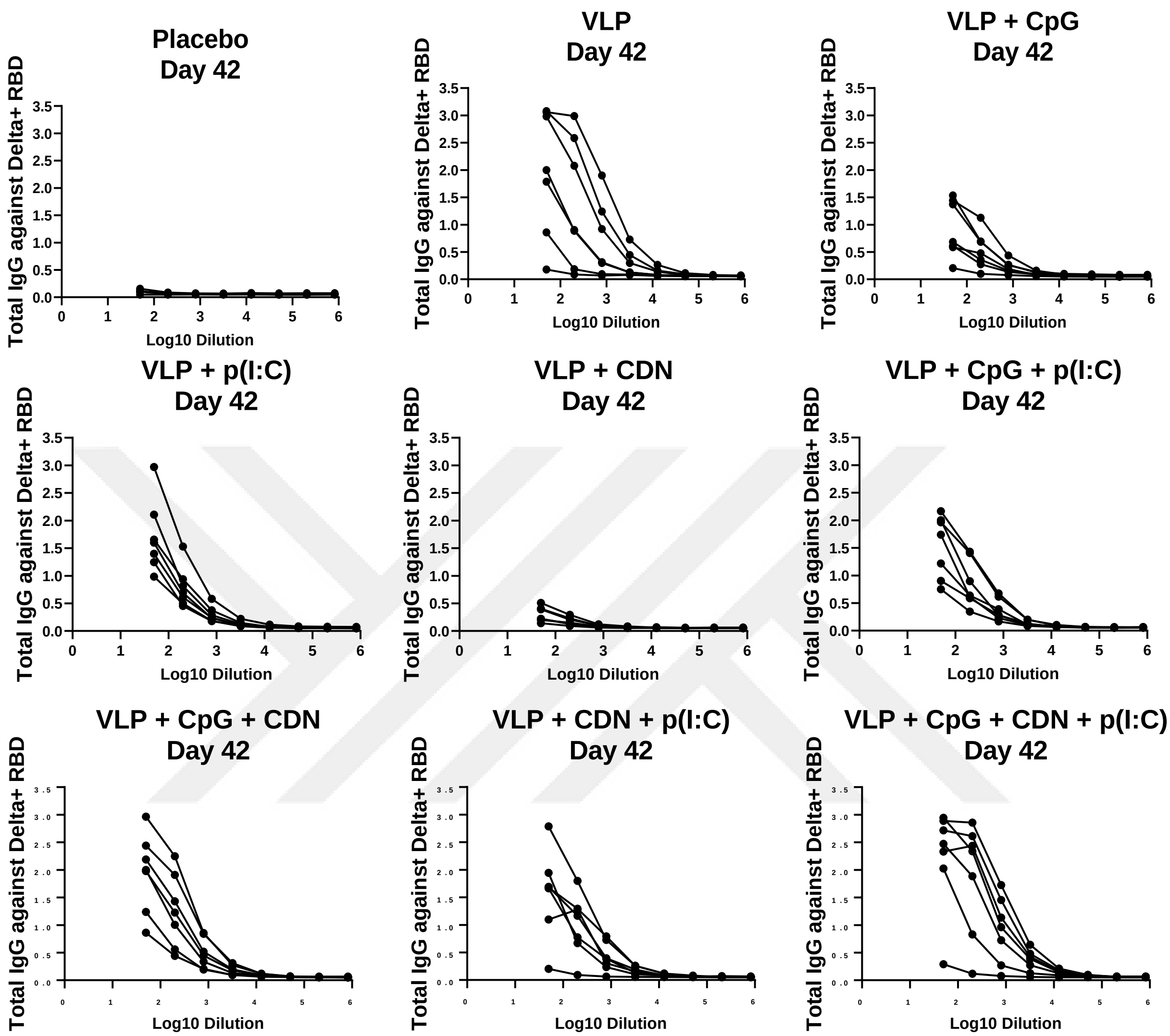

Figure A.21. Total IgG responses of the mice injected with VLP with single, dual or triple adjuvant combinations with K-type CpG ODN, poly(I:C), and 2,3-cGAMP one month after the second injection against Delta+ RBD protein. Each graph represents one group of mice injected with the corresponding vaccine combination.

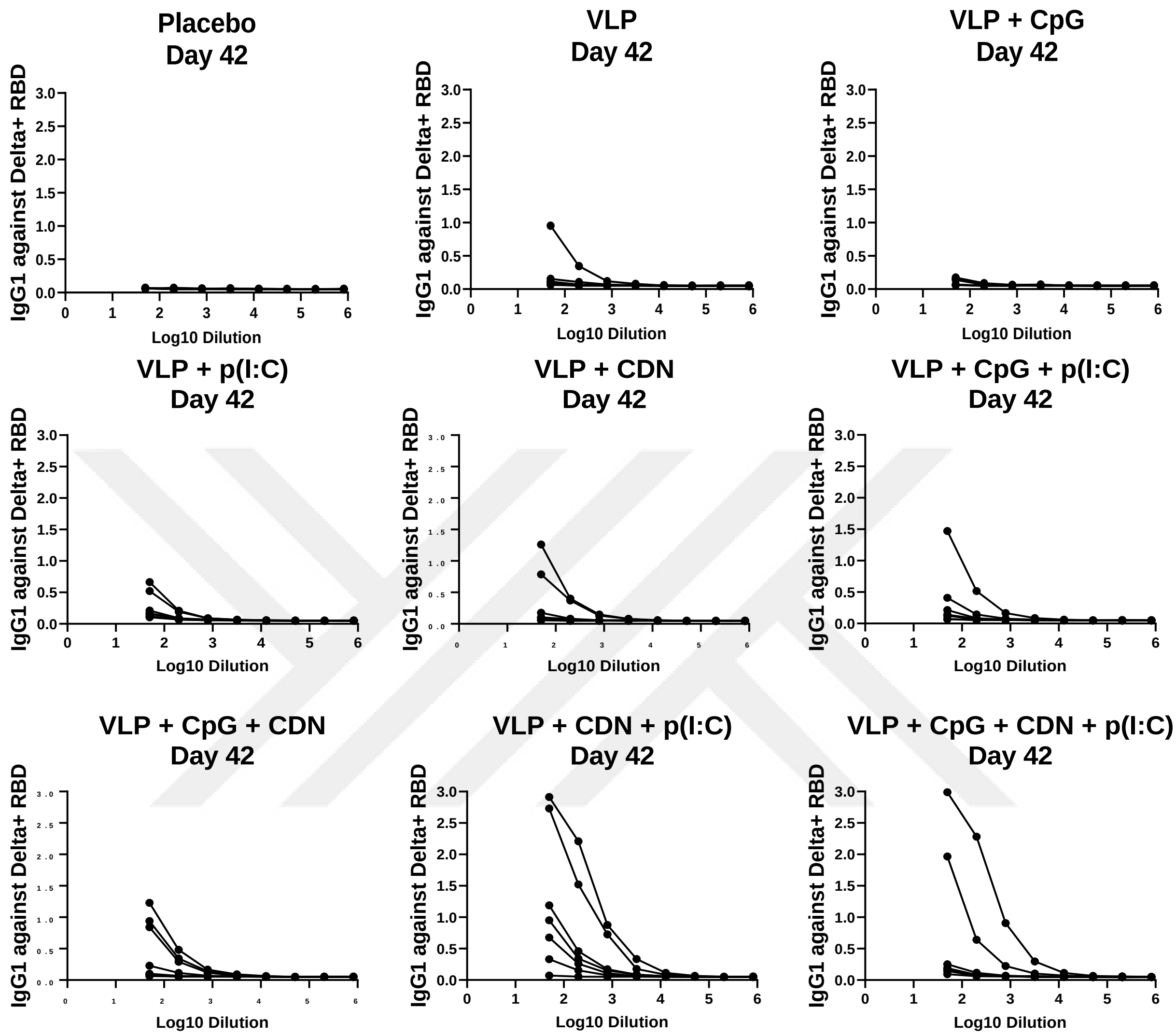

Figure A.22. IgG1 responses of the mice injected with VLP with single, dual or triple adjuvant combinations with K-type CpG ODN, poly(I:C), and 2,3-cGAMP one month after the second injection against Delta+ RBD protein. Each graph represents one group of mice injected with the corresponding vaccine combination.

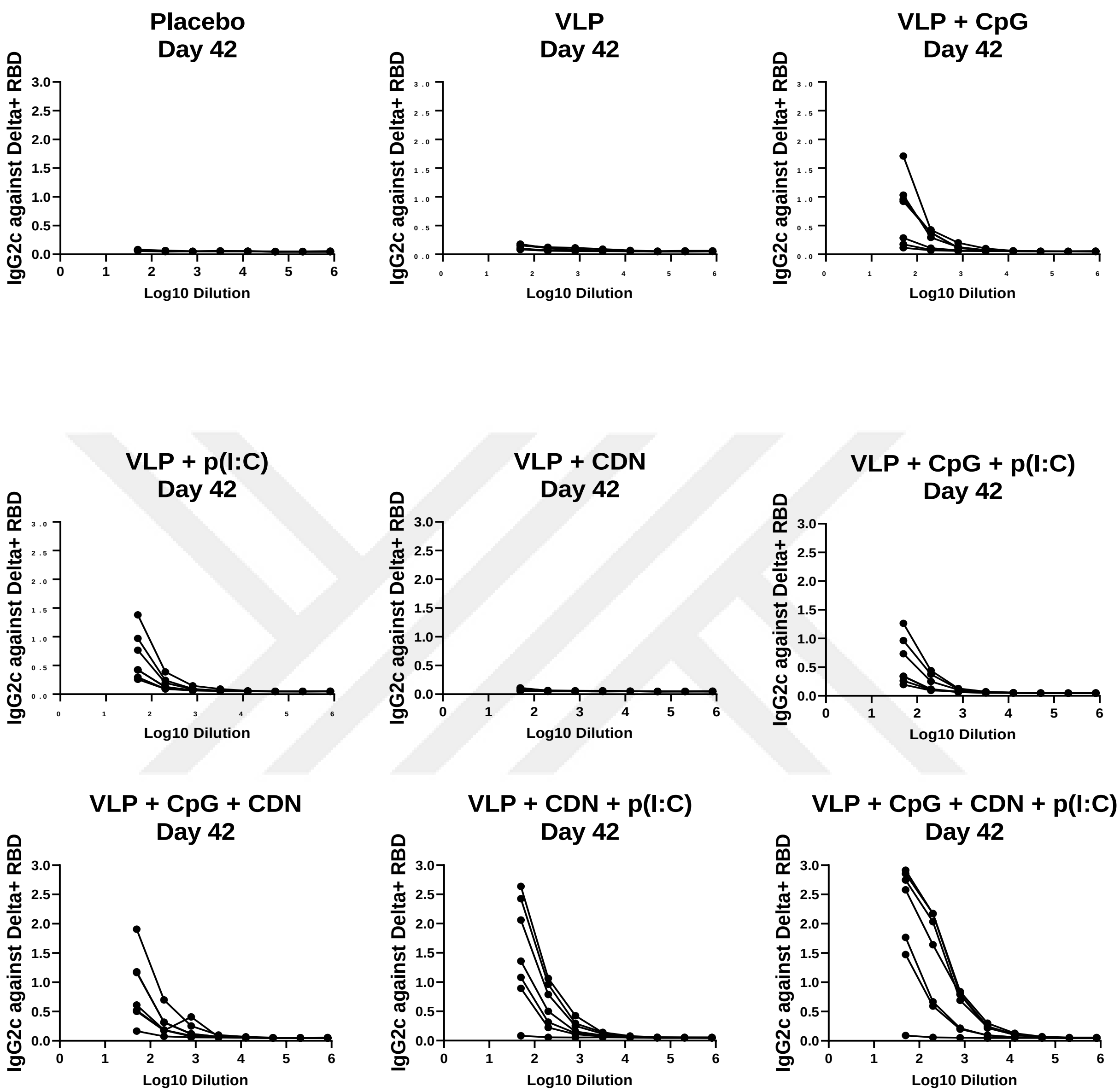

Figure A.23. IgG2c responses of the mice injected with VLP with single, dual or triple adjuvant combinations with K-type CpG ODN, poly(I:C), and 2,3-cGAMP one month after the second injection against Delta+ RBD protein. Each graph represents one group of mice injected with the corresponding vaccine combination.

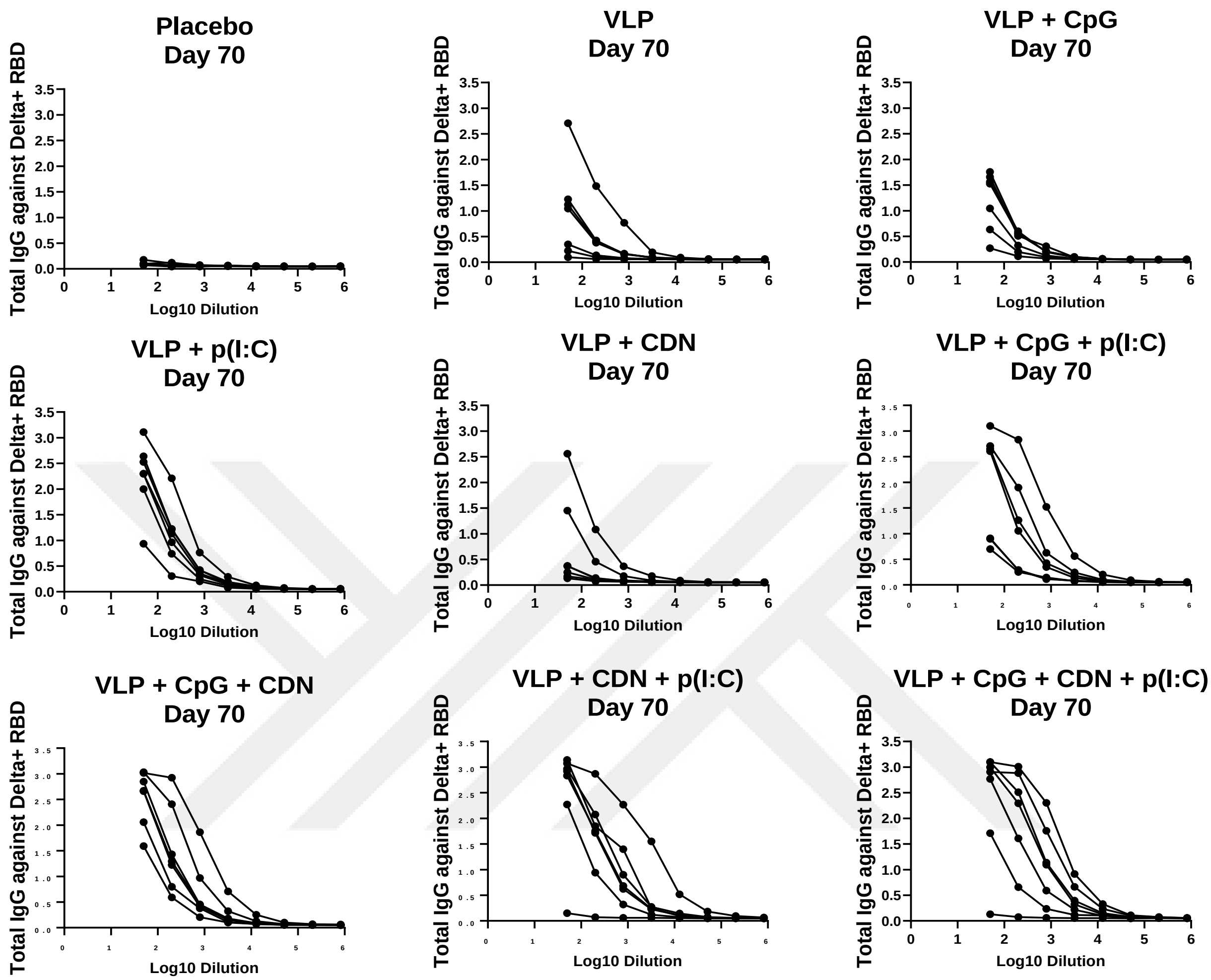

Figure A.24. Total IgG responses of the mice injected with VLP with single, dual or triple adjuvant combinations with K-type CpG ODN, poly(I:C), and 2,3-cGAMP two months after the second injection against Delta+ RBD protein. Each graph represents one group of mice injected with the corresponding vaccine combination.

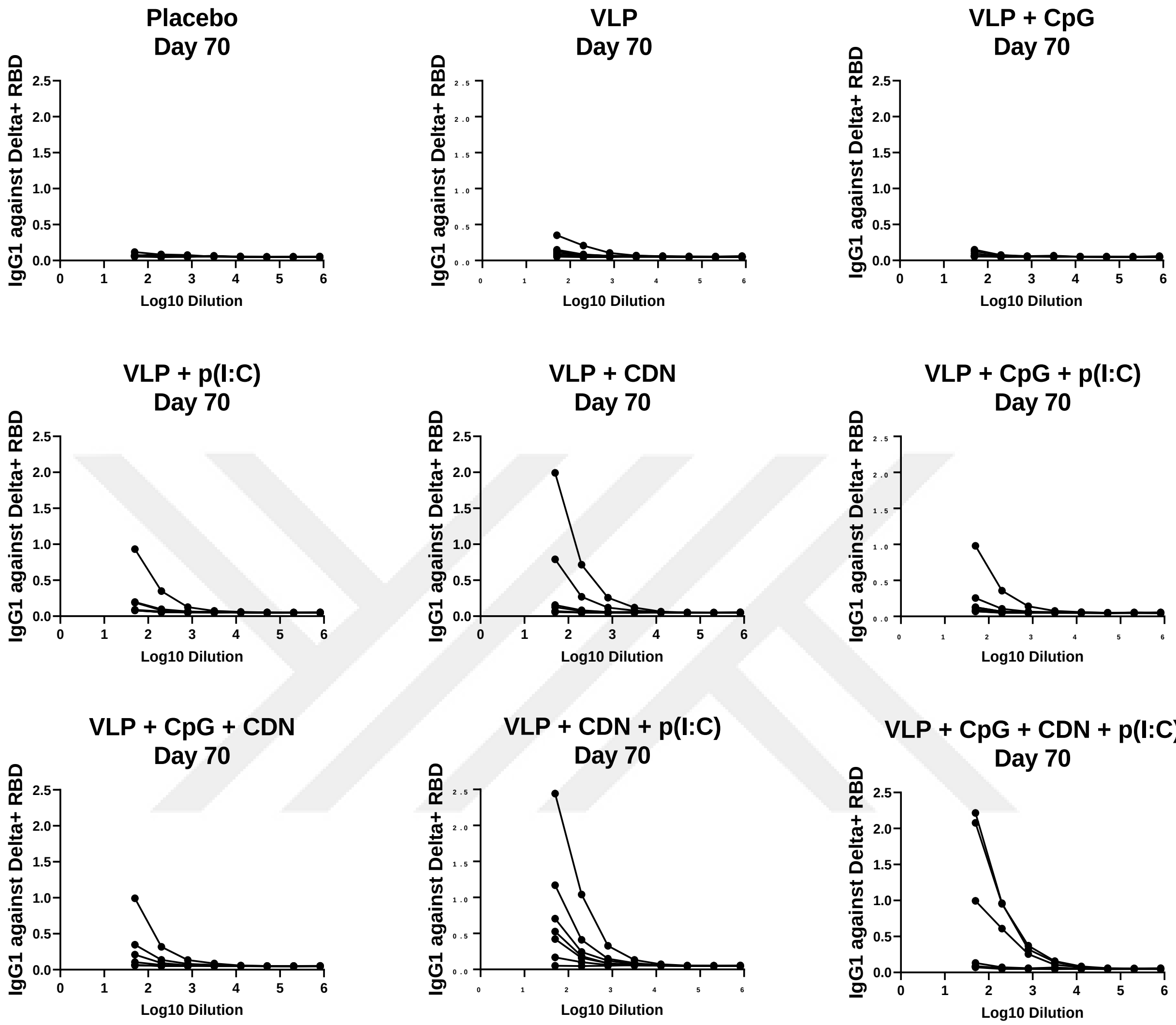

Figure A.25. IgG1 responses of the mice injected with VLP with single, dual or triple adjuvant combinations with K-type CpG ODN, poly(I:C), and 2,3-cGAMP two months after the second injection against Delta+ RBD protein. Each graph represents one group of mice injected with the corresponding vaccine combination.

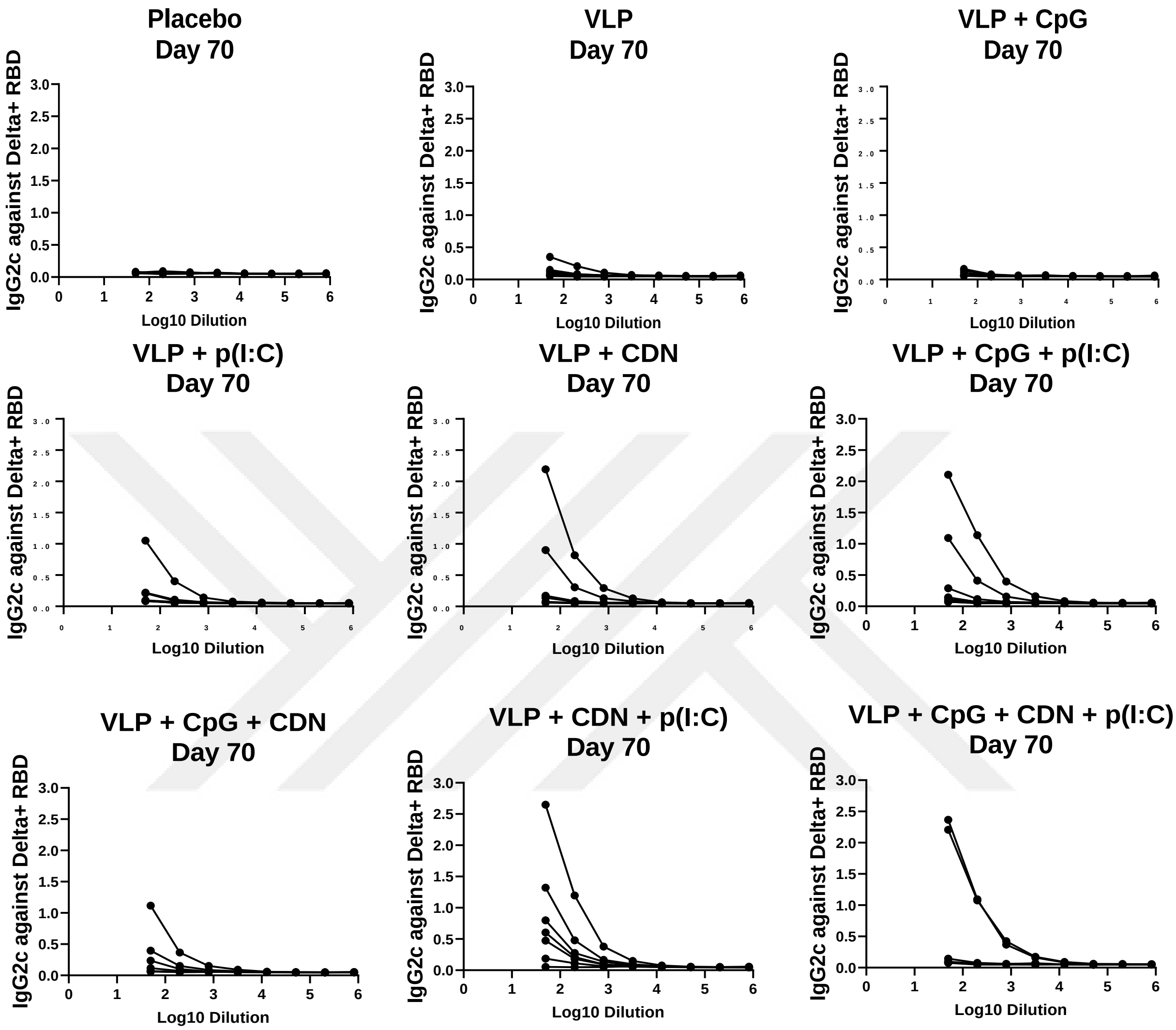

Figure A.26. IgG2c responses of the mice injected with VLP with single, dual or triple adjuvant combinations with K-type CpG ODN, poly(I:C), and 2,3-cGAMP two months after the second injection against Delta+ RBD protein. Each graph represents one group of mice injected with the corresponding vaccine combination.

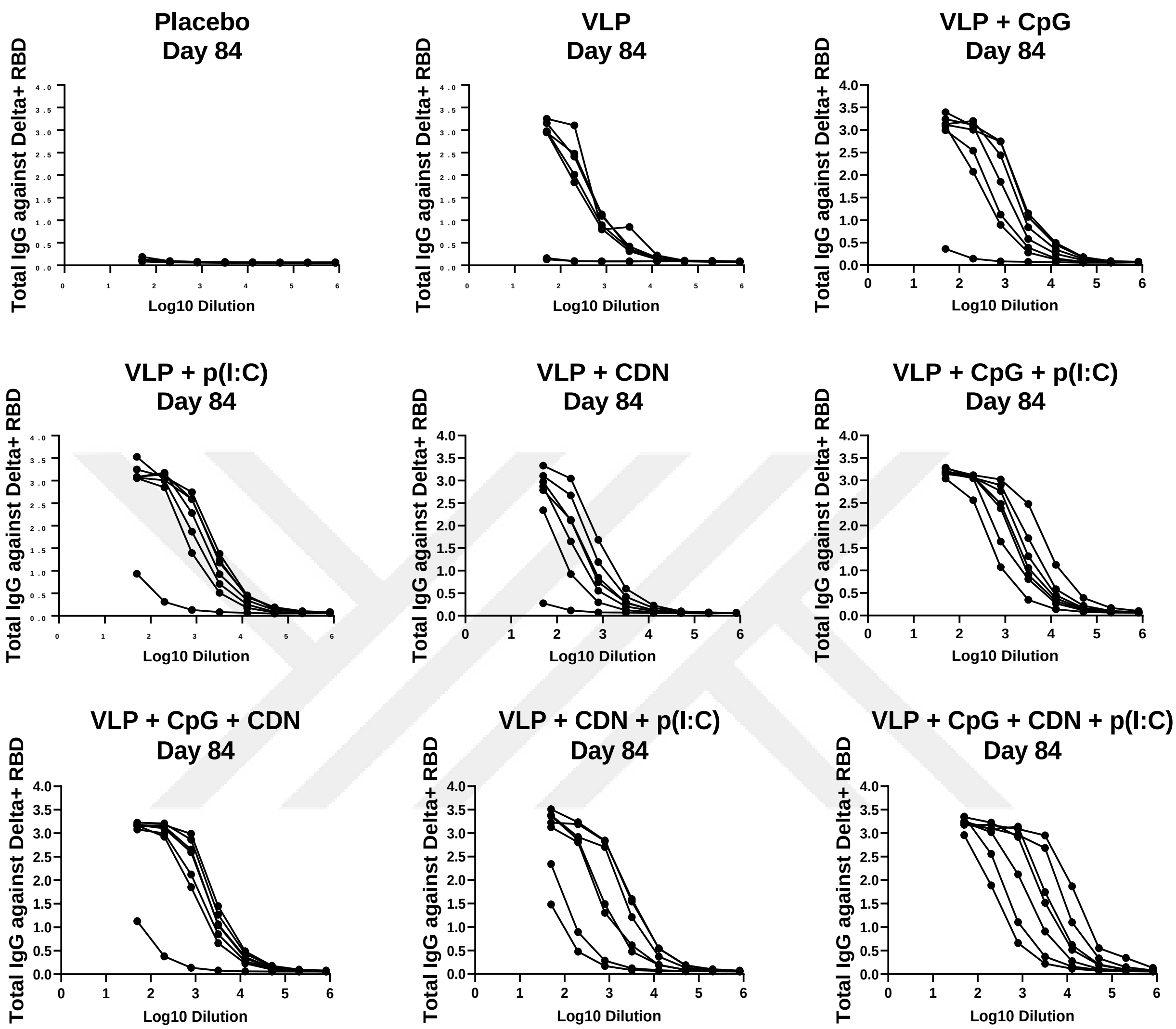

Figure A.27. Total IgG responses of the mice injected with VLP with single, dual or triple adjuvant combinations with K-type CpG ODN, poly(I:C), and 2,3-cGAMP two weeks after the third injection against Delta+ RBD protein. Each graph represents one group of mice injected with the corresponding vaccine combination.

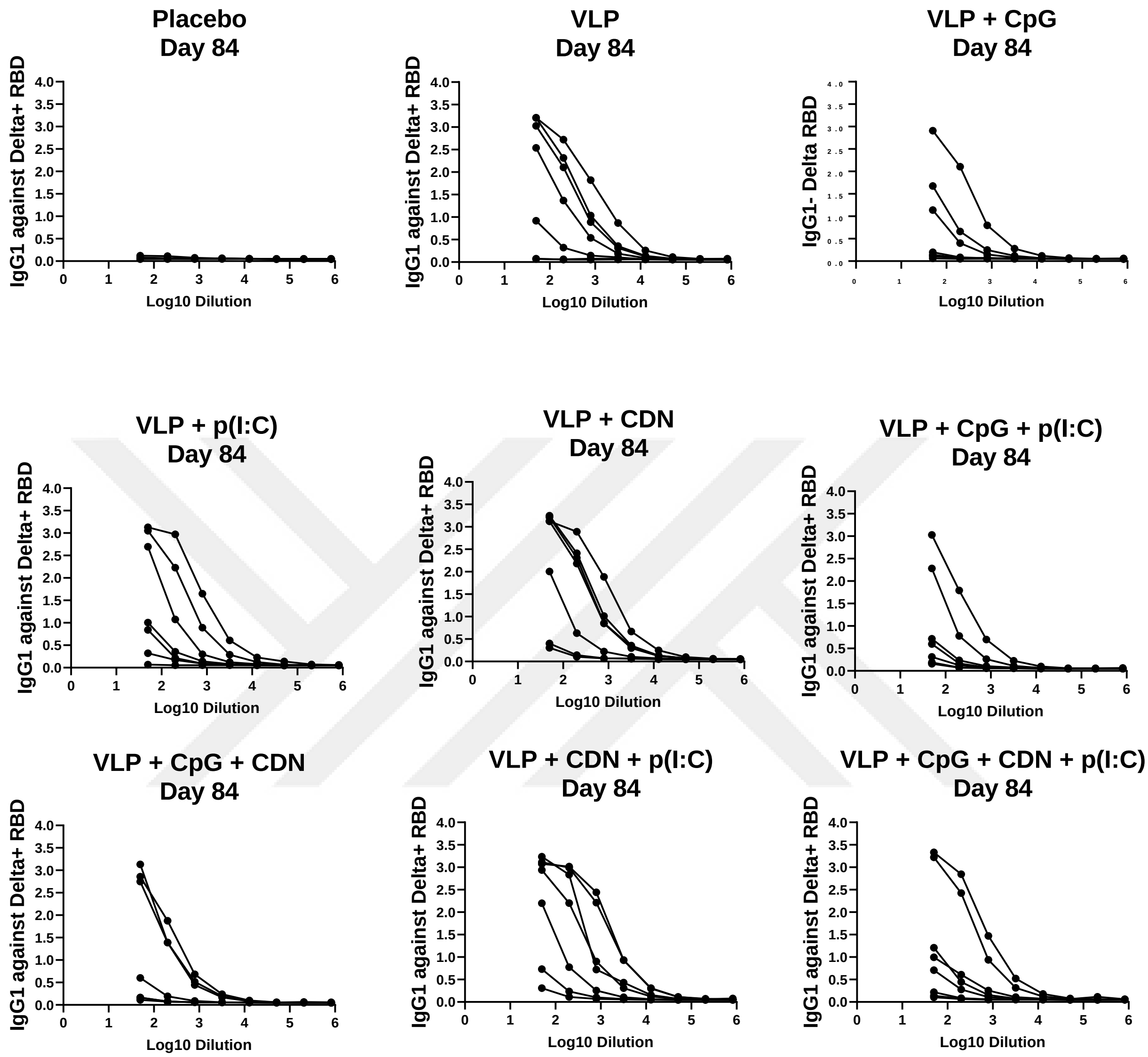

Figure A.28. IgG1 responses of the mice injected with VLP with single, dual or triple adjuvant combinations with K-type CpG ODN, poly(I:C), and 2,3-cGAMP two weeks after the third injection against Delta+ RBD protein. Each graph represents one group of mice injected with the corresponding vaccine combination.

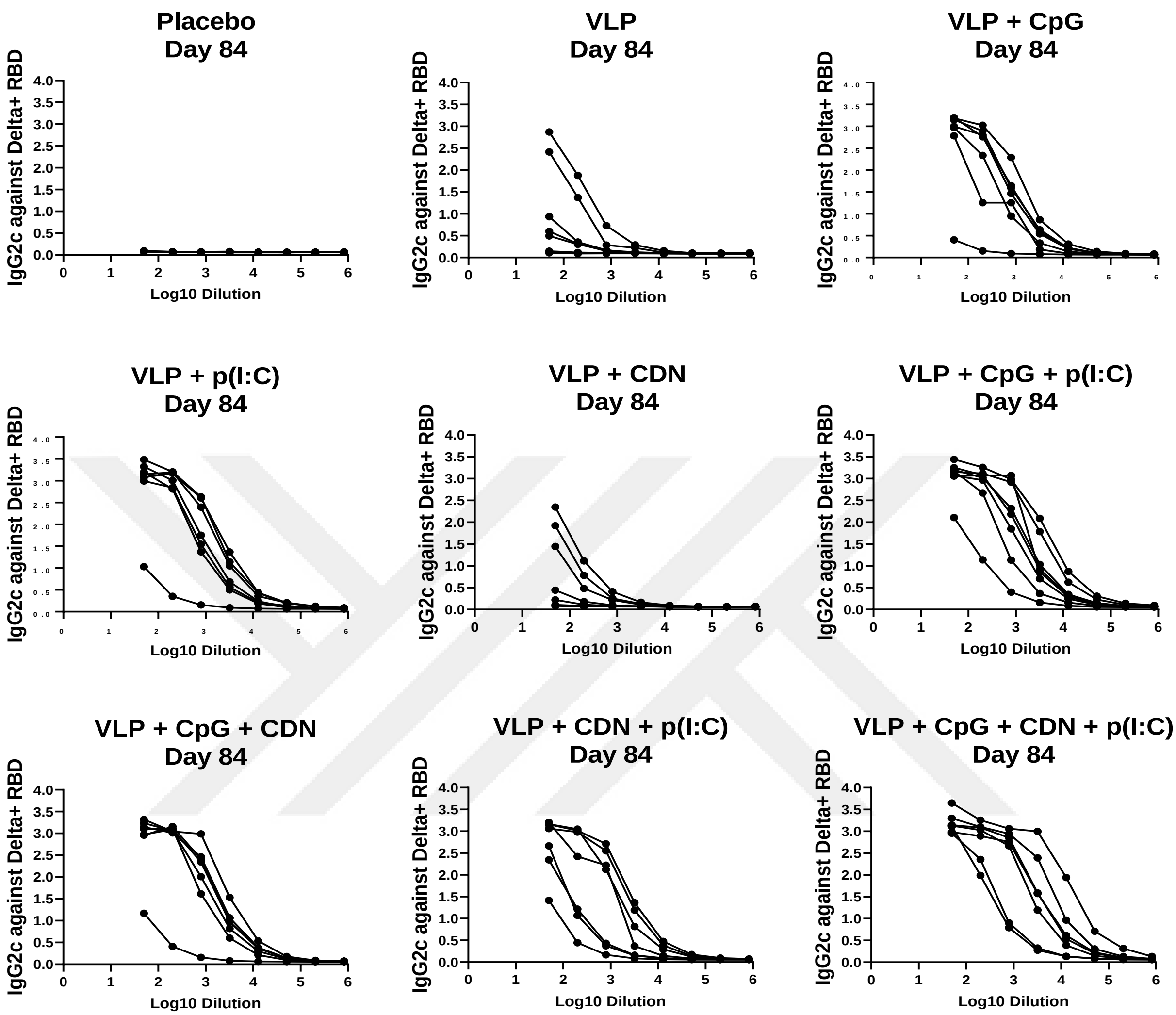

Figure A.29. IgG2c responses of the mice injected with VLP with single, dual or triple adjuvant combinations with K-type CpG ODN, poly(I:C), and 2,3-cGAMP two weeks after the third injection against Delta+ RBD protein. Each graph represents one group of mice injected with the corresponding vaccine combination.

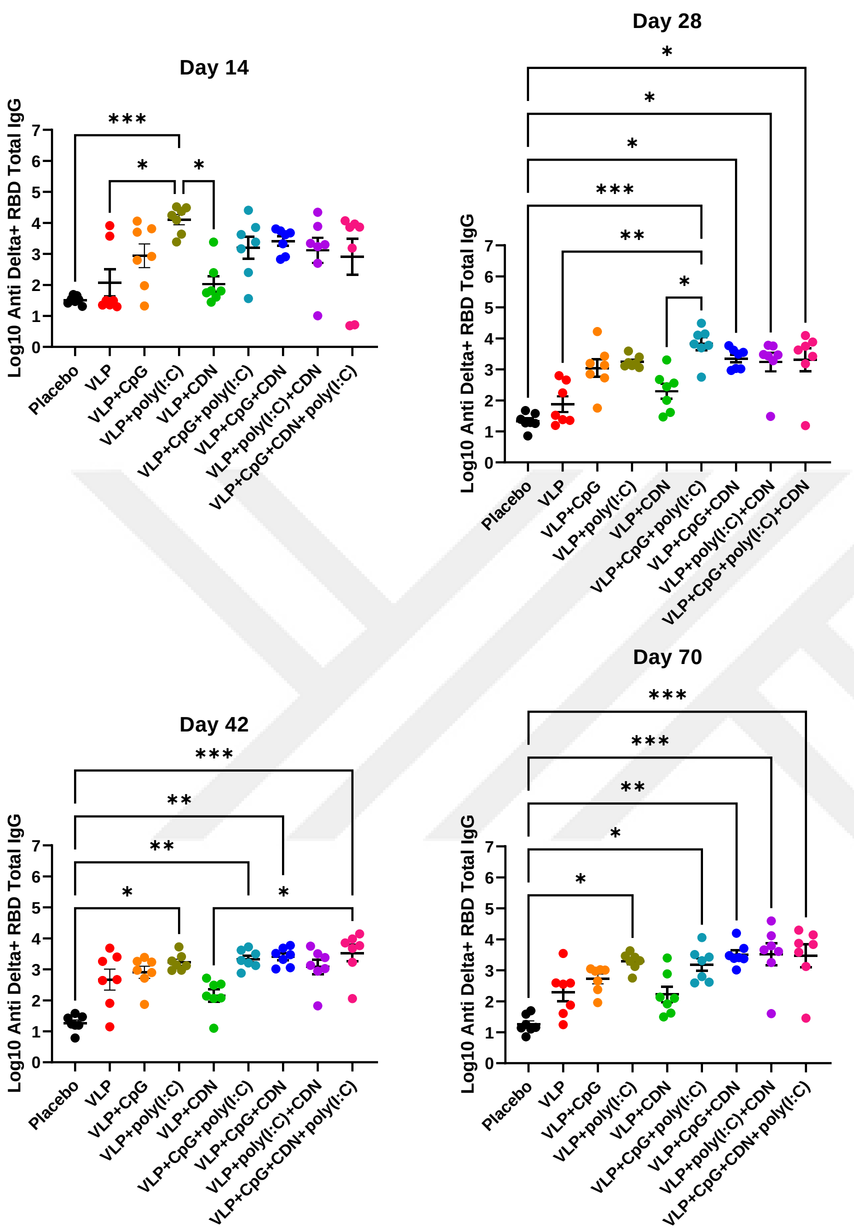
Day 14
Day 28
Day 42
Day 70
Log10 Anti Delta+ RBD Total IgG
Placebo
VLP
VLP+CpG
VLP+poly(I:C)
VLP+CDN
VLP+CpG+poly(I:C)
VLP+CpG+CDN
VLP+poly(I:C)+CDN
VLP+CpG+CDN+poly(I:C)
VLP+CpG+poly(I:C)+CDN

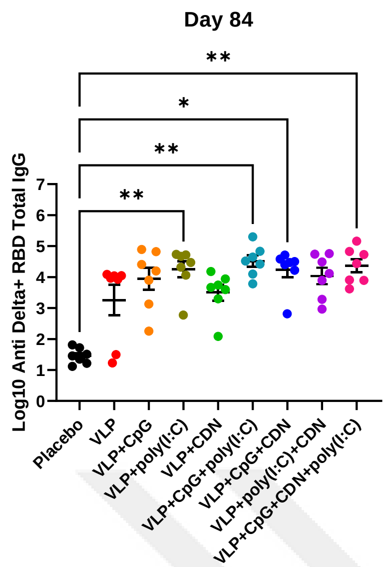

Figure A.30. Antibody responses of vaccinated male C57BL/6 mice (n=7/group) against Delta^{+} RBD protein. Cellular immune response against Delta^{+} RBD protein A) two weeks after the primary injection; B) two weeks after the booster injection; C) four weeks after the primary injection D) eight weeks after the booster injection; E) two weeks after the third dose of vaccination. Groups were compared with one-way ANOVA with Kruskal-Wallis test. P < .05, **P < .01, *P < .001, ***P < .0001.

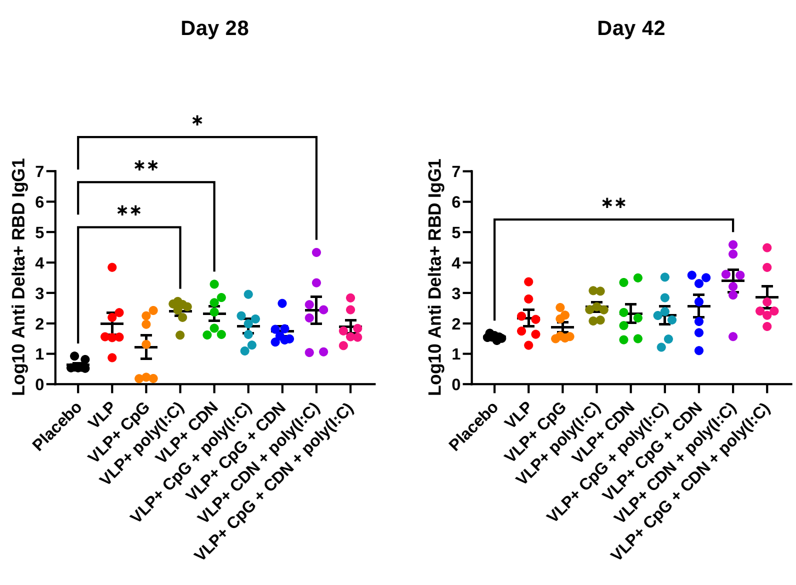

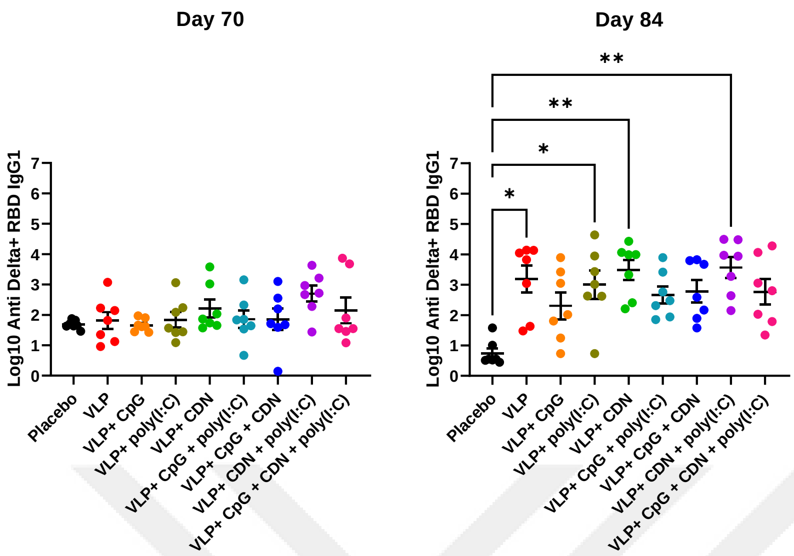

Figure A.31. IgG1 responses of vaccinated male C57BL/6 mice (n=7/group) against Delta$^+$ RBD protein. Cellular immune response against Delta$^+$ RBD protein. A) two weeks after the booster injection; B) four weeks after the primary injection C) eight weeks after the booster injection; D) two weeks after the third vaccination dose. Groups were compared with one-way ANOVA with Kruskal-Wallis test. P < .05, **P < .01, *P < .001, ***P < .0001.

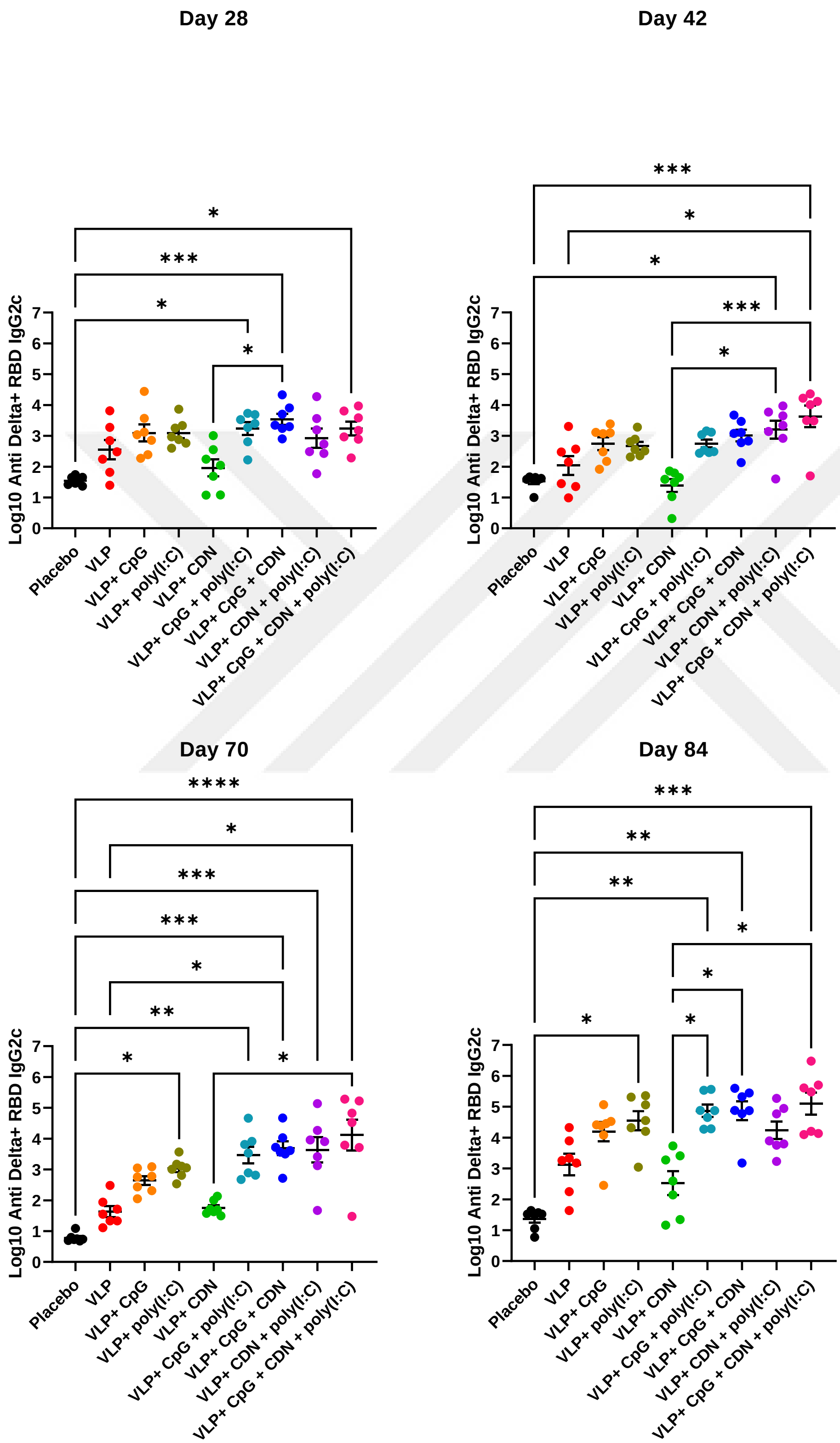

Figure A.32. IgG2c responses of vaccinated male C57BL/6 mice (n=7/group) against Delta⁺ RBD protein. Cellular immune response against Delta⁺ RBD protein. A) two weeks after the booster injection; B) four weeks after the primary injection C) eight weeks after the booster injection; D) two weeks after the third vaccination dose. Groups were compared with one-way ANOVA with Kruskal-Wallis test. P < .05, **P < .01, *P < .001, ***P < .0001.

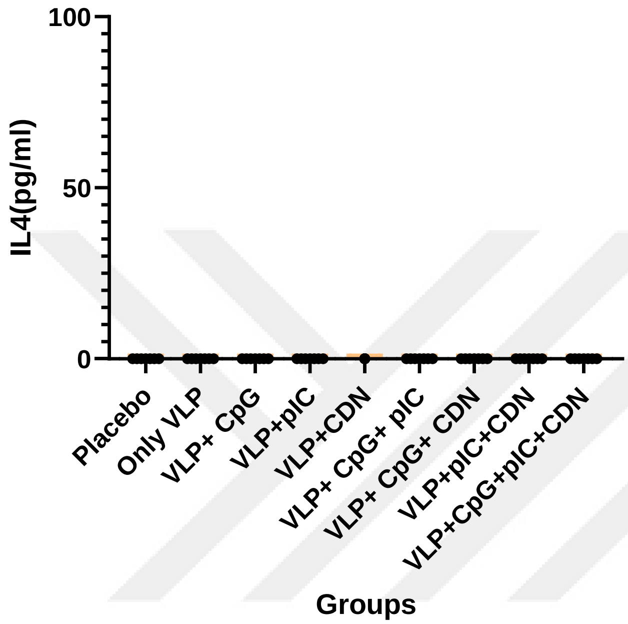

Figure A33. The Antigen Recall Assay using immunized mice spleen cells to assess IL4 secretion by ELISA. Spleen cells were incubated with VLP (0.5ug/well) for 48 hours, and secreted IL-4 amounts compared among groups. Vaccinated groups were compared with one-way ANOVA followed by the Kruskal-Wallis test for multiple comparisons. *P < 0.05, **P < 0.01, ***P <0 .001, ****P <0 .0001.

CHAPTER 7

COPYRIGHT PERMISSIONS

Copyright permission for Figure 1.6

SPRINGER NATURE LICENSE
TERMS AND CONDITIONS
Aug 17, 2023

This Agreement between Bilkent University -- Yasemin Ceylan ("You") and Springer Nature ("Springer Nature") consists of your license details and the terms and conditions provided by Springer Nature and Copyright Clearance Center.

License Number	5610840463577
License date	Aug 16, 2023
Licensed Content Publisher	Springer Nature
Licensed Content Publication	Springer eBook
Licensed Content Title	Developments in Vaccine AdjuvantsAdjuvants
Licensed Content Author	Farrhana Ziana Firdaus, Mariusz Skwarczynski, Istvan Toth
Licensed Content Date	Jan 1, 2022
Type of Use	Thesis/Dissertation
Requestor type	academic/university or research institute
Format	print and electronic

Portion	figures/tables/illustrations
Number of figures/tables/illustrations	1
Will you be translating?	no
Circulation/distribution	1 - 29
Author of this Springer Nature content	no
Title	INVESTIGATING IN VIVO UTILIZATION OF VLP VACCINES ADJUVANTED WITH SINGLE, DUAL, OR TRIPLE PATHOGEN-ASSOCIATED MOLECULAR PATTERNS
Institution name	Bilkent University
Expected presentation date	Aug 2023
Portions	Figure 1. Timeline of licensed adjuvants discovery
Requestor Location	Bilkent University Bilkent Universitesi, SB Blok, Kat:2 Ankara, 06800 Turkey Attn: Bilkent University
Total	0.00 USD